Non-equilibrium Statistical Theory for Singular Fluid Stresses

Masato Itami

January 2016

Contents

Chapter 1

Introduction

1.1 Theory of equilibrium systems

When we consider the flow of air, there is no need to consider the motion of atoms of which air consists. Different methods for describing physical phenomena are employed depending on space-time scales, which means that there are hierarchies in nature. Statistical mechanics aims at establishing relations between different hierarchies. As a typical example where the connection between microscopic structure and macroscopic properties is well understood, there is known to be equilibrium statistical mechanics which relates macroscopic thermodynamics to microscopic mechanical laws in equilibrium. In this section, we first review thermodynamics and equilibrium statistical mechanics.

1.1.1 Thermodynamics

In equilibrium systems, macroscopic behavior is systematically described by a universal framework—thermodynamics [1]. In thermodynamics, characteristic quantities to be measured are heat capacity at constant volume C_V and pressure P as a function of temperature T and volume V. The heat capacity $C_V(T,V)$ and the pressure $P(T,V)$ represent heat and mechanical properties of equilibrium systems, respectively. The relation $P = P(T,V)$ is called the equation of state. The heat capacity and the equation of state fully characterize thermodynamic properties of a single-component system in equilibrium. For instance, we can obtain internal energy U as a function of temperature T and volume V by using them. The temperature dependence of the internal energy $U(T,V)$ is determined by the heat capacity $C_V(T,V)$ using

$$\frac{\partial U(T,V)}{\partial T} = C_V(T,V), \tag{1.1}$$

and the volume dependence of the internal energy $U(T,V)$ is determined by the equation of state using

$$\frac{\partial U(T,V)}{\partial V} = T\frac{\partial P(T,V)}{\partial T} - P(T,V). \tag{1.2}$$

Note that the heat capacity $C_V(T,V)$ and the equation of state are not independent because (1.1) and (1.2) lead to

$$\frac{\partial C_V(T,V)}{\partial V} = T\frac{\partial^2 P(T,V)}{\partial T^2}, \tag{1.3}$$

which means that the volume dependence of the heat capacity $C_V(T,V)$ is determined using only the equation of state, or the mechanical property.

In thermodynamics, the most fundamental and useful quantity is the thermodynamic entropy S. The entropy is defined as the unique extensive quantity, up to an affine transformation of scale, characterizing feasibility of adiabatic processes, which is called the entropy principle [2]. Thus, the entropy describes a measure of the irreversibility of thermodynamics. By introducing the entropy, we can formalize the framework of thermodynamics and derive thermodynamic properties in an elegant manner. When the entropy S is expressed as a function of internal energy U and volume V, the functional form of the entropy $S(U,V)$ determines all of the thermodynamic properties, which means that we can obtain the heat capacity and the equation of state from the entropy $S(U,V)$. The entropy is also directly related to the second law of thermodynamics:

$$\Delta S \geq 0, \tag{1.4}$$

where ΔS is the change of entropy in an adiabatic process. We can operationally determine the entropy $S(U,V)$ through the use of the fundamental thermodynamic relation:

$$dU = TdS - PdV, \tag{1.5}$$

and the measurement of the heat capacity and the equation of state. If we want to determine the entropy $S(U,V)$ without the measurement starting from a microscopic description of an equilibrium system, we have to employ equilibrium statistical mechanics.

1.1.2 Equilibrium statistical mechanics

On the basis of a microscopic description of equilibrium systems, the principle of equal a priori probabilities reproduces the results obtained in the framework of thermodynamics. This is established as equilibrium statistical mechanics [3]. Explicitly, by considering the law of large numbers, we obtain the thermal equilibrium values of macroscopic mechanical quantities in isolated systems using the microcanonical distribution. In the framework of equilibrium statistical mechanics, the thermodynamic entropy $S(U,V)$ is given by Boltzmann's formula

$$S(U,V) = k_{\mathrm{B}} \log W(U,V), \tag{1.6}$$

where k_{B} is the Boltzmann constant and $W(U,V)$ is the number of microstates consistent with the given macrostate (U,V). The important thing here is that this entropy

is found to satisfy the fundamental thermodynamic relation (1.5), and as the result all of the thermodynamic properties are obtained from $S(U, V)$. Note that (1.6) asymptotically holds in the thermodynamic limit.

What is the significance of equilibrium statistical mechanics beyond thermodynamics? First, when we choose a microscopic Hamiltonian, we can predict thermodynamic properties of the system without measurements. In other words, we can explore the microscopic origin of macroscopic phenomena in equilibrium systems. Second, we can discuss fluctuations of thermodynamic and mechanical quantities. For example, by using equilibrium statistical mechanics, the heat capacity can be expressed in terms of the fluctuation of the internal energy of a system interacting with a heat bath. Third, we have the possibility of calculating universal quantities of different materials such as critical exponents in critical phenomena. We can neither obtain theoretically scaling exponents nor verify the Widom scaling hypothesis without equilibrium statistical mechanics where the renormalization group is a powerful tool for critical phenomena. Due to the above reasons, equilibrium statistical mechanics is indispensable for understanding macroscopic behavior in equilibrium systems.

1.1.3 Einstein theory

Between macroscopic thermodynamics and microscopic mechanics, there is the mesoscopic Einstein theory which describes rare fluctuations of thermodynamic variables in equilibrium systems. By considering that $W(U, V)$ is directly related to the probability density of U and V, (1.6) leads to

$$\lim_{\substack{V\to\infty \\ N/V:\text{fix}}} \frac{1}{V} \log P(u) = s(u), \tag{1.7}$$

where s is the thermodynamic entropy density per unit volume, u is the internal energy density per unit volume, and $P(u)$ is the probability density of u. This equation (1.7) means that the rare fluctuations of u are expressed in terms of the thermodynamic entropy in an isolated system. In general thermodynamic systems, the large deviation function of thermodynamic variables is expressed in terms of the thermodynamic function. Thus, by using the Einstein theory, we know the rare fluctuations of thermodynamic variables in equilibrium systems without microscopic mechanics.

1.2 Theory of non-equilibrium systems

In contrast to equilibrium systems, there is still no theory describing the general behavior of non-equilibrium systems although much effort has been devoted to the investigation of steady-state thermodynamics and non-equilibrium statistical mechanics [4–6]. When fluids are out of equilibrium but still remain in local equilibrium, their macroscopic dynamical behavior is universally described by the hydrodynamic equations [7]. A microscopic understanding of the hydrodynamic equations for the case of dilute gases was established through the Boltzmann equation [8], whereas it remains

Table 1.1 Classification of equilibrium and non-equilibrium theories.

	Equilibrium	Local equilibrium
Macroscopic	Thermodynamics	Fluid mechanics
Mesoscopic	Einstein theory	Onsager theory
Microscopic	Mechanics	Mechanics

unclear for a general fluid. Thus, we aim at the construction of statistical mechanics for fluid phenomena. In this section, we review fluid mechanics, the Onsager theory, and non-equilibrium statistical mechanics, which, in equilibrium, correspond to thermodynamics, the Einstein theory, and equilibrium statistical mechanics, respectively. We show the classification of well-established equilibrium and non-equilibrium theories in Table 1.1.

1.2.1 Fluid mechanics

In this subsection, in order to understand the hydrodynamic equations which universally describe the time evolution of macroscopic density fields in local equilibrium, we consider the Navier–Stokes equations on the basis of the description of a Hamiltonian particle system. We study a system consisting of N particles of mass m in a cube of side length L. For simplicity, periodic boundary conditions are assumed. Let $(\boldsymbol{r}_i, \boldsymbol{p}_i)$ $(1 \leq i \leq N)$ be the position and momentum of the ith particle. A collection of the positions and momenta of all particles is denoted by $\Gamma = (\boldsymbol{r}_1, \boldsymbol{p}_1, \ldots, \boldsymbol{r}_N, \boldsymbol{p}_N)$, which represents the microscopic state of the system. The Hamiltonian of the system is given by

$$H(\Gamma) = \sum_{i=1}^{N} \left[\frac{|\boldsymbol{p}_i|^2}{2m} + \frac{1}{2} \sum_{j(\neq i)} \Phi(|\boldsymbol{r}_i - \boldsymbol{r}_j|) \right], \tag{1.8}$$

where Φ is a short-range interaction potential between two particles. Γ_t denotes the solution of the Hamiltonian equations at time t for any state Γ at $t = 0$. Then, the equation of motion for the ith particle is written as

$$\frac{\mathrm{d}p_i^a}{\mathrm{d}t} = -\sum_{j(\neq i)} \frac{\partial \Phi(|\boldsymbol{r}_i - \boldsymbol{r}_j|)}{\partial r_i^a}. \tag{1.9}$$

Throughout this subsection, the superscripts a and b take values x, y, or z, which represents the index of the Cartesian coordinates, and we employ Einstein's summation convention for repeated indices appearing in one term. For convenience, we abbreviate $\partial/\partial t$ and $\partial/\partial r^a$ as ∂_t and ∂^a, respectively.

Let ξ_{micro} be the largest length scale appearing in the molecular description, and ξ_{macro} be the minimum length characterizing macroscopic behavior. We assume that there exists a cut-off length Λ that satisfies $\xi_{\mathrm{micro}} \ll \Lambda \ll \xi_{\mathrm{macro}}$. The total mass, the total momentum, and the total energy are conserved quantities in this system.

Corresponding to the conserved quantities, mass, momentum, and energy density fields are defined by

$$\rho(\boldsymbol{r};\Gamma) \equiv \sum_i m\mathcal{D}(\boldsymbol{r}-\boldsymbol{r}_i), \tag{1.10}$$

$$\pi^a(\boldsymbol{r};\Gamma) \equiv \sum_i p_i^a \mathcal{D}(\boldsymbol{r}-\boldsymbol{r}_i), \tag{1.11}$$

$$h(\boldsymbol{r};\Gamma) \equiv \sum_i \left[\frac{|\boldsymbol{p}_i|^2}{2m} + \frac{1}{2}\sum_{j(\neq i)} \Phi(|\boldsymbol{r}_i-\boldsymbol{r}_j|)\right] \mathcal{D}(\boldsymbol{r}-\boldsymbol{r}_i), \tag{1.12}$$

respectively, with

$$\mathcal{D}(\boldsymbol{r}-\boldsymbol{r}_i) \equiv \begin{cases} 3/(4\pi\Lambda^3), & |\boldsymbol{r}-\boldsymbol{r}_i| \leq \Lambda, \\ 0, & |\boldsymbol{r}-\boldsymbol{r}_i| > \Lambda. \end{cases} \tag{1.13}$$

Because $\xi_{\text{micro}} \ll \Lambda$, it is expected from the law of large numbers that these density fields take typical values with respect to a probability density. On the other hand, the condition $\Lambda \ll \xi_{\text{macro}}$ leads to the result that the typical value of each density field is independent of the cut-off length Λ. Thus, these density fields are regarded as macroscopic density fields without ambiguity. Here, we define the local velocity field by $u^a(\boldsymbol{r};\Gamma) \equiv \pi^a(\boldsymbol{r};\Gamma)/\rho(\boldsymbol{r};\Gamma)$. For any physical quantity A, we abbreviate $A(\boldsymbol{r};\Gamma_t)$ as A_t. The density fields satisfy the following continuity equations:

$$\partial_t \rho_t + \partial^a(\rho_t u_t^a) = 0, \tag{1.14}$$

$$\partial_t \pi_t^a + \partial^b(\pi_t^a u_t^b) = \partial^b \sigma_t^{ab}, \tag{1.15}$$

$$\partial_t h_t + \partial^a(h_t u_t^a) = \partial^a(\sigma_t^{ba} u_t^b - q_t^a), \tag{1.16}$$

with

$$\begin{aligned}\sigma^{ab}(\boldsymbol{r};\Gamma) = &-\sum_{i=1}^N \frac{[p_i^a - mu^a(\boldsymbol{r};\Gamma)][p_i^b - mu^b(\boldsymbol{r};\Gamma)]}{m}\mathcal{D}(\boldsymbol{r}-\boldsymbol{r}_i) \\ &-\sum_{i<j}\left[-\frac{\partial\Phi(|\boldsymbol{r}_i-\boldsymbol{r}_j|)}{\partial|\boldsymbol{r}_i-\boldsymbol{r}_j|}\right]\frac{\left(r_i^a-r_j^a\right)\left(r_i^b-r_j^b\right)}{|\boldsymbol{r}_i-\boldsymbol{r}_j|}\mathcal{S}(\boldsymbol{r};\boldsymbol{r}_i,\boldsymbol{r}_j),\end{aligned} \tag{1.17}$$

$$\begin{aligned}q^a(\boldsymbol{r};\Gamma) = &\sum_{i=1}^N \left[\frac{|\boldsymbol{p}_i - m\boldsymbol{u}(\boldsymbol{r};\Gamma)|^2}{2m} + \frac{1}{2}\sum_{j(\neq i)}\Phi(|\boldsymbol{r}_i-\boldsymbol{r}_j|)\right]\frac{p_i^a - mu^a(\boldsymbol{r};\Gamma)}{m}\mathcal{D}(\boldsymbol{r}-\boldsymbol{r}_i) \\ &+\sum_{i<j}\frac{[p_i^b - mu^b(\boldsymbol{r};\Gamma)] + [p_j^b - mu^b(\boldsymbol{r};\Gamma)]}{2m} \\ &\times\left[-\frac{\partial\Phi(|\boldsymbol{r}_i-\boldsymbol{r}_j|)}{\partial|\boldsymbol{r}_i-\boldsymbol{r}_j|}\right]\frac{\left(r_i^a-r_j^a\right)\left(r_i^b-r_j^b\right)}{|\boldsymbol{r}_i-\boldsymbol{r}_j|}\mathcal{S}(\boldsymbol{r};\boldsymbol{r}_i,\boldsymbol{r}_j),\end{aligned} \tag{1.18}$$

where σ^{ab} is the microscopic expression of the ab component of the stress tensor that is the a-component of the force on the unit area perpendicular to the b-axis, q^a is the microscopic expression of the heat flux, and

$$\mathcal{S}(\boldsymbol{r};\boldsymbol{r}_i,\boldsymbol{r}_j) \equiv \int_0^1 \mathrm{d}\xi\, \mathcal{D}(\boldsymbol{r}-\boldsymbol{r}_i-(\boldsymbol{r}_j-\boldsymbol{r}_i)\xi), \tag{1.19}$$

which satisfies

$$(r_j^a - r_i^a)\partial^a \mathcal{S}(\boldsymbol{r};\boldsymbol{r}_i,\boldsymbol{r}_j) = \mathcal{D}(\boldsymbol{r}-\boldsymbol{r}_i) - \mathcal{D}(\boldsymbol{r}-\boldsymbol{r}_j). \tag{1.20}$$

It can be directly confirmed that

$$\sigma^{ab}(\boldsymbol{r};\Gamma) = \sigma^{ba}(\boldsymbol{r};\Gamma). \tag{1.21}$$

Note that, when there are interactions between particles across the periodic boundary, the right-hand sides of (1.17) and (1.18) must be modified to take a non-zero value on the shortest line connecting two interacting particles across the periodic boundary. In order to obtain the hydrodynamic equations from (1.14), (1.15), and (1.16), what we have to do is to express σ^{ab} and q^a in terms of ρ, π^a, and h. However, by using only the microscopic expressions, we cannot do that.

Here, we phenomenologically derive the hydrodynamic equations based on the second law of thermodynamics [9, 10]. We define the internal energy density by

$$\begin{aligned}\varepsilon(\boldsymbol{r};\Gamma) &\equiv h(\boldsymbol{r};\Gamma) - \frac{1}{2}\rho(\boldsymbol{r};\Gamma)|\boldsymbol{u}(\boldsymbol{r};\Gamma)|^2 \\ &= \sum_i \left[\frac{|\boldsymbol{p}_i - m\boldsymbol{u}(\boldsymbol{r};\Gamma)|^2}{2m} + \frac{1}{2}\sum_{j(\neq i)}\Phi(|\boldsymbol{r}_i-\boldsymbol{r}_j|)\right]\mathcal{D}(\boldsymbol{r}-\boldsymbol{r}_i).\end{aligned} \tag{1.22}$$

Then, using (1.14), (1.15), and (1.16), we obtain

$$\partial_t \varepsilon_t + \partial^a(\varepsilon_t u_t^a) = \sigma_t^{ba}\partial^a u_t^b - \partial^a q_t^a. \tag{1.23}$$

Denoting the material derivative as

$$\mathrm{D}_t = \partial_t + u_t^a \partial^a, \tag{1.24}$$

and using (1.14), (1.23) is rewritten as

$$\rho_t \mathrm{D}_t\left(\frac{\varepsilon_t}{\rho_t}\right) = \sigma_t^{ba}\partial^a u_t^b - \partial^a q_t^a. \tag{1.25}$$

In fluid mechanics, it is assumed that thermodynamic quantities and thermodynamic relations are valid for all time at each macroscopic position, which is called the assumption of local equilibrium thermodynamics. Then, by recalling (1.5), we obtain

$$T_t \mathrm{D}_t\left(\frac{s_t}{\rho_t}\right) = \mathrm{D}_t\left(\frac{\varepsilon_t}{\rho_t}\right) + p_t \mathrm{D}_t\left(\frac{1}{\rho_t}\right), \tag{1.26}$$

where s is the entropy density which is determined as a function of ε and ρ, T is the temperature, and p is the thermodynamic pressure. Note that T and p are determined from s. Using (1.25) and (1.26), we have

$$\rho_t T_t \mathrm{D}_t \left(\frac{s_t}{\rho_t} \right) = (\sigma_t^{ba} + p_t \delta^{ba}) \partial^a u_t^b - \partial^a q_t^a. \tag{1.27}$$

By recalling (1.21), (1.27) is rewritten as

$$\partial_t s_t + \partial^a \left(s_t u_t^a + \frac{q_t^a}{T_t} \right) = \Sigma_t \tag{1.28}$$

with

$$\Sigma_t = \frac{1}{2T_t} (\sigma_t^{ab} + p_t \delta^{ab})(\partial^a u_t^b + \partial^b u_t^a) - \frac{q_t^a}{T_t^2} \partial^a T_t. \tag{1.29}$$

Note that because of the periodic boundary conditions, the second term in the left-hand side of (1.28) does not contribute to the increment of the total entropy defined by

$$S_{\mathrm{tot}} = \int \mathrm{d}^3 \boldsymbol{r} \; s(\varepsilon(\boldsymbol{r}), \rho(\boldsymbol{r})). \tag{1.30}$$

By recalling the assumption of local equilibrium thermodynamics, the second law of thermodynamics implies $\Sigma_t \geq 0$ for any $\partial^a u_t^b$ and $\partial^a T_t$. Here, we further assume that $\sigma_t^{ab} + p_t \delta^{ab}$ and q_t^a depend linearly on $\partial^a u_t^b$ and $\partial^a T_t$. Then, the second law of thermodynamics leads to

$$\sigma_t^{ab} + p_t \delta^{ab} = \eta (\partial^a u_t^b + \partial^b u_t^a) + \left(\zeta - \frac{2}{3} \eta \right) \partial^c u_t^c \delta^{ab}, \tag{1.31}$$

$$q_t^a = -\kappa \partial^a T_t, \tag{1.32}$$

where η, ζ, and κ are the viscosity, the bulk viscosity, and the thermal conductivity, respectively. The transport coefficients η, ζ, and κ are non-negative and may depend on thermodynamic variables. Substituting (1.31) and (1.32) into (1.14), (1.15), and (1.16), we obtain the Navier–Stokes equations.

1.2.2 Onsager theory

In the framework of fluid mechanics, the transport coefficients are the quantities to be measured. In general, it is difficult to obtain some properties of transport coefficients when we give a microscopic description of systems. In this subsection, we review Onsager theory which universally describes the relaxation process of thermodynamic variables and elucidate important properties of transport coefficients [11–16].

Let $\boldsymbol{X} = (X^i)_{i=1}^N$ be a complete set of unconstrained thermodynamic extensive variables of an isolated system. The Onsager theory formulates the deterministic

dynamics of thermodynamic variables in relaxation processes to the equilibrium state. The time evolution is simply expressed as

$$\frac{\mathrm{d}X^i}{\mathrm{d}t} = L^{ij}\frac{\partial S(\boldsymbol{X})}{\partial X^j}, \tag{1.33}$$

where we employ Einstein's summation convention for repeated indices appearing in one term, $S(\boldsymbol{X})$ is the thermodynamic entropy of the system, $\partial S(\boldsymbol{X})/\partial X_j$ corresponds to the thermodynamic force, and L^{ij} is called the Onsager coefficient. The important consequence of Onsager theory is the Onsager reciprocal relations

$$L^{ij} = L^{ji}. \tag{1.34}$$

This non-trivial result was derived by studying fluctuation at equilibrium. Onsager assumed that the most probable regression process from a given non-equilibrium state produced by a spontaneous fluctuation is equivalent to the relaxation dynamics, which is called the regression hypothesis. Concretely, the regression process is assumed to be described by a Langevin equation

$$\frac{\mathrm{d}X^i}{\mathrm{d}t} = L^{ij}\frac{\partial S(\boldsymbol{X})}{\partial X^j} + l^{ij}\xi^j, \tag{1.35}$$

where ξ^j is a Gaussian white noise with zero mean and covariance $\left\langle \xi^i(t)\xi^j(t')\right\rangle = \delta(t-t')$. According to equilibrium statistical mechanics, the stationary probability density of $\boldsymbol{X}$ is determined as

$$P_{\mathrm{eq}}(\boldsymbol{X}) = \frac{1}{Z}\exp\left[S(\boldsymbol{X})\right], \tag{1.36}$$

where Z is the normalization constant. Then, the time-reversibility of microscopic systems provides a non-trivial relation

$$\sum_k l^{ik}l^{jk} = 2L^{ij}, \tag{1.37}$$

which leads to (1.34). The relation (1.37) is referred to as the fluctuation-dissipation relation of the second kind.

The Onsager theory was extended to a complete set of macroscopic slow variables in Ref. [17], which includes (fluctuating) hydrodynamics. The fluctuation-dissipation relation (1.37) gives the Green–Kubo formula for the transport coefficients as shown in Ref. [18]. Note that the Onsager reciprocal relations are not useful for fluid mechanics because there are no non-diagonal transport coefficients in the hydrodynamic equations.

1.2.3 Non-equilibrium statistical mechanics

We here consider the derivation of the Navier–Stokes equations from the viewpoint of statistical mechanics. Explicitly, by taking the average of (1.17) and (1.18) using some distribution, we want to derive (1.31) and (1.32). By recalling the equilibrium theories, we may assume that a local equilibrium distribution is valid for all time at each macroscopic position. However, in Ref. [19], it is shown that this assumption leads to

$$\left\langle \sigma^{ab}(\boldsymbol{r}) \right\rangle_{\mathrm{leq}} = -p(\boldsymbol{r})\delta^{ab}, \tag{1.38}$$

$$\left\langle q^{a}(\boldsymbol{r}) \right\rangle_{\mathrm{leq}} = 0, \tag{1.39}$$

where $\langle \cdot \rangle_{\mathrm{leq}}$ denotes the expectation value with respect to the local equilibrium distribution. In other words, local equilibrium statistical mechanics gives only the Euler equations. Thus, we have to study the statistical distribution more carefully.

Key relations for deriving the Navier–Stokes equations from the viewpoint of statistical mechanics were developed in non-equilibrium statistical mechanics. We explain the recent developments in non-equilibrium statistical mechanics. Although it had been difficult to obtain useful relations for fluctuations beyond the linear response regime, non-trivial relations that are generally valid far from equilibrium, including the fluctuation theorem [20–28] and the Jarzynski equality [29], were developed for the last two decades as a result of the time-reversal symmetry of microscopic mechanics. Thanks to such universal relations, we can easily derive the well-known relations, such as the second law of thermodynamics, the McLennan ensembles, the Green–Kubo relations, and the Kawasaki nonlinear response relation [30, 31]. Moreover, the newly discovered universal relations were confirmed by the laboratory experiments using small systems which are strongly influenced by fluctuations in their environment [32–34]. It should be noted that the universal relations were also utilized to estimate the rotary torque of F_1-ATPase [35].

Recently, by using a non-equilibrium identity similar to the fluctuation theorems and assuming a local Gibbs distribution at the initial time, the Navier–Stokes equations with the Green–Kubo formula for the transport coefficients were derived for an isolated Hamiltonian system [36]. Then, can we perfectly understand fluid mechanics from the microscopic point of view? There are many unsolved problems. In general, by using the Green–Kubo formula, we cannot know how transport coefficients depend on physical quantities. We cannot determine macroscopic boundary conditions starting from a microscopic mechanical description. We also cannot derive Kolmogorov's power law for turbulence on the basis of the microscopic mechanical description.

1.3 Statistical mechanics for fluid mechanics: Stokes' law

Among many problems of statistical mechanics for fluid mechanics, we consider the relation between phenomena described by the solution of hydrodynamic equations and the results of non-equilibrium statistical mechanics in Chapter 2. Concretely, we study the friction coefficient of a macroscopic sphere in a viscous fluid at low Reynolds number because this is one of the most fundamental problem when we study the dynamics of matter in fluids. In general, the linear response formulas are valid for all fluids in the linear response regime, whereas the transport coefficients take different forms depending on the nature of fluids. Thus, the connection between the linear response formula for the friction coefficient and the expressions of the friction coefficient obtained by the hydrodynamic equations has been unclear.

By solving the hydrodynamic equations, we obtain that the friction coefficient is proportional to the viscosity and the radius of the sphere, which is known as Stokes' law. In addition, using non-equilibrium identities, we obtain the linear response formulas for the friction coefficient and the viscosity. The former is expressed in terms of the stress correlation on the surface of the sphere, whereas the latter is expressed in terms of the stress correlation in the bulk of the fluid. Thus, in order to derive Stokes' law from the linear response formulas, what we have to do is to relate the surface stress correlation to the bulk stress correlation. This is not an easy task. If we assume that the surface correlation length is of the same order as the bulk correlation length, we cannot obtain the proper dependence of the Stokes friction coefficient on the size of the sphere. Furthermore, there has been no research in which a surface correlation is related to a bulk correlation in a viscous fluid.

In Chapter 2, we relate the surface stress correlation to the bulk stress correlation with the aid of large deviation theory, especially the contraction principle, and then derive Stokes' law without explicitly employing the hydrodynamic equations.

1.4 Limitations of fluid mechanics: adiabatic piston problem

Macroscopic non-equilibrium phenomena are described by evolution equations for slow modes associated with conservation laws and symmetry breaking [9]. As explained above, the equations for standard liquids and gases are well established as the hydrodynamic equations of mass, momentum, and energy density fields, and heat conduction and sound propagation in solids are also well established [7]. The validity of the description was carefully investigated in small-scale experiments [37], which suggested that the behavior near a solid wall shows deviations from calculation results based on the standard hydrodynamic equations. Furthermore, a stimulating prediction that a liquid droplet is nucleated in a sheared solid may be another example that

is not described by the established continuum equations [38].

As another typical example, we focus on the following adiabatic piston problem [1, 39–42]. A freely movable wall of mass M with one degree of freedom separates a long tube into two regions, each of which is filled with rarefied gas particles of mass m. The wall is assumed to be thermally insulating and frictionless. It is also assumed that $\sqrt{\epsilon} = m/M$ is a small parameter, which controls the amount of energy transferred through the wall. It should be noted that we need to work with a very small system for observing the motion of the wall in a laboratory experiment because ϵ in macroscopic systems is too small (less than 10^{-10}). If the wall were fixed, the energy could not be transferred through the wall. Such a wall is referred to as "adiabatic" in the thermodynamic sense. However, we note that the wall is not strictly adiabatic because the energy is transferred from the hot side to the cold side through the fluctuation of the wall, which is sometimes pointed out in the previous papers. Thus, the wall can be regarded as a "Brownian" wall. The gases in the left and right regions are initially prepared at the same pressure p but different temperatures $T_{\rm L}$ and $T_{\rm R}$, respectively. Each gas is well approximated by an ideal gas, and it is also assumed that the pressure and temperature of gas particles before colliding with the wall are kept constant over time in each region. In this case, the standard hydrodynamic equations suggest that the wall does not move due to the equal pressure. However, perturbation methods for kinetic equations and molecular dynamics simulations reveal that the wall moves towards the hot side owing to the energy transfer from the hot side to the cold side through the fluctuation of the wall. Recently, a phenomenological mechanism for the emergence of the motion from the cross-coupling between momentum and heat flux has been proposed in Refs. [43, 44].

In order to study the adiabatic piston problem, the local detailed balance condition is useful. The local detailed balance condition states that when the system in contact with a single heat bath obeys the canonical distribution at the temperature of the heat bath, the ratio of probability density of the forward path and of the backward path is quantitatively related to the entropy production in the heat baths. The condition holds in many systems including Hamiltonian systems [27] and Langevin systems [28]. The condition can be helpful in defining heat in small systems where heat is not identified yet. By using a model with the local detailed balance condition, we can define heat in the model. Furthermore, since the local detailed balance condition immediately leads to most of the non-trivial relations that are generally valid far from equilibrium [26, 31], it plays a fundamental role in analyzing non-equilibrium systems. Nevertheless, it should be noted that the local detailed balance condition is not obviously valid because the entropy production depends on a level of description [45].

In Chapter 3, we provide a model for the adiabatic piston problem by using a continuous-time Markov jump process. Then, we elucidate the energetics of the model on the basis of the local detailed balance condition, and then derive the expression for the heat transferred from each gas to the wall. Furthermore, by using the condition, we obtain the linear response formula for the steady velocity of the wall and steady energy flux through the wall. By using perturbation expansion in a small parameter

ϵ, we calculate the steady velocity up to order ϵ.

In Chapter 4, we focus on the wall consisting of many atoms instead of the wall with one degree of freedom. Then, we show that temperature gaps appearing on the solid surface generate a force. We provide a quantitative estimation of the force, which turns out to be large enough to be observed by a macroscopic measurement.

1.5 Organization

The remainder of this thesis is organized as follows. In Chapter 2, we derive Stokes' law from Kirkwood's formula and the Green–Kubo formula with the aid of large deviation theory. This chapter corresponds to the paper [M. Itami and S. Sasa, J. Stat. Phys. **161**, 532–552 (2015)]. In Chapter 3, we elucidate the energetics of the adiabatic piston problem on the basis of the local detailed balance condition, and then derive the linear response formula. This chapter corresponds to the paper [M. Itami and S. Sasa, J. Stat. Phys. **158**, 37–56 (2015)]. In Chapter 4, we show that temperature gaps appearing on the solid-gas surfaces generate a force, and provide a quantitative estimation of the force. This chapter corresponds to the paper [M. Itami and S. Sasa, Phys. Rev. E **89**, 052106 (2014)]. Finally, Chapter 5 is devoted to the summary and conclusions. Note that we use different notations in each section.

Chapter 2

Derivation of Stokes' law from Kirkwood's formula and the Green–Kubo formula via large deviation theory

2.1 Introduction

When liquids and gases are out of equilibrium but still remain in local equilibrium, their macroscopic dynamical behavior is precisely described by the hydrodynamic equations [7]. A microscopic understanding of the hydrodynamic equations for the case of dilute gases was established through the Boltzmann equation [8], whereas it remains unclear for a general fluid. Non-trivial relations that are generally valid far from equilibrium, including the fluctuation theorems [20–27] and the Jarzynski equality [29], have been developed over the past two decades as a result of the time-reversal symmetry of microscopic mechanics. Thanks to such universal relations, we can easily re-derive certain well-known relations, such as the McLennan ensembles, the Green–Kubo formula, and the Kawasaki nonlinear response relation [30, 31]. Furthermore, by using a non-equilibrium identity similar to the fluctuation theorems and assuming a local Gibbs distribution at the initial time, the Navier–Stokes equation was derived for an isolated Hamiltonian system [36]. Based on these achievements, we believe this is an opportune moment to reconsider fluid dynamics from the viewpoint of statistical mechanics.

In this chapter, we study the friction coefficient of a macroscopic sphere in a fluid. Starting from microscopic mechanics, Kirkwood first derived the linear response formula for the friction coefficient, γ_{K}, in the form [46]

$$\gamma_{\mathrm{K}} = \frac{1}{3k_{\mathrm{B}}T} \int_0^\tau dt \ \langle \boldsymbol{F}_t \cdot \boldsymbol{F}_0 \rangle_{\mathrm{eq}} \,, \tag{2.1}$$

where $k_{\rm B}$ is the Boltzmann constant, T is the temperature of the fluid, $\langle\,\cdot\,\rangle_{\rm eq}$ denotes a canonical ensemble average at temperature T, and $\boldsymbol{F}_t$ is the total force exerted on the sphere by the fluid at time t. The upper limit of the integral τ should be much larger than the correlation time of the force $\boldsymbol{F}_t$ and much smaller than the relaxation time of the momentum of the sphere. This will be discussed in detail in Sect. 2.3. Note that τ could go to infinity if we take the heavy mass limit for the sphere [47–49]. The theoretical results were confirmed by numerical experiments [50–54].

By focusing on a special class of fluids, we can obtain a more explicit expression for the friction coefficient. For instance, the friction coefficient for a dilute gas, $\gamma_{\rm dg}$, has the form [55, 56]

$$\gamma_{\rm dg} = \frac{8}{3}\rho\mathcal{R}^2\sqrt{2\pi m k_{\rm B}T}, \tag{2.2}$$

where ρ is the number density of gas particles, $\mathcal{R}$ is the radius of the sphere, and m is the mass of a gas particle. As another typical example, the friction coefficient for a viscous fluid at low Reynolds number, $\gamma_{\rm S}$, is given by [7]

$$\gamma_{\rm S} = \mathcal{C}\eta\mathcal{R}, \tag{2.3}$$

where η is the viscosity of the fluid. The numerical coefficient $\mathcal{C}$ is equal to 4π for the slip boundary condition where the velocity of the fluid normal to the sphere at the boundary is equal to that of the sphere in this direction and the shear stresses on the sphere are equal to zero, and 6π for the stick boundary condition where the velocity of the fluid at the boundary is equal to that of the sphere. The expression (2.3) is known as Stokes' law.

Kirkwood's formula can be derived on the basis of a mechanical system, meaning that the validity of the formula is generally independent of the nature of the fluid within the linear response regime. Thus, Kirkwood's formula (2.1) corresponds to (2.2) for a dilute gas, which was confirmed by Green [56]. Furthermore, (2.1) corresponds to (2.3) for a viscous incompressible fluid at low Reynolds number, as confirmed by Zwanzig [57] on the basis of fluctuating hydrodynamics [7, 58] and Faxén's law [59] in the case of the stick boundary condition. Note that the linear response formula (2.1) is effective because the Reynolds number is low.

We now consider the derivation of Stokes' law (2.3) from Kirkwood's formula (2.1) without explicitly employing the hydrodynamic equations. According to the Green–Kubo formula [18], the viscosity of the fluid, η, can be expressed in terms of the stress correlation in the bulk of the fluid as

$$\eta = \frac{1}{k_{\rm B}T}\int_0^\tau dt \int d^3\boldsymbol{r}\,\langle\sigma^{xy}(\boldsymbol{r}_0,0)\sigma^{xy}(\boldsymbol{r},t)\rangle_{\rm eq}\,, \tag{2.4}$$

where $\sigma^{xy}(\boldsymbol{r},t)$ is the x-component of the force on the unit area perpendicular to the y-axis at position $\boldsymbol{r}$ and time t (this is the xy component of the stress tensor $\overleftrightarrow{\boldsymbol{\sigma}}$), and $\boldsymbol{r}_0$ is an arbitrary position in the bulk of the fluid. Note that τ is much larger than the correlation time of σ^{xy}, and much smaller than the relaxation time of the momentum density field of the fluid. Precisely speaking, the condition of this τ is

different from that of τ in Kirkwood's formula, but we assume that there exists some τ that satisfies both conditions. Because the right-hand side of (2.1) can be expressed in terms of the stress correlation on the surface of the sphere, we can obtain Stokes' law (2.3) from Kirkwood's formula (2.1) and the Green–Kubo formula (2.4) if the surface stress correlation is related to the bulk stress correlation.

The main contribution of this chapter is to establish the connection between the bulk and surface stress fluctuations. The basic concept is simple. The probability density of surface stress fluctuations is obtained from the probability density of bulk stress fluctuations by integrating out the other degrees of freedom. This procedure can be conducted in an elegant manner with the aid of large deviation theory.

The remainder of this chapter is organized as follows. In Sect. 2.2, we explain the setup of our model, and we review Kirkwood's formula from the Hamiltonian description of particle systems in Sect. 2.3. We derive the probability density of bulk stress fluctuations under two phenomenological assumptions in Sect. 2.4. We then express the probability density of surface stress fluctuations by integrating the probability density of bulk stress fluctuations. We apply a saddle-point method to this expression, and obtain the exact form of the probability density of surface stress fluctuations. By combining the obtained expression with Kirkwood's formula, we derive Stokes' law. These highlights are presented in Sect. 2.5. The final section is devoted to a brief summary and some concluding remarks.

Throughout this chapter, the superscripts a, b and α, β represent the indices in Cartesian coordinates (x, y, z) and spherical coordinates (r, θ, φ), respectively, where $(x, y, z) = (r\sin\theta\cos\varphi, r\sin\theta\sin\varphi, r\cos\theta)$ with $r \geq 0, 0 \leq \theta \leq \pi, 0 \leq \varphi \leq 2\pi$. In addition, we employ Einstein's summation convention for repeated indices appearing in one term.

2.2 Model

We provide a three-dimensional mechanical description of our setup. A schematic illustration is shown in Fig. 2.1. The system consists of N bath particles of mass m and radius r_{bp}, and one macroscopic sphere of mass M and radius $\mathcal{R}$ in a cube of side length L. We assume that M and $\mathcal{R}$ are much larger than m and r_{bp}, respectively. For simplicity, periodic boundary conditions are assumed. Let $(\boldsymbol{r}_i, \boldsymbol{p}_i)$ $(1 \leq i \leq N)$ be the position and momentum of the ith bath particle, and $(\boldsymbol{R}, \boldsymbol{P})$ be those of the sphere. A collection of the positions and momenta of all particles is denoted by $\Gamma = (\boldsymbol{r}_1, \boldsymbol{p}_1, \ldots, \boldsymbol{r}_N, \boldsymbol{p}_N, \boldsymbol{R}, \boldsymbol{P})$, which represents the microscopic state of the system.

The Hamiltonian of the system is given by

$$H(\Gamma) = \sum_{i=1}^{N} \left[\frac{|\boldsymbol{p}_i|^2}{2m} + \sum_{j>i} \Phi_{\mathrm{int}}(|\boldsymbol{r}_i - \boldsymbol{r}_j|) + \Phi_{\mathrm{sp}}(|\boldsymbol{r}_i - \boldsymbol{R}|) \right] + \frac{|\boldsymbol{P}|^2}{2M}, \tag{2.5}$$

where Φ_{int} is a short-range interaction potential between two bath particles, and Φ_{sp}

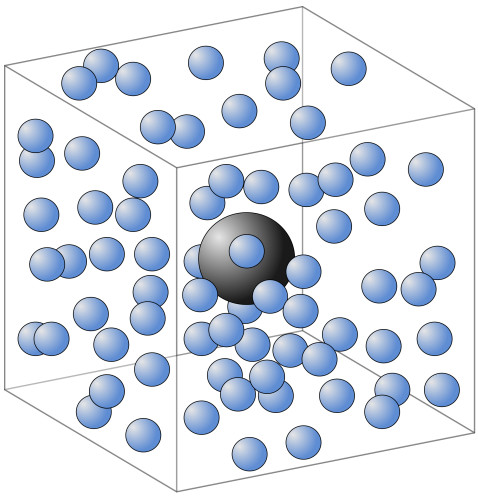

Fig. 2.1 Schematic illustration of our setup. The system consists of N bath particles of mass m and radius r_{bp}, and one macroscopic sphere of mass M and radius $\mathcal{R}$ in a cube of side length L.

is that between a bath particle and the sphere. We assume

$$\Phi_{\mathrm{sp}}(\chi) \to \infty, \qquad \text{as } \chi \to \mathcal{R} + r_{\mathrm{bp}}, \tag{2.6}$$

$$\Phi_{\mathrm{sp}}(\chi) = 0, \qquad \text{for } \chi \geq \mathcal{R} + r_{\mathrm{bp}} + \xi_0, \tag{2.7}$$

where $\xi_0 \simeq r_{\mathrm{bp}}$. Γ_t denotes the solution of the Hamiltonian equations at time t for any state Γ at $t = 0$. In this setup, the energy is conserved, i.e.,

$$H(\Gamma_t) = H(\Gamma), \tag{2.8}$$

and Liouville's theorem

$$\left| \frac{\partial \Gamma_t}{\partial \Gamma} \right| = 1 \tag{2.9}$$

holds. The total force acting on the sphere is given by

$$\begin{aligned} \boldsymbol{F}(\Gamma) &= -\frac{\partial H(\Gamma)}{\partial \boldsymbol{R}} \\ &= -\sum_{i=1}^{N} \frac{\partial \Phi_{\mathrm{sp}}(|\boldsymbol{r}_i - \boldsymbol{R}|)}{\partial \boldsymbol{R}}. \end{aligned} \tag{2.10}$$

For convenience, we abbreviate $\boldsymbol{F}(\Gamma_t)$ as $\boldsymbol{F}_t$. The equation of motion for the sphere is written as $\partial_t \boldsymbol{P}_t = \boldsymbol{F}_t$.

We assume that the system is initially in equilibrium at temperature T. Then, the initial probability density of Γ is given by

$$f_{\mathrm{eq}}(\Gamma) = \exp\left[-\frac{H(\Gamma) - \Psi_{\mathrm{eq}}}{k_{\mathrm{B}} T} \right], \tag{2.11}$$

where $\Psi_{\rm eq}$ is the normalization constant.

2.3 Kirkwood's formula

2.3.1 Derivation

To consider the relaxation of the momentum of the sphere, we apply an impulsive force $M\boldsymbol{V}\delta(t)$ to the sphere when the system is in equilibrium at temperature T. Then, the probability density just after $t = 0$ is represented by

$$f_0(\Gamma; \boldsymbol{V}) = \exp\left[-\frac{H(\Gamma) - \boldsymbol{P}\cdot\boldsymbol{V} - \Psi(\boldsymbol{V})}{k_{\rm B}T}\right], \tag{2.12}$$

where $\Psi(\boldsymbol{V})$ is the normalization constant and $f_0(\Gamma; \boldsymbol{0}) = f_{\rm eq}(\Gamma)$. Using (2.8) and (2.9), the probability density at time t is obtained as

$$\begin{aligned} f_t(\Gamma) &= f_0(\Gamma_{-t}; \boldsymbol{V}) \\ &= \exp\left[-\frac{H(\Gamma) - \boldsymbol{P}_{-t}\cdot\boldsymbol{V} - \Psi(\boldsymbol{V})}{k_{\rm B}T}\right]. \end{aligned} \tag{2.13}$$

In the following, the expectation values with respect to $f_0(\Gamma; \boldsymbol{V})$ and $f_t(\Gamma)$ are denoted by $\langle\,\cdot\,\rangle_0^{\boldsymbol{V}}$ and $\langle\,\cdot\,\rangle_t$, respectively. In particular, $\langle\,\cdot\,\rangle_0^{\boldsymbol{0}}$ corresponds to $\langle\,\cdot\,\rangle_{\rm eq}$.

We derive the exact formula for the friction coefficient for any $\boldsymbol{V}$. Using (2.13) and $\partial_t \boldsymbol{P}_{-t} = -\boldsymbol{F}_{-t}$, we obtain

$$\begin{aligned} f_t(\Gamma) &= f_0(\Gamma; \boldsymbol{V}) + \int_0^t ds\ \partial_s f_s(\Gamma) \\ &= f_0(\Gamma; \boldsymbol{V}) - \int_0^t ds\ f_s(\Gamma)\frac{\boldsymbol{F}_{-s}\cdot\boldsymbol{V}}{k_{\rm B}T}. \end{aligned} \tag{2.14}$$

In addition, because $\boldsymbol{F}$ is independent of the momenta, we obtain

$$\langle \boldsymbol{F}\rangle_0^{\boldsymbol{V}} = \langle \boldsymbol{F}\rangle_{\rm eq} = \boldsymbol{0}. \tag{2.15}$$

Then, (2.14) and (2.15) lead to

$$\begin{aligned} \langle F^a\rangle_t &= -\frac{1}{k_{\rm B}T}\int d\Gamma \int_0^t ds\ f_s(\Gamma) F^a F^b_{-s} V^b \\ &= -\frac{1}{k_{\rm B}T}\int_0^t ds \int d\Gamma_{-s}\ f_0(\Gamma_{-s}; \boldsymbol{V}) F^a F^b_{-s} V^b \\ &= -\gamma^{ab}_t(\boldsymbol{V}) V^b \end{aligned} \tag{2.16}$$

with

$$\gamma^{ab}_t(\boldsymbol{V}) \equiv \frac{1}{k_{\rm B}T}\int_0^t ds\ \left\langle F^a_s F^b\right\rangle_0^{\boldsymbol{V}}, \tag{2.17}$$

which is valid for any $\boldsymbol{V}$. Note that V^b is not equal to P_t^b/M in (2.16), and thus the time dependence of $\langle F^a \rangle_t$ is described by that of $\gamma_t^{ab}(\boldsymbol{V})$. Furthermore, in general, $\langle F^a \rangle_t$ is a nonlinear function of $\boldsymbol{V}$.

Next, we focus on the linear response regime. The dependence of γ_t^{ab} on $\boldsymbol{V}$ is neglected. Within this regime, we can rewrite (2.17) as

$$\gamma_t^{ab}(\boldsymbol{0}) = \gamma_t \delta^{ab} \tag{2.18}$$

with

$$\begin{aligned} \gamma_t &= \frac{1}{k_{\mathrm{B}}T} \int_0^t ds \ \langle F_s^z F^z \rangle_{\mathrm{eq}} \\ &= \frac{1}{3k_{\mathrm{B}}T} \int_0^t ds \ \langle F_s^a F^a \rangle_{\mathrm{eq}} , \end{aligned} \tag{2.19}$$

where we have employed the isotropic property of the system in equilibrium. The expression (2.19) is the linear response formula for the friction coefficient, first derived by Kirkwood [46].

2.3.2 Time dependence of the friction coefficient

We denote the correlation time of $\boldsymbol{F}_t$ and the relaxation time of $\boldsymbol{P}$ by τ_{micro} and τ_{macro}, respectively. We assume the separation of time scales represented by $\tau_{\mathrm{micro}} \ll \tau_{\mathrm{macro}}$. Here, (2.15) and $\langle \boldsymbol{P} \rangle_0^{\boldsymbol{V}} = M\boldsymbol{V}$ lead to

$$\begin{aligned} \left\langle P^a F^b \right\rangle_0^{\boldsymbol{V}} &= \int d\Gamma \ f_0(\Gamma; \boldsymbol{V}) \left(P^a - MV^a \right) F^b \\ &= 0. \end{aligned} \tag{2.20}$$

Using $\partial_t \boldsymbol{P}_t = \boldsymbol{F}_t$ and (2.20), we can rewrite (2.17) as

$$\begin{aligned} \gamma_t^{ab}(\boldsymbol{V}) &= \frac{1}{k_{\mathrm{B}}T} \left[\left\langle P_t^a F^b \right\rangle_0^{\boldsymbol{V}} - \left\langle P^a F^b \right\rangle_0^{\boldsymbol{V}} \right] \\ &= \frac{1}{k_{\mathrm{B}}T} \left\langle P_t^a F^b \right\rangle_0^{\boldsymbol{V}} . \end{aligned} \tag{2.21}$$

Thus, we find $\gamma_t^{ab}(\boldsymbol{V}) = 0$ for any $\boldsymbol{V}$ when $t \gg \tau_{\mathrm{macro}}$, because the correlation between P^a and F^b is considered to take about τ_{macro}. Furthermore, by considering (2.17), we obtain $\gamma_0^{ab}(\boldsymbol{V}) = 0$ for any $\boldsymbol{V}$. Keeping these two limiting cases in mind, we conjecture the following time dependence of $\gamma_t^{ab}(\boldsymbol{V})$. $\gamma_t^{ab}(\boldsymbol{V})$ increases when $0 < t \simeq \tau_{\mathrm{micro}}$. After that, $\gamma_t^{ab}(\boldsymbol{V})$ remains constant when $\tau_{\mathrm{micro}} \ll t \ll \tau_{\mathrm{macro}}$. Eventually, $\gamma_t^{ab}(\boldsymbol{V})$ gradually tends to zero when $t \simeq \tau_{\mathrm{macro}}$. By recalling (2.17), we can express this behavior as

$$\left\langle F_t^a F^b \right\rangle_0^{\boldsymbol{V}} \begin{cases} > 0, & \text{for } 0 < t \simeq \tau_{\mathrm{micro}}, \\ = 0, & \text{for } \tau_{\mathrm{micro}} \ll t \ll \tau_{\mathrm{macro}}, \\ < 0, & \text{for } \tau \simeq \tau_{\mathrm{macro}}. \end{cases} \tag{2.22}$$

In the linear response regime, we denote the constant value of γ_t during the time interval $\tau_{\mathrm{micro}} \ll t \ll \tau_{\mathrm{macro}}$ as γ. Using this particular value of γ, τ_{macro} can be expressed as M/γ. This γ is the linear friction coefficient.

2.3.3 Other expressions

We hereafter focus on the equilibrium case in which Γ is chosen according to the canonical ensemble $f_{\mathrm{eq}}(\Gamma)$, and consider a finite time interval $[0, \tau]$ that satisfies $\tau_{\mathrm{micro}} \ll \tau \ll \tau_{\mathrm{macro}}$. Because the motion of the sphere can be ignored up to τ, we assume that the center of the sphere is fixed at the origin. Throughout this chapter, for any physical quantity $A(\Gamma)$, we define the time-averaged quantity by

$$\bar{A}(\Gamma) \equiv \frac{1}{\tau} \int_0^\tau dt\ A(\Gamma_t). \tag{2.23}$$

Then, we can rewrite (2.19) as

$$\gamma = \frac{\tau}{2k_{\mathrm{B}}T} \left\langle \left(\bar{F}^z\right)^2 \right\rangle_{\mathrm{eq}}. \tag{2.24}$$

In this derivation, it should be noted that $\langle F_t^z F_s^z \rangle_{\mathrm{eq}}$ is a function of $|t-s|$, and that $\langle F_t^z F^z \rangle_{\mathrm{eq}} = 0$ when $\tau_{\mathrm{micro}} \ll t \ll \tau_{\mathrm{macro}}$.

We can also express the force F_t^a by the surface integration of a stress $\sigma_{\mathrm{sp}}^{ab}$:

$$F^a(\Gamma) = \mathcal{R}^2 \int d\Omega\ n^b \sigma_{\mathrm{sp}}^{ab}(\mathcal{R}, \Omega; \Gamma), \tag{2.25}$$

where Ω is a solid angle and $\boldsymbol{n} \equiv (\sin\theta\cos\varphi, \sin\theta\sin\varphi, \cos\theta)$. By direct calculation, we find

$$\sigma_{\mathrm{sp}}^{ab}(\boldsymbol{r}; \Gamma) = -\sum_{i=1}^{N} \left[-\frac{\partial \Phi_{\mathrm{sp}}(|\boldsymbol{r}_i - \boldsymbol{R}|)}{\partial R^a} \right] \left(R^b - r_i^b\right) D(\boldsymbol{r}; \boldsymbol{r}_i, \boldsymbol{R}) \tag{2.26}$$

with

$$D(\boldsymbol{r}; \boldsymbol{r}_i, \boldsymbol{R}) = \int_0^1 d\xi\ \delta\left(\boldsymbol{r} - \boldsymbol{r}_i - (\boldsymbol{R} - \boldsymbol{r}_i)\xi\right). \tag{2.27}$$

Indeed, by substituting (2.26) into (2.25), we obtain (2.10), where we have used the divergence theorem and

$$(R^b - r_i^b)\partial^b D(\boldsymbol{r}; \boldsymbol{r}_i, \boldsymbol{R}) = \delta(\boldsymbol{r} - \boldsymbol{r}_i) - \delta(\boldsymbol{r} - \boldsymbol{R}). \tag{2.28}$$

Furthermore, the stress tensor can be defined in spherical coordinates by

$$\begin{bmatrix} \sigma_{\mathrm{sp}}^{xx} & \sigma_{\mathrm{sp}}^{xy} & \sigma_{\mathrm{sp}}^{xz} \\ \sigma_{\mathrm{sp}}^{yx} & \sigma_{\mathrm{sp}}^{yy} & \sigma_{\mathrm{sp}}^{yz} \\ \sigma_{\mathrm{sp}}^{zx} & \sigma_{\mathrm{sp}}^{zy} & \sigma_{\mathrm{sp}}^{zz} \end{bmatrix} = Q \begin{bmatrix} \sigma_{\mathrm{sp}}^{rr} & \sigma_{\mathrm{sp}}^{r\theta} & \sigma_{\mathrm{sp}}^{r\varphi} \\ \sigma_{\mathrm{sp}}^{\theta r} & \sigma_{\mathrm{sp}}^{\theta\theta} & \sigma_{\mathrm{sp}}^{\theta\varphi} \\ \sigma_{\mathrm{sp}}^{\varphi r} & \sigma_{\mathrm{sp}}^{\varphi\theta} & \sigma_{\mathrm{sp}}^{\varphi\varphi} \end{bmatrix} Q^{\mathrm{T}} \tag{2.29}$$

with

$$Q = \begin{bmatrix} \sin\theta\cos\varphi & \cos\theta\cos\varphi & -\sin\varphi \\ \sin\theta\sin\varphi & \cos\theta\sin\varphi & \cos\varphi \\ \cos\theta & -\sin\theta & 0 \end{bmatrix}, \tag{2.30}$$

where Q^{T} denotes the transpose of Q. We then obtain

$$F^z(\Gamma) = \mathcal{R}^2 \int d\Omega \ \left[\cos\theta\ \sigma_{\mathrm{sp}}^{rr}(\mathcal{R},\Omega;\Gamma) - \sin\theta\ \sigma_{\mathrm{sp}}^{\theta r}(\mathcal{R},\Omega;\Gamma)\right]. \tag{2.31}$$

Here, it is convenient to define the stress $\sigma_*(\Gamma)$ that represents the z-component of the force per unit area on the surface of the sphere. From (2.31) and $F^z(\Gamma) = 4\pi\mathcal{R}^2\sigma_*(\Gamma)$, we have

$$\sigma_*(\Gamma) = \frac{1}{4\pi}\int d\Omega \ \left[\cos\theta\ \sigma_{\mathrm{sp}}^{rr}(\mathcal{R},\Omega;\Gamma) - \sin\theta\ \sigma_{\mathrm{sp}}^{\theta r}(\mathcal{R},\Omega;\Gamma)\right]. \tag{2.32}$$

The formula (2.24) is rewritten as

$$\gamma = \frac{(4\pi\mathcal{R}^2)^2\tau}{2k_{\mathrm{B}}T}\left\langle(\bar{\sigma}_*)^2\right\rangle_{\mathrm{eq}}. \tag{2.33}$$

The linear friction coefficient is expressed in terms of the correlation of the time-averaged stress at the surface, $\bar{\sigma}_*$.

2.4 Stress fluctuations in equilibrium viscous fluids

Our goal is to derive Stokes' law (2.3) from Kirkwood's formula (2.33) without explicitly employing the Stokes equations that are a linearized form of the Navier–Stokes equations in the low Reynolds number limit. Stokes' law (2.3) contains the viscosity of the fluid η. Instead of introducing η as a parameter of the Stokes equations, we define η from the stress fluctuations in the bulk of the fluid by the Green–Kubo formula (2.4). Thus, to derive Stokes' law, we must relate the bulk stress correlation to the surface stress correlation. In this section, we derive the probability density of coarse-grained time-averaged stress fluctuations in equilibrium viscous fluids.

2.4.1 The Green–Kubo formula

We first consider the microscopic expression of the stress $\sigma^{ab}(\boldsymbol{r};\Gamma)$ in the bulk of the equilibrium fluid. For the momentum density of the bath particles

$$\Pi^a(\boldsymbol{r};\Gamma) \equiv \sum_{i=1}^{N} p_i^a \delta(\boldsymbol{r} - \boldsymbol{r}_i), \tag{2.34}$$

$\sigma^{ab}(\boldsymbol{r};\Gamma)$ is defined to satisfy the following continuity equation:

$$\partial_t \Pi^a(\boldsymbol{r};\Gamma_t) = \partial^b\left[\sigma^{ab}(\boldsymbol{r};\Gamma_t) + \sigma_{\mathrm{sp}}^{ab}(\boldsymbol{r};\Gamma_t)\right]. \tag{2.35}$$

Note that the stress $\sigma^{ab}(\boldsymbol{r};\Gamma)$ corresponds to the force per unit area $\sigma^{ab}(\boldsymbol{r};\Gamma)n^b$ exerted on a virtual surface described by the unit vector n^b from the outer side, where the unit vector is perpendicular to the surface and directed toward the outer region. $\sigma^{ab}_{\rm sp}$ was given in (2.26). Here, $\sigma^{ab}(\boldsymbol{r};\Gamma)$ is calculated as

$$\begin{aligned}\sigma^{ab}(\boldsymbol{r};\Gamma) = &-\sum_{i=1}^{N}\frac{p_i^a p_i^b}{m}\delta\left(\boldsymbol{r}-\boldsymbol{r}_i\right)\\ &-\sum_{i<j}\left[-\frac{\partial\Phi_{\rm int}(|\boldsymbol{r}_i-\boldsymbol{r}_j|)}{\partial|\boldsymbol{r}_i-\boldsymbol{r}_j|}\right]\frac{\left(r_i^a-r_j^a\right)\left(r_i^b-r_j^b\right)}{|\boldsymbol{r}_i-\boldsymbol{r}_j|}D(\boldsymbol{r};\boldsymbol{r}_i,\boldsymbol{r}_j).\end{aligned} \tag{2.36}$$

It can be directly confirmed that

$$\sigma^{ab}(\boldsymbol{r};\Gamma) = \sigma^{ba}(\boldsymbol{r};\Gamma). \tag{2.37}$$

Note that, when there are interactions between bath particles across the periodic boundary, the right-hand side of (2.36) must be modified to take a non-zero value on the shortest line connecting two interacting bath particles.

By employing the microscopic expression of the stress, the Green–Kubo formula (2.4) is precisely expressed as

$$\eta = \frac{1}{k_{\rm B}T}\int_0^\tau dt\int d^3\boldsymbol{r}\,\langle\sigma^{xy}(\boldsymbol{r}_0;\Gamma)\sigma^{xy}(\boldsymbol{r};\Gamma_t)\rangle_{\rm eq}\,, \tag{2.38}$$

where τ is chosen such that $\tau^{\rm fluid}_{\rm micro} \ll \tau \ll \tau^{\rm fluid}_{\rm macro}$. $\tau^{\rm fluid}_{\rm micro}$ is the correlation time of σ^{xy}, and $\tau^{\rm fluid}_{\rm macro}$ is the relaxation time of $\mathbf{\Pi}$. In general, this τ is different from that in Kirkwood's formula (2.33). Here, we assume that the same value of τ can be chosen in the two formulas, and use the same notation. One may notice the long-time tail of the stress correlation, which apparently breaks the separation of time scales. We assume that this long-time tail only appears in the regime $t \gtrsim \tau$, because it originates from long wavelength fluctuations of locally conserved quantities. Therefore, we continue the argument without considering the long-time tail problem.

2.4.2 Macroscopic fluctuation theory

Let $\xi_{\rm micro}$ be the largest length scale appearing in the molecular description, and $\xi_{\rm macro}$ be the minimum length characterizing macroscopic behavior. In the case of viscous liquids, $\xi_{\rm micro}$ may be estimated as $r_{\rm bp}$, and $\xi_{\rm macro}$ is given by $\mathcal{R}$. Because $\xi_{\rm micro} \ll \xi_{\rm macro}$, we can choose Λ to satisfy $\xi_{\rm micro} \ll \Lambda \ll \xi_{\rm macro}$. We then define the coarse-grained time-averaged stresses by

$$\hat{\sigma}^{ab}(\boldsymbol{r}) = \frac{1}{\Lambda^3}\int_{\mathcal{V}(\boldsymbol{r})} d^3\boldsymbol{r}'\;\bar{\sigma}^{ab}(\boldsymbol{r}') \tag{2.39}$$

with $\mathcal{V}(\boldsymbol{r}) \equiv \prod_a [r^a - \Lambda/2, r^a + \Lambda/2]$. In terms of $\hat{\sigma}^{ab}(\boldsymbol{r})$, the Green–Kubo formula (2.38) is expressed as

$$\eta = \frac{\tau \Lambda^3}{2k_{\mathrm{B}}T} \left\langle (\hat{\sigma}^{xy}(\boldsymbol{r}))^2 \right\rangle_{\mathrm{eq}}. \tag{2.40}$$

We also note that

$$\frac{\tau \Lambda^3}{2k_{\mathrm{B}}T} \left\langle \hat{\sigma}^{xy}(\boldsymbol{r}) \hat{\sigma}^{xy}(\boldsymbol{r}') \right\rangle_{\mathrm{eq}} \simeq 0 \tag{2.41}$$

for $|\boldsymbol{r} - \boldsymbol{r}'| \geq \Lambda$, because the correlation length of the stress field is on the order of ξ_{micro}. The relations (2.40) and (2.41) can be summarized as

$$\left\langle \hat{\sigma}^{xy}(\boldsymbol{r}) \hat{\sigma}^{xy}(\boldsymbol{r}') \right\rangle_{\mathrm{eq}} = \frac{2k_{\mathrm{B}}T\eta}{\tau \Lambda^3} \mathcal{S}(|\boldsymbol{r} - \boldsymbol{r}'|), \tag{2.42}$$

where $\mathcal{S}(d) = 1$ for $d \ll \Lambda$ and $\mathcal{S}(d) \simeq 0$ for $d \geq \Lambda$.

We now formulate a macroscopic fluctuation theory for the coarse-grained time-averaged stresses $\hat{\sigma}^{ab}$. Because $\hat{\sigma}^{ab}(\boldsymbol{r})$ are obtained by integrating the microscopic stress over the region $\mathcal{V}(\boldsymbol{r})$, it is reasonable, by considering the central limit theorem, to expect these $\hat{\sigma}^{ab}(\boldsymbol{r})$ to obey a Gaussian distribution. Here, we adapt the continuum description with the space mesh (ultraviolet cutoff) Λ. In this description, $\mathcal{S}(|\boldsymbol{r} - \boldsymbol{r}'|)/\Lambda^3 \to \delta(\boldsymbol{r} - \boldsymbol{r}')$, and thus (2.42) is rewritten as

$$\left\langle \hat{\sigma}^{xy}(\boldsymbol{r}) \hat{\sigma}^{xy}(\boldsymbol{r}') \right\rangle_{\mathrm{eq}} = \frac{2k_{\mathrm{B}}T\eta}{\tau} \delta(\boldsymbol{r} - \boldsymbol{r}'). \tag{2.43}$$

Next, we consider the statistical properties of the stresses. We start with the following decomposition of $\hat{\sigma}^{ab}$ into traceless and trace parts:

$$\hat{\sigma}^{ab}(\boldsymbol{r}) = -\hat{p}(\boldsymbol{r})\delta^{ab} + \hat{s}^{ab}(\boldsymbol{r}) \tag{2.44}$$

with

$$\hat{p}(\boldsymbol{r}) \equiv -\frac{\hat{\sigma}^{xx}(\boldsymbol{r}) + \hat{\sigma}^{yy}(\boldsymbol{r}) + \hat{\sigma}^{zz}(\boldsymbol{r})}{3}, \tag{2.45}$$

where $\hat{p}$ and $\hat{s}^{ab}$ are called the mean pressure and the stress deviator tensor, respectively. Because $\hat{s}^{ab}$ is traceless, we have

$$\hat{s}^{xx}(\boldsymbol{r}) + \hat{s}^{yy}(\boldsymbol{r}) + \hat{s}^{zz}(\boldsymbol{r}) = 0. \tag{2.46}$$

Using the isotropic property and the assumption that the correlation length of the stress fluctuations is much less than Λ, we can express

$$\left\langle \hat{s}^{ab}(\boldsymbol{r}) \hat{s}^{a'b'}(\boldsymbol{r}') \right\rangle_{\mathrm{eq}} = \left[B_1 \delta^{aa'} \delta^{bb'} + B_2 \delta^{ab'} \delta^{ba'} + B_3 \delta^{ab} \delta^{a'b'} \right] \delta(\boldsymbol{r} - \boldsymbol{r}'), \tag{2.47}$$

where the constants B_1, B_2, and B_3 are determined below. By recalling (2.37), we obtain $\hat{\sigma}^{ab}(\boldsymbol{r}) = \hat{\sigma}^{ba}(\boldsymbol{r})$, and then we find that

$$\left\langle \hat{s}^{xy}(\boldsymbol{r}) \hat{s}^{xy}(\boldsymbol{r}') \right\rangle_{\mathrm{eq}} = \left\langle \hat{s}^{yx}(\boldsymbol{r}) \hat{s}^{xy}(\boldsymbol{r}') \right\rangle_{\mathrm{eq}}, \tag{2.48}$$

which leads to $B_1 = B_2$. Using (2.46), we also have

$$\langle (\hat{s}^{xx}(\boldsymbol{r}) + \hat{s}^{yy}(\boldsymbol{r}) + \hat{s}^{zz}(\boldsymbol{r}))\,(\hat{s}^{xx}(\boldsymbol{r'}) + \hat{s}^{yy}(\boldsymbol{r'}) + \hat{s}^{zz}(\boldsymbol{r'}))\rangle_{\mathrm{eq}} = 0, \tag{2.49}$$

which gives $B_3 = -2B_1/3$. Finally, the Green–Kubo formula (2.43) leads to

$$B_1 = \frac{2k_{\mathrm{B}}T\eta}{\tau}. \tag{2.50}$$

We summarize these relations as

$$\left\langle \hat{s}^{ab}(\boldsymbol{r})\hat{s}^{a'b'}(\boldsymbol{r'}) \right\rangle_{\mathrm{eq}} = \frac{2k_{\mathrm{B}}T\eta}{\tau}\Delta^{aba'b'}\delta(\boldsymbol{r} - \boldsymbol{r'}) \tag{2.51}$$

with

$$\Delta^{aba'b'} = \delta^{aa'}\delta^{bb'} + \delta^{ab'}\delta^{ba'} - \frac{2}{3}\delta^{ab}\delta^{a'b'}. \tag{2.52}$$

Condition (2.51) is necessary, but the statistical distribution of $\hat{\sigma}^{ab}$ is not completely determined. The problem is to derive the statistical property of $\hat{p}$. Because we are studying incompressible fluids, the pressure fluctuation arising from the density fluctuations need not be taken into account. Rather, we assume that $\hat{p}$ is determined from the balance of time-averaged forces in each region, which is expressed as $\partial^b\hat{\sigma}^{ab}(\boldsymbol{r}) = 0$. We express this in coordinate-free form as

$$\nabla \cdot \overleftrightarrow{\hat{\boldsymbol{\sigma}}}(\boldsymbol{r}) = \boldsymbol{0}. \tag{2.53}$$

It is obvious that the expectation values of the stresses satisfy the balance condition in the equilibrium cases. However, assumption (2.53) means that fluctuating stresses are already balanced in the macroscopic fluctuation theory.

2.4.3 Probability density of stresses

For later convenience, we express $\Delta^{aba'b'} = \Delta^{ij}$ with $g(ab) = i$ and $g(a'b') = j$, where $g(xx) = 1$, $g(yy) = 2$, $g(zz) = 3$, $g(xy) = g(yx) = 4$, $g(yz) = g(zy) = 5$, and $g(zx) = g(xz) = 6$. That is, Δ is interpreted as a 6×6 matrix. (We use the same symbol Δ without confusion.) Explicitly, the matrix Δ is expressed as

$$\Delta = \begin{bmatrix} 4/3 & -2/3 & -2/3 & 0 & 0 & 0 \\ -2/3 & 4/3 & -2/3 & 0 & 0 & 0 \\ -2/3 & -2/3 & 4/3 & 0 & 0 & 0 \\ 0 & 0 & 0 & 1 & 0 & 0 \\ 0 & 0 & 0 & 0 & 1 & 0 \\ 0 & 0 & 0 & 0 & 0 & 1 \end{bmatrix}. \tag{2.54}$$

As the probability density of $\hat{s}^{ab}$ is expressed using the inverse of Δ, we calculate the kth eigenvalue ϵ_k and corresponding eigenvector ϕ_k^j defined by

$$\sum_{j=1}^{6} \Delta^{ij}\phi_k^j = \epsilon_k\phi_k^i. \tag{2.55}$$

We find that

$$\epsilon_k = \begin{cases} 0 & \text{for } k = 1 \\ 2 & \text{for } k = 2, 3 \\ 1 & \text{for } k = 4, 5, 6 \end{cases} . \tag{2.56}$$

The zero-eigenvector is calculated as $\phi_1^j = 1/\sqrt{3}$ for $j = 1, 2, 3$ and $\phi_1^j = 0$ for $j = 4, 5, 6$. Although the matrix Δ is singular, we can define the pseudo-inverse of Δ as

$$\sum_{j=1}^{6} (\Delta^{-1})^{ij} \phi_1^j = 0, \tag{2.57}$$

and

$$\sum_{j=1}^{6} (\Delta^{-1})^{ij} \phi_k^j = \epsilon_k^{-1} \phi_k^i \tag{2.58}$$

for $k \geq 2$. A straightforward calculation yields

$$\Delta^{-1} = \begin{bmatrix} 1/3 & -1/6 & -1/6 & 0 & 0 & 0 \\ -1/6 & 1/3 & -1/6 & 0 & 0 & 0 \\ -1/6 & -1/6 & 1/3 & 0 & 0 & 0 \\ 0 & 0 & 0 & 1 & 0 & 0 \\ 0 & 0 & 0 & 0 & 1 & 0 \\ 0 & 0 & 0 & 0 & 0 & 1 \end{bmatrix} . \tag{2.59}$$

We identify $(\Delta^{-1})^{aba'b'}$ with $(\Delta^{-1})^{ij}$ by $i = g(ab)$ and $j = g(a'b')$.

Now, we write the probability density of $\{\hat{p}(\boldsymbol{r}), \hat{s}^{ab}(\boldsymbol{r})\}$ such that the statistical properties of the macroscopic stress fields $\{\hat{p}(\boldsymbol{r}), \hat{s}^{ab}(\boldsymbol{r})\}$ are reproduced. Because the macroscopic stress fields obey the Gaussian distribution on the restricted configuration space given by (2.46) and (2.53), the expression is

$$\begin{aligned} \mathcal{P}\left(\{\hat{p}(\boldsymbol{r}), \hat{s}^{ab}(\boldsymbol{r})\}\right) = C \exp\left[-\frac{\tau}{4k_{\mathrm{B}}T\eta} \int d^3\boldsymbol{r}\ \hat{s}^{ab}(\boldsymbol{r}) (\Delta^{-1})^{aba'b'} \hat{s}^{a'b'}(\boldsymbol{r}) \right] \\ \times \prod_{\boldsymbol{r}} \delta\Big(\hat{s}^{xx}(\boldsymbol{r}) + \hat{s}^{yy}(\boldsymbol{r}) + \hat{s}^{zz}(\boldsymbol{r}) \Big) \\ \times \prod_{\boldsymbol{r}} \prod_{a} \delta\Big(\partial^b \hat{s}^{ab}(\boldsymbol{r}) - \partial^a \hat{p}(\boldsymbol{r}) \Big). \end{aligned} \tag{2.60}$$

where C is the normalization constant.

Because the traceless condition (2.46) can be written as

$$\phi_1^{g(ab)} \hat{s}^{ab}(\boldsymbol{r}) = 0, \tag{2.61}$$

we find that $\hat{s}^{ab}(\Delta^{-1})^{aba'b'} \hat{s}^{a'b'}$ in (2.60) can be replaced by $\hat{s}^{ab}(\tilde{\Delta}^{-1})^{aba'b'} \hat{s}^{a'b'}$ with

$$(\tilde{\Delta}^{-1})^{ij} = (\Delta^{-1})^{ij} + \psi^i \phi_1^j + \psi^j \phi_1^i, \tag{2.62}$$

where ψ^i is an arbitrary vector. Explicitly, this is written as

$$\tilde{\Delta}^{-1} = \Delta^{-1} + \begin{bmatrix} 2q_1 & q_1+q_2 & q_1+q_3 & q_4 & q_5 & q_6 \\ q_1+q_2 & 2q_2 & q_2+q_3 & q_4 & q_5 & q_6 \\ q_1+q_3 & q_2+q_3 & 2q_3 & q_4 & q_5 & q_6 \\ q_4 & q_4 & q_4 & 0 & 0 & 0 \\ q_5 & q_5 & q_5 & 0 & 0 & 0 \\ q_6 & q_6 & q_6 & 0 & 0 & 0 \end{bmatrix}. \tag{2.63}$$

With the particular choices $q_1 = q_2 = 1/3$, $q_3 = -1/6$, and $q_4 = q_5 = q_6 = 0$, $\tilde{\Delta}^{-1}$ takes the simpler form:

$$\tilde{\Delta}^{-1} = \begin{bmatrix} 1 & 1/2 & 0 & 0 & 0 & 0 \\ 1/2 & 1 & 0 & 0 & 0 & 0 \\ 0 & 0 & 0 & 0 & 0 & 0 \\ 0 & 0 & 0 & 1 & 0 & 0 \\ 0 & 0 & 0 & 0 & 1 & 0 \\ 0 & 0 & 0 & 0 & 0 & 1 \end{bmatrix}. \tag{2.64}$$

Note that $\tilde{\Delta}^{-1}$ is the pseudo-inverse of $\tilde{\Delta}$ given by

$$\tilde{\Delta} = \begin{bmatrix} 4/3 & -2/3 & 0 & 0 & 0 & 0 \\ -2/3 & 4/3 & 0 & 0 & 0 & 0 \\ 0 & 0 & 0 & 0 & 0 & 0 \\ 0 & 0 & 0 & 1 & 0 & 0 \\ 0 & 0 & 0 & 0 & 1 & 0 \\ 0 & 0 & 0 & 0 & 0 & 1 \end{bmatrix}, \tag{2.65}$$

where $\tilde{\Delta}$ is obtained by setting the (zz) column and the (zz) row to zero in the matrix Δ .

The transformation of variables from $\hat{s}^{ab}$ to $\hat{\sigma}^{ab}$ yields

$$\begin{aligned} \mathcal{P}\left(\{\hat{p}(\boldsymbol{r}), \hat{\sigma}^{ab}(\boldsymbol{r})\}\right) &= C' \exp\left[-\tau \mathcal{I}\left(\{\hat{p}(\boldsymbol{r}), \hat{\sigma}^{ab}(\boldsymbol{r})\}\right)\right] \\ &\quad \times \prod_{\boldsymbol{r}} \delta\Big(\hat{\sigma}^{xx}(\boldsymbol{r}) + \hat{\sigma}^{yy}(\boldsymbol{r}) + \hat{\sigma}^{zz}(\boldsymbol{r}) + 3\hat{p}(\boldsymbol{r})\Big) \delta\Big(\nabla \cdot \overleftrightarrow{\hat{\boldsymbol{\sigma}}}(\boldsymbol{r})\Big) \end{aligned} \tag{2.66}$$

with

$$\begin{aligned} &\mathcal{I}\left(\{\hat{p}(\boldsymbol{r}), \hat{\sigma}^{ab}(\boldsymbol{r})\}\right) \\ &\quad = \frac{1}{4k_{\mathrm{B}}T\eta} \int d^3\boldsymbol{r} \ \left(\hat{\sigma}^{ab}(\boldsymbol{r}) + \hat{p}(\boldsymbol{r})\delta^{ab}\right) (\tilde{\Delta}^{-1})^{aba'b'} \left(\hat{\sigma}^{a'b'}(\boldsymbol{r}) + \hat{p}(\boldsymbol{r})\delta^{a'b'}\right), \end{aligned} \tag{2.67}$$

where C' is the normalization constant. Because $\tau \gg \tau_{\mathrm{micro}}$, $\mathcal{I}(\{\hat{p}(\boldsymbol{r}), \hat{\sigma}^{ab}(\boldsymbol{r})\})$ corresponds to a large deviation function in probability theory [60, 61].

Finally, we consider the stress tensor in spherical coordinates. This is denoted by $\hat{\sigma}^{\alpha\beta}$, where α and β represent r, θ, or φ. With a similar method, we obtain

$$\mathcal{P}\left(\{\hat{p}(\boldsymbol{r}),\hat{\sigma}^{\alpha\beta}(\boldsymbol{r})\}\right) = C''\exp\left[-\tau\mathcal{I}\left(\{\hat{p}(\boldsymbol{r}),\hat{\sigma}^{\alpha\beta}(\boldsymbol{r})\}\right)\right] \times\prod_{\boldsymbol{r}}\delta\Big(\hat{\sigma}^{rr}(\boldsymbol{r})+\hat{\sigma}^{\theta\theta}(\boldsymbol{r})+\hat{\sigma}^{\varphi\varphi}(\boldsymbol{r})+3\hat{p}(\boldsymbol{r})\Big)\delta\Big(\nabla\cdot\overleftrightarrow{\hat{\boldsymbol{\sigma}}}(\boldsymbol{r})\Big) \tag{2.68}$$

with

$$\mathcal{I}\left(\{\hat{p}(\boldsymbol{r}),\hat{\sigma}^{\alpha\beta}(\boldsymbol{r})\right) = \frac{1}{4k_{\mathrm{B}}T\eta}\int_{\mathcal{R}}^{\infty}dr\int_0^{\pi}d\theta\int_0^{2\pi}d\varphi\, r^2\sin\theta \times\left(\hat{\sigma}^{\alpha\beta}(\boldsymbol{r})+\hat{p}(\boldsymbol{r})\delta^{\alpha\beta}\right)(\tilde{\Delta}^{-1})^{\alpha\beta\alpha'\beta'}\left(\hat{\sigma}^{\alpha'\beta'}(\boldsymbol{r})+\hat{p}(\boldsymbol{r})\delta^{\alpha'\beta'}\right), \tag{2.69}$$

where C'' is the normalization constant and we have taken the limit $L\to\infty$. $\tilde{\Delta}$ is obtained by setting the $(\varphi\varphi)$ column and the $(\varphi\varphi)$ row to zero in Δ . Note that the fourth-order isotropic tensor $\Delta^{aba'b'}$ takes the same form as in Cartesian coordinates.

Because $\mathcal{R}\gg r_{\mathrm{bp}}$ and the interaction potential between the sphere and a bath particle depends only on the distance between them, the momentum of the tangential direction at the surface of the sphere is conserved. This yields the boundary condition

$$\hat{\sigma}^{\theta r}(\mathcal{R},\Omega)=\hat{\sigma}^{\varphi r}(\mathcal{R},\Omega)=0. \tag{2.70}$$

2.5 Stress fluctuation at surface

Let us return to Kirkwood's formula (2.33). We want to calculate the friction constant γ from the fluctuation intensity of $\bar{\sigma}_*$. We first connect $\bar{\sigma}_*$ with $\hat{\sigma}^{\alpha\beta}$. By recalling that $\mathcal{R}\gg r_{\mathrm{bp}}$ and using (2.6) and (2.36), we obtain

$$\sigma^{ab}(\mathcal{R},\Omega;\Gamma)=0 \tag{2.71}$$

at the surface of the sphere. From (2.7) and (2.26), we obtain

$$\sigma^{ab}_{\mathrm{sp}}(\mathcal{R}+r_{\mathrm{bp}}+\xi_0,\Omega;\Gamma)=0. \tag{2.72}$$

The continuity of the total coarse-grained time-averaged stresses leads to

$$\hat{\sigma}^{ab}(\mathcal{R},\Omega)=\frac{1}{\Lambda^2}\int_{S(\mathcal{R},\Omega)}d\Omega'\;\bar{\sigma}^{ab}_{\mathrm{sp}}(\mathcal{R},\Omega'), \tag{2.73}$$

where $S(\mathcal{R},\Omega)$ is the region on the surface of the sphere represented by

$$\left[\theta-\frac{\Lambda}{2\mathcal{R}},\theta+\frac{\Lambda}{2\mathcal{R}}\right]\times\left[\varphi-\frac{\Lambda}{2\mathcal{R}\sin\theta},\varphi+\frac{\Lambda}{2\mathcal{R}\sin\theta}\right]. \tag{2.74}$$

Therefore, from (2.32) and (2.73), we find that $\bar{\sigma}_*$ in (2.33) is connected to $\hat{\sigma}^{\alpha\beta}$ by the relation

$$\bar{\sigma}_* = \frac{1}{4\pi}\int d\Omega\ \left[\cos\theta\ \hat{\sigma}^{rr}(\mathcal{R},\Omega) - \sin\theta\ \hat{\sigma}^{r\theta}(\mathcal{R},\Omega)\right]. \tag{2.75}$$

The probability density of $\bar{\sigma}_*$ is determined from the statistical properties of $\hat{\sigma}^{\alpha\beta}$ in the bulk under conditions (2.70) and (2.75). This relation is formally written as

$$P(\bar{\sigma}_*) = \int_{\bar{\sigma}_*:\mathrm{fix}} \mathcal{D}\hat{p}\mathcal{D}\hat{\sigma}^{\alpha\beta}\ \mathcal{P}\left(\{\hat{p}(\boldsymbol{r}),\hat{\sigma}^{\alpha\beta}(\boldsymbol{r})\}\right), \tag{2.76}$$

where "$\bar{\sigma}_*$:fix" in the integral represents the condition given in (2.75).

2.5.1 Saddle-point method

We now evaluate the right-hand side of (2.76). In the asymptotic regime $\tau \gg \tau_{\mathrm{micro}}$, the functional integral may be accurately evaluated by the saddle-point method. By introducing the Lagrange multiplier field $\boldsymbol{\lambda}(\boldsymbol{r}) = (\lambda^r(\boldsymbol{r}),\lambda^\theta(\boldsymbol{r}),\lambda^\varphi(\boldsymbol{r}))$ to take constraint (2.53) into account, we obtain

$$P(\bar{\sigma}_*) = C'''\exp\left[-\tau I(\bar{\sigma}_*)\right] \tag{2.77}$$

with

$$I(\bar{\sigma}_*) = \min_{\substack{\{\hat{\sigma}^{\alpha\beta}(\boldsymbol{r})\}\\ \bar{\sigma}_*:\mathrm{fix}}} \frac{1}{4k_{\mathrm{B}}T\eta}\int_{\mathcal{R}}^{\infty} dr\int_0^{\pi} d\theta\int_0^{2\pi} d\varphi\ \mathcal{L}\left(\{\hat{\sigma}^{\alpha\beta}(\boldsymbol{r})\}\right), \tag{2.78}$$

and

$$\mathcal{L}\left(\{\hat{\sigma}^{\alpha\beta}(\boldsymbol{r})\}\right) = r^2\sin\theta\left[\hat{s}^{\alpha\beta}(\boldsymbol{r})(\tilde{\Delta}^{-1})^{\alpha\beta\alpha'\beta'}\hat{s}^{\alpha'\beta'}(\boldsymbol{r}) + \boldsymbol{\lambda}(\boldsymbol{r})\cdot\left(\nabla\cdot\overleftrightarrow{\hat{\boldsymbol{\sigma}}}(\boldsymbol{r})\right)\right], \tag{2.79}$$

where C''' is the normalization constant, and $\hat{s}^{\alpha\beta}(\boldsymbol{r}) = \hat{\sigma}^{\alpha\beta}(\boldsymbol{r}) + \hat{p}(\boldsymbol{r})\delta^{\alpha\beta}$ with $\hat{p}(\boldsymbol{r}) = -(\hat{\sigma}^{rr}(\boldsymbol{r}) + \hat{\sigma}^{\theta\theta}(\boldsymbol{r}) + \hat{\sigma}^{\varphi\varphi}(\boldsymbol{r}))/3$. Note that the saddle-point method for the large deviation function has been rigorously verified under certain conditions. This is called the contraction principle [61] in probability theory. In Appendix 2.A, we present a derivation of the probability density of $\bar{\sigma}_*$ within the framework of fluctuating hydrodynamics.

As a reference for the argument below, we explicitly write $\nabla\cdot\overleftrightarrow{\hat{\boldsymbol{\sigma}}}$ and $\hat{s}^{\alpha\beta}(\tilde{\Delta}^{-1})^{\alpha\beta\alpha'\beta'}\hat{s}^{\alpha'\beta'}$ as

$$\nabla\cdot\overleftrightarrow{\hat{\boldsymbol{\sigma}}} = \begin{pmatrix} \frac{\partial\hat{\sigma}^{rr}}{\partial r} + \frac{1}{r}\frac{\partial\hat{\sigma}^{r\theta}}{\partial\theta} + \frac{1}{r\sin\theta}\frac{\partial\hat{\sigma}^{\varphi r}}{\partial\varphi} + \frac{2\hat{\sigma}^{rr}-\hat{\sigma}^{\theta\theta}-\hat{\sigma}^{\varphi\varphi}}{r} + \frac{\hat{\sigma}^{r\theta}}{r\tan\theta} \\ \frac{\partial\hat{\sigma}^{r\theta}}{\partial r} + \frac{1}{r}\frac{\partial\hat{\sigma}^{\theta\theta}}{\partial\theta} + \frac{1}{r\sin\theta}\frac{\partial\hat{\sigma}^{\theta\varphi}}{\partial\varphi} + \frac{\hat{\sigma}^{\theta\theta}-\hat{\sigma}^{\varphi\varphi}}{r\tan\theta} + \frac{3\hat{\sigma}^{r\theta}}{r} \\ \frac{\partial\hat{\sigma}^{\varphi r}}{\partial r} + \frac{1}{r}\frac{\partial\hat{\sigma}^{\theta\varphi}}{\partial\theta} + \frac{1}{r\sin\theta}\frac{\partial\hat{\sigma}^{\varphi\varphi}}{\partial\varphi} + \frac{2\hat{\sigma}^{\theta\varphi}}{r\tan\theta} + \frac{3\hat{\sigma}^{\varphi r}}{r} \end{pmatrix}, \tag{2.80}$$

and

$$\begin{aligned}\hat{s}^{\alpha\beta}(\tilde{\Delta}^{-1})^{\alpha\beta\alpha'\beta'}\hat{s}^{\alpha'\beta'} &= (\hat{\sigma}^{rr}+\hat{p})^2+(\hat{\sigma}^{rr}+\hat{p})\left(\hat{\sigma}^{\theta\theta}+\hat{p}\right)+\left(\hat{\sigma}^{\theta\theta}+\bar{p}\right)^2 \\ &\quad +(\hat{\sigma}^{r\theta})^2+(\hat{\sigma}^{\theta\varphi})^2+(\hat{\sigma}^{\varphi r})^2 \\ &= \frac{(\hat{\sigma}^{rr})^2+(\hat{\sigma}^{\theta\theta})^2+(\hat{\sigma}^{\varphi\varphi})^2-\hat{\sigma}^{rr}\hat{\sigma}^{\theta\theta}-\hat{\sigma}^{\theta\theta}\hat{\sigma}^{\varphi\varphi}-\hat{\sigma}^{\varphi\varphi}\hat{\sigma}^{rr}}{3} \\ &\quad +(\hat{\sigma}^{r\theta})^2+(\hat{\sigma}^{\theta\varphi})^2+(\hat{\sigma}^{\varphi r})^2, \end{aligned} \tag{2.81}$$

respectively, where we have used (2.44), (2.45), and (2.64).

Next, we calculate the right-hand side of (2.78). We start with the variation

$$\begin{aligned}&\delta\int_{\mathcal{R}}^{\infty}dr\int_0^{\pi}d\theta\int_0^{2\pi}d\varphi\;\mathcal{L}\left(\{\hat{\sigma}^{\alpha\beta}(\boldsymbol{r})\}\right) \\ &\quad=\int_{\mathcal{R}}^{\infty}dr\int_0^{\pi}d\theta\int_0^{2\pi}d\varphi\;\left\{\partial^{\alpha'}\left[\frac{\partial\mathcal{L}}{\partial\left(\partial^{\alpha'}\hat{\sigma}^{\alpha\beta}\right)}\delta\hat{\sigma}^{\alpha\beta}\right]\right. \\ &\qquad\left.+\left[\frac{\partial\mathcal{L}}{\partial\hat{\sigma}^{\alpha\beta}}-\partial^{\alpha'}\left(\frac{\partial\mathcal{L}}{\partial\left(\partial^{\alpha'}\hat{\sigma}^{\alpha\beta}\right)}\right)\right]\delta\hat{\sigma}^{\alpha\beta}+\frac{\partial\mathcal{L}}{\partial\lambda^{\alpha}}\delta\lambda^{\alpha}\right\}. \end{aligned} \tag{2.82}$$

The first term of the right-hand side corresponds to the surface contribution. We find that

$$\int_0^{2\pi}d\varphi\;\partial^{\varphi}\left[\frac{\partial\mathcal{L}}{\partial\left(\partial^{\varphi}\hat{\sigma}^{\alpha\beta}\right)}\delta\hat{\sigma}^{\alpha\beta}\right]=0 \tag{2.83}$$

because of the periodic boundary of φ, and

$$\int_0^{\pi}d\theta\;\partial^{\theta}\left[\frac{\partial\mathcal{L}}{\partial\left(\partial^{\theta}\hat{\sigma}^{\alpha\beta}\right)}\delta\hat{\sigma}^{\alpha\beta}\right]=0, \tag{2.84}$$

because

$$\frac{\partial\mathcal{L}}{\partial\left(\partial^{\theta}\hat{\sigma}^{\alpha\beta}\right)}=0 \tag{2.85}$$

at $\theta=0$ and π. Furthermore, as a result of (2.70), $\hat{\sigma}^{r\theta}$ and $\hat{\sigma}^{\varphi r}$ are fixed to zero at the surface. Then,

$$\delta\hat{\sigma}^{r\theta}=\delta\hat{\sigma}^{\varphi r}=0 \tag{2.86}$$

at $r=\mathcal{R}$. Thus, the first term of the right-hand side of (2.82) becomes

$$\int_{\mathcal{R}}^{\infty}dr\int_0^{\pi}d\theta\int_0^{2\pi}d\varphi\;\partial^{r}\left[\frac{\partial\mathcal{L}}{\partial\left(\partial^{r}\hat{\sigma}^{rr}\right)}\delta\hat{\sigma}^{rr}\right]. \tag{2.87}$$

Here, we impose

$$\left.\frac{\partial\mathcal{L}}{\partial\left(\partial^{r}\hat{\sigma}^{rr}\right)}\right|_{r=\mathcal{R}}=0 \tag{2.88}$$

as the boundary condition of the variational problem. This is called a natural boundary condition, and explicitly gives

$$\lambda^r(\mathcal{R}, \Omega) = 0. \tag{2.89}$$

With this setup, the surface contribution of the variation vanishes, and we obtain the Euler–Lagrange equations

$$\frac{\partial \mathcal{L}}{\partial \hat{\sigma}^{\alpha\beta}} - \partial^{\alpha'} \left(\frac{\partial \mathcal{L}}{\partial \left(\partial^{\alpha'} \hat{\sigma}^{\alpha\beta} \right)} \right) = 0. \tag{2.90}$$

Using (2.79), (2.80), and (2.81), we can write (2.90) as

$$\begin{cases} \hat{\sigma}^{rr} = -\hat{p} + \dfrac{\partial \lambda^r}{\partial r}, \\ \hat{\sigma}^{\theta\theta} = -\hat{p} + \left(\dfrac{1}{r} \dfrac{\partial \lambda^\theta}{\partial \theta} + \dfrac{\lambda^r}{r} \right), \\ \hat{\sigma}^{\varphi\varphi} = -\hat{p} + \left(\dfrac{1}{r \sin\theta} \dfrac{\partial \lambda^\varphi}{\partial \varphi} + \dfrac{\lambda^r}{r} + \dfrac{\lambda^\theta}{r \tan\theta} \right), \\ \hat{\sigma}^{r\theta} = \dfrac{1}{2} \left(\dfrac{1}{r} \dfrac{\partial \lambda^r}{\partial \theta} + \dfrac{\partial \lambda^\theta}{\partial r} - \dfrac{\lambda^\theta}{r} \right), \\ \hat{\sigma}^{\theta\varphi} = \dfrac{1}{2} \left(\dfrac{1}{r \sin\theta} \dfrac{\partial \lambda^\theta}{\partial \varphi} + \dfrac{1}{r} \dfrac{\partial \lambda^\varphi}{\partial \theta} - \dfrac{\lambda^\varphi}{r \tan\theta} \right), \\ \hat{\sigma}^{\varphi r} = \dfrac{1}{2} \left(\dfrac{1}{r \sin\theta} \dfrac{\partial \lambda^r}{\partial \varphi} + \dfrac{\partial \lambda^\varphi}{\partial r} - \dfrac{\lambda^\varphi}{r} \right). \end{cases} \tag{2.91}$$

Note that (2.45) is equivalent to

$$\nabla \cdot \boldsymbol{\lambda} = 0 \tag{2.92}$$

in the expression of (2.91). By solving (2.53), (2.91), and (2.92) with boundary conditions (2.70), (2.75), and (2.89), we obtain the probability density of $\bar{\sigma}_*$. The set of equations (2.53), (2.91), and (2.92) coincide with the Stokes equations

$$\eta \nabla^2 \boldsymbol{u} = \nabla \hat{p}, \tag{2.93}$$

$$\nabla \cdot \boldsymbol{u} = 0, \tag{2.94}$$

when we set $\boldsymbol{\lambda}(\boldsymbol{r}) = 2\eta \boldsymbol{u}(\boldsymbol{r})$. We may interpret $\boldsymbol{u}(\boldsymbol{r})$ as the macroscopic fluctuating velocity of the fluid generated by $\bar{\sigma}_*$.

By referring to the solution of the Stokes equations, we obtain

$$\lambda^r(\boldsymbol{r}) = \left(1 - \frac{\mathcal{R}}{r}\right) 2\mathcal{R}\bar{\sigma}_* \cos\theta, \tag{2.95}$$

$$\lambda^\theta(\boldsymbol{r}) = -\left(1 - \frac{\mathcal{R}}{2r}\right) 2\mathcal{R}\bar{\sigma}_* \sin\theta, \tag{2.96}$$

$$\lambda^\varphi(\boldsymbol{r}) = 0, \tag{2.97}$$

$$\hat{p}(\boldsymbol{r}) = p_\infty - \frac{\mathcal{R}^2}{r^2}\bar{\sigma}_* \cos\theta, \tag{2.98}$$

where p_∞ is a constant. Then, (2.91) leads to

$$\hat{\sigma}^{rr}(\boldsymbol{r}) = -p_\infty + \frac{3\mathcal{R}^2\bar{\sigma}_* \cos\theta}{r^2}, \tag{2.99}$$

$$\hat{\sigma}^{\theta\theta}(\boldsymbol{r}) = \hat{\sigma}^{\varphi\varphi}(\boldsymbol{r}) = -p_\infty, \tag{2.100}$$

$$\hat{\sigma}^{r\theta}(\boldsymbol{r}) = \hat{\sigma}^{\theta\varphi}(\boldsymbol{r}) = \hat{\sigma}^{\varphi r}(\boldsymbol{r}) = 0. \tag{2.101}$$

Substituting these relations into (2.78), we obtain

$$\begin{aligned} I(\bar{\sigma}_*) &= \frac{1}{4k_\mathrm{B}T\eta} \int_{\mathcal{R}}^{\infty} dr\ r^2 \int d\Omega\ 3 \left(\frac{\mathcal{R}^2\bar{\sigma}_* \cos\theta}{r^2}\right)^2 \\ &= \frac{(\bar{\sigma}_*)^2}{2} \frac{2\pi\mathcal{R}^3}{k_\mathrm{B}T\eta}. \end{aligned} \tag{2.102}$$

This immediately yields

$$\left\langle (\bar{\sigma}_*)^2 \right\rangle_{\mathrm{eq}} = \frac{k_\mathrm{B}T\eta}{2\pi\mathcal{R}^3\tau}. \tag{2.103}$$

Combining this with Kirkwood's formula (2.33), we arrive at Stokes' law

$$\gamma = \frac{(4\pi\mathcal{R}^2)^2\tau}{2k_\mathrm{B}T} \left\langle (\bar{\sigma}_*)^2 \right\rangle_{\mathrm{eq}} = 4\pi\eta\mathcal{R}. \tag{2.104}$$

2.5.2 Stokes' law for a macroscopic sphere with a rough surface

Because we have studied a macroscopic sphere with a smooth surface represented by a spherical symmetric interaction potential, the version of Stokes' law we have obtained corresponds to that with the slip boundary condition in hydrodynamics. Indeed, we used the boundary condition (2.70). In reality, the surface of a sphere is assumed to be rough. Although the precise microscopic description of such a surface is not simple, it should be claimed that the boundary conditions (2.70) are not imposed in the macroscopic fluctuation theory. In this case, the natural boundary conditions

$$\boldsymbol{\lambda}(\mathcal{R}, \Omega) = \boldsymbol{0} \tag{2.105}$$

are imposed, so that the Euler–Lagrange equation can be obtained.

By referring to the solution of the Stokes equations with these modified boundary conditions, we obtain

$$\lambda^r(\boldsymbol{r}) = \left(1 - \frac{3\mathcal{R}}{2r} + \frac{\mathcal{R}^3}{2r^3}\right)\frac{4\mathcal{R}\bar{\sigma}_* \cos\theta}{3}, \tag{2.106}$$

$$\lambda^\theta(\boldsymbol{r}) = -\left(1 - \frac{3\mathcal{R}}{4r} - \frac{\mathcal{R}^3}{4r^3}\right)\frac{4\mathcal{R}\bar{\sigma}_* \sin\theta}{3}, \tag{2.107}$$

$$\lambda^\varphi(\boldsymbol{r}) = 0, \tag{2.108}$$

$$\hat{p}(\boldsymbol{r}) = p'_\infty - \frac{\mathcal{R}^2}{r^2}\bar{\sigma}_* \cos\theta, \tag{2.109}$$

where p'_∞ is a constant. Then, (2.91) leads to

$$\hat{\sigma}^{rr}(\boldsymbol{r}) = -p'_\infty + \left(\frac{3\mathcal{R}^2}{r^2} - \frac{2\mathcal{R}^4}{r^4}\right)\bar{\sigma}_* \cos\theta, \tag{2.110}$$

$$\hat{\sigma}^{\theta\theta}(\boldsymbol{r}) = \hat{\sigma}^{\varphi\varphi}(\boldsymbol{r}) = -p'_\infty + \frac{\mathcal{R}^4}{r^4}\bar{\sigma}_* \cos\theta, \tag{2.111}$$

$$\hat{\sigma}^{r\theta}(\boldsymbol{r}) = -\frac{\mathcal{R}^4}{r^4}\bar{\sigma}_* \sin\theta, \tag{2.112}$$

$$\hat{\sigma}^{\theta\varphi}(\boldsymbol{r}) = \hat{\sigma}^{\varphi r}(\boldsymbol{r}) = 0. \tag{2.113}$$

Thus, we have that

$$\begin{aligned} I(\bar{\sigma}_*) &= \int_{\mathcal{R}}^{\infty} dr \int d\Omega\, \frac{r^2}{4k_{\mathrm{B}}T\eta}\left\{3\left[\left(\frac{\mathcal{R}^2}{r^2} - \frac{\mathcal{R}^4}{r^4}\right)\bar{\sigma}_* \cos\theta\right]^2 + \left[\frac{\mathcal{R}^4}{r^4}\bar{\sigma}_* \sin\theta\right]^2\right\} \\ &= (\bar{\sigma}_*)^2 \frac{2\pi}{4k_{\mathrm{B}}T\eta}\int_{\mathcal{R}}^{\infty} dr\, r^2\left(\frac{2\mathcal{R}^4}{r^4} - \frac{4\mathcal{R}^6}{r^6} + \frac{10\mathcal{R}^8}{3r^8}\right) \\ &= \frac{(\bar{\sigma}_*)^2}{2}\frac{4\pi\mathcal{R}^3}{3k_{\mathrm{B}}T\eta}, \end{aligned} \tag{2.114}$$

which leads to

$$\left\langle(\bar{\sigma}_*)^2\right\rangle_{\mathrm{eq}} = \frac{3k_{\mathrm{B}}T\eta}{4\pi\mathcal{R}^3\tau}. \tag{2.115}$$

The substitution of (2.115) into Kirkwood's formula (2.33) yields

$$\gamma = \frac{(4\pi\mathcal{R}^2)^2\tau}{2k_{\mathrm{B}}T}\left\langle(\bar{\sigma}_*)^2\right\rangle_{\mathrm{eq}} = 6\pi\eta\mathcal{R}. \tag{2.116}$$

This is Stokes' law for cases with the stick boundary condition in hydrodynamics.

2.6 Concluding Remarks

In this chapter, we have derived Stokes' law from Kirkwood's formula and the Green–Kubo formula in the linear-response regime where the Stokes equations are valid. In this derivation, we did not assume the Stokes equations to describe Stokes flow, but rather formulated the relation between the stress fluctuations in the bulk and the stress fluctuation at the surface with the aid of large deviation theory.

The heart of this derivation is the contraction principle, which is a standard technique in large deviation theory [61]. In the present case, we first used a phenomenological basis to apply the large deviation function to stress fluctuations in the bulk, and then applied the contraction principle. See [62] for another application of the contraction principle to the calculation of a large deviation function for time-averaged quantities. A similar argument has been employed to derive a generating function for the current fluctuation in stochastic non-equilibrium lattice gases [63]. Such a phenomenological argument is called the additivity principle, and the condition of its validity can be discussed within the framework of fluctuating hydrodynamics [64]. Similarly, our derivation can also be formulated within fluctuating hydrodynamics, as briefly explained in Appendix 2.A. Although there is no one-to-one correspondence between our argument and that in the additivity principle, there may be a universal concept behind these two arguments. Determining a theoretical framework that provides a microscopic understanding of the phenomenological arguments would be an interesting problem.

In this chapter, we studied the force from a viscous fluid. More complex cases can be discussed using a similar formulation. For example, a cross-over from the dilute case (2.2) to the viscous case (2.3), which has been observed in numerical experiments [54], may be one of our next targets. A simple but less trivial example may be a Brownian particle under a temperature gradient [65–68]. To elucidate the mechanism of the driving force and the friction force in this system, we must consider macroscopic fluctuation theory from microscopic mechanics, where the fluctuation of the energy flux should be taken into account [43]. Furthermore, the study of the force to a small system from an active environment is a hot topic in recent non-equilibrium statistical mechanics [69]. Examples of active environments include cytoskeleton networks (under chemical reaction) [70–73], granular materials [74–77], and the assembly of small biological elements [78–81]. The law of the force from an active environment may be given by a phenomenological description in accordance with experimental observations. However, the nature of the force is highly non-trivial. Thus, we believe that developing the theory by which the nature of the force from an active environment can be described would be a significant achievement.

Finally, let us return to the formula described in (2.78). This claims that the large deviation function on the surface is determined from the variational principle associated with the large deviation function in the bulk. Note that the large deviation function is called entropy, because the large deviation of the fluctuations of thermo-

dynamic variables is equal to the thermodynamic entropy. Here, one may recall the so-called bulk-boundary correspondence in quantum many-body systems [82–86]. For the moment, we do not have any evidence for a direct connection with such theories, but it may be interesting to imagine such a possibility.

2.A Fluctuating hydrodynamics

We describe a viscous incompressible fluid at low Reynolds number by the fluctuating hydrodynamic equations in spherical coordinates. We denote by $\boldsymbol{u}(\boldsymbol{r},t)$, $p(\boldsymbol{r},t)$, $\overleftrightarrow{\boldsymbol{\sigma}}(\boldsymbol{r},t)$, and $\overleftrightarrow{\boldsymbol{s}}(\boldsymbol{r},t)$ the velocity, pressure, stress tensor, and random stress tensor at position $\boldsymbol{r}$ and time t, respectively. In this case, each component of the stress tensor is written as

$$\sigma^{rr} = -p + 2\eta\frac{\partial u^r}{\partial r} + s^{rr}, \tag{2.117}$$

$$\sigma^{\theta\theta} = -p + 2\eta\left(\frac{1}{r}\frac{\partial u^\theta}{\partial\theta} + \frac{u^r}{r}\right) + s^{\theta\theta}, \tag{2.118}$$

$$\sigma^{\varphi\varphi} = -p + 2\eta\left(\frac{1}{r\sin\theta}\frac{\partial u^\varphi}{\partial\varphi} + \frac{u^r}{r} + \frac{u^\theta}{r\tan\theta}\right) + s^{\varphi\varphi}, \tag{2.119}$$

$$\sigma^{r\theta} = \eta\left(\frac{1}{r}\frac{\partial u^r}{\partial\theta} + \frac{\partial u^\theta}{\partial r} - \frac{u^\theta}{r}\right) + s^{r\theta}, \tag{2.120}$$

$$\sigma^{\theta\varphi} = \eta\left(\frac{1}{r\sin\theta}\frac{\partial u^\theta}{\partial\varphi} + \frac{1}{r}\frac{\partial u^\varphi}{\partial\theta} - \frac{u^\varphi}{r\tan\theta}\right) + s^{\theta\varphi}, \tag{2.121}$$

$$\sigma^{\varphi r} = \eta\left(\frac{1}{r\sin\theta}\frac{\partial u^r}{\partial\varphi} + \frac{\partial u^\varphi}{\partial r} - \frac{u^\varphi}{r}\right) + s^{\varphi r}. \tag{2.122}$$

We assume that the temperature T and density ρ of the fluid are constant and homogeneous. Because we are focusing on incompressible fluid, we assume that the bulk viscosity ζ is equal to zero and that $\nabla\cdot\boldsymbol{u} = 0$. This is written as

$$\frac{\partial u^r}{\partial r} + \frac{2u^r}{r} + \frac{1}{r}\frac{\partial u^\theta}{\partial\theta} + \frac{u^\theta}{r\tan\theta} + \frac{1}{r\sin\theta}\frac{\partial u^\varphi}{\partial\varphi} = 0. \tag{2.123}$$

Furthermore, the time evolution equation of $\boldsymbol{u}(\boldsymbol{r},t)$ is assumed to be given by

$$\rho\frac{\partial\boldsymbol{u}}{\partial t} = \nabla\cdot\overleftrightarrow{\boldsymbol{\sigma}}, \tag{2.124}$$

because the Reynolds number is sufficiently low. Finally, the random stresses are assumed to be zero-mean Gaussian white noises with covariance

$$\left\langle s^{\alpha\beta}(r,\Omega,t)s^{\alpha'\beta'}(r',\Omega',t')\right\rangle = 2k_{\mathrm{B}}T\eta\Delta^{\alpha\beta\alpha'\beta'}\frac{\delta(r-r')\delta(\Omega-\Omega')}{r^2}\delta(t-t'), \tag{2.125}$$

$$\Delta^{\alpha\beta\alpha'\beta'} = \delta^{\alpha\alpha'}\delta^{\beta\beta'} + \delta^{\alpha\beta'}\delta^{\beta\alpha'} - \frac{2}{3}\delta^{\alpha\beta}\delta^{\alpha'\beta'}. \tag{2.126}$$

where we have used $\zeta = 0$. Note that (2.125) leads to

$$s^{rr} + s^{\theta\theta} + s^{\varphi\varphi} = 0. \tag{2.127}$$

By recalling (2.117), (2.118), (2.119), and (2.123), we also have

$$\sigma^{rr} + \sigma^{\theta\theta} + \sigma^{\varphi\varphi} + 3p = 0. \tag{2.128}$$

For any time-dependent quantity $A(t)$, we denote its path during the time interval $[0, \tau]$ by $[A]$. Then, using (2.125) and the Gaussian property of $s^{\alpha\beta}$, we obtain the probability density of $\{[p], [\sigma^{\alpha\beta}], [u^\alpha]\}$ in the form

$$\begin{aligned}\mathcal{P}\left(\{[p], [\sigma^{\alpha\beta}], [u^\alpha]\}\right) = C_0 \exp\left[-\tau \mathcal{I}\left(\{[p], [\sigma^{\alpha\beta}], [u^\alpha]\}\right)\right] \\ \times \prod_t \prod_{\boldsymbol{r}} \delta\left(\rho \partial_t \boldsymbol{u} - \nabla \cdot \overleftrightarrow{\boldsymbol{\sigma}}\right) \\ \times \prod_t \prod_{\boldsymbol{r}} \delta\left(\nabla \cdot \boldsymbol{u}\right) \delta\left(\sigma^{rr} + \sigma^{\theta\theta} + \sigma^{\varphi\varphi} + 3p\right)\end{aligned} \tag{2.129}$$

with

$$\mathcal{I}\left(\{[p], [\sigma^{\alpha\beta}], [u^\alpha]\}\right) = \frac{1}{4 k_{\mathrm{B}} T \eta \tau} \int_0^\tau dt \int_{\mathcal{R}}^\infty dr\, r^2 \int d\Omega\, s^{\alpha\beta} (\tilde{\Delta}^{-1})^{\alpha\beta\alpha'\beta'} s^{\alpha'\beta'}, \tag{2.130}$$

where C_0 is the normalization constant and $s^{\alpha\beta}$ in the right-hand side is related to $(p, \sigma^{\alpha\beta}, u^\alpha)$ through (2.117)–(2.122). By applying the contraction principle to (2.129), we obtain the probability density of the surface stress fluctuations as

$$\begin{aligned}P(\bar{\sigma}_*) &= \int_{\bar{\sigma}_*:\mathrm{fix}} \mathcal{D}p \mathcal{D}\sigma^{\alpha\beta} \mathcal{D}u^\alpha\, \mathcal{P}\left(\{[p], [\sigma^{\alpha\beta}], [u^\alpha]\}\right) \\ &= C_0' \exp\left[-\tau I(\bar{\sigma}_*)\right]\end{aligned} \tag{2.131}$$

with

$$I(\bar{\sigma}_*) = \min_{\substack{\{[\sigma^{\alpha\beta}], [u^\alpha]\} \\ \bar{\sigma}_*:\mathrm{fix}}} \frac{1}{4 k_{\mathrm{B}} T \eta \tau} \int_0^\tau dt \int_{\mathcal{R}}^\infty dr \int_0^\pi d\theta \int_0^{2\pi} d\varphi\, \mathcal{L}\left(\{[\sigma^{\alpha\beta}], [u^\alpha]\}\right), \tag{2.132}$$

and

$$\begin{aligned}\mathcal{L}\left(\{[\sigma^{\alpha\beta}], [u^\alpha]\}\right) = r^2 \sin\theta \Big[s^{\alpha\beta} (\tilde{\Delta}^{-1})^{\alpha\beta\alpha'\beta'} s^{\alpha'\beta'} \\ + \boldsymbol{\lambda}_1 \cdot \left(\rho \partial_t \boldsymbol{u} - \nabla \cdot \overleftrightarrow{\boldsymbol{\sigma}}\right) + \lambda_2 \left(\nabla \cdot \boldsymbol{u}\right) \Big],\end{aligned} \tag{2.133}$$

where C_0' is the normalization constant, $\boldsymbol{\lambda}_1(\boldsymbol{r}, t)$ and $\lambda_2(\boldsymbol{r}, t)$ are the Lagrange multiplier fields, $p = -(\sigma^{rr} + \sigma^{\theta\theta} + \sigma^{\varphi\varphi})/3$, and "$\bar{\sigma}_*$:fix" represents the condition given in

$$\bar{\sigma}_* = \frac{1}{4\pi\tau} \int_0^\tau dt \int d\Omega\, \left[\cos\theta\, \sigma^{rr}(\mathcal{R}, \Omega, t) - \sin\theta\, \sigma^{r\theta}(\mathcal{R}, \Omega, t)\right]. \tag{2.134}$$

If a time-independent configuration with $\boldsymbol{u} = \boldsymbol{0}$ is the minimizer of (2.132), we obtain the same result as in (2.77)–(2.79).

Chapter 3

Non-equilibrium statistical mechanics for adiabatic piston problem

3.1 Introduction

One of the important problems in small systems is to provide an energetic interpretation of phenomena. In macroscopic systems, the thermodynamics is established with operationally identifying work as the energy transferred to a system accompanied with macroscopic volume change of the system caused by a macroscopic force and heat as the other energy transferred to the system through microscopic degrees of freedom. On the other hand, although we can consider the energy transferred to a small system, it is still unsolved in the small system how to decompose the transferred energy into work and heat so as to be consistent with the results of the thermodynamics. Sekimoto provided a reasonable definition of heat in Langevin systems [87, 88], while there are other stochastic systems where the energetics is still not fully understood.

In this chapter, we consider the energetics of the adiabatic piston problem [1,39–42]. We provide a model for the adiabatic piston problem by using a continuous-time Markov jump process. By correctly calculating the local detailed balance condition, we clarify that the entropy production depends on waiting times between jumps. Furthermore, we provide the definition of heat in our model, and then elucidate the energetics.

This chapter is organized as follows. In Sect. 3.2, we explain our model. In Sect. 3.3, we elucidate the energetics of our model on the basis of the local detailed balance condition. In Sect. 3.4, we derive several types of fluctuation theorems and the formal expression of the steady-state distribution. In Sect. 3.5, we first show the Onsager theory for the adiabatic piston problem, and after that we derive the linear response formula. We finally calculate one of the time-correlation functions explicitly, and derive the steady velocity of the wall up to order ϵ. The final section is devoted to a brief summary and remarks. In Appendix 3.A, we confirm the validity of our

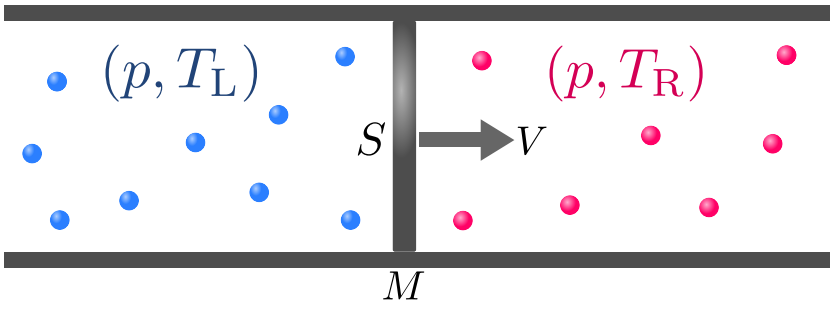

Fig. 3.1 Schematic illustration of our model. A wall of mass M with velocity V separates a infinitely long tube of cross-sectional area S into two regions, each of which is filled with rarefied gas particles of mass m. The gases in the left and right regions are initially prepared at equal pressure p but different temperatures T_{L} and T_{R}, respectively.

model on the basis of Hamiltonian systems. Throughout this chapter, β represents the inverse temperature and the Boltzmann constant k_{B} is set to unity. The subscripts or superscripts L and R represent quantities on the left and right side, respectively.

3.2 Model

3.2.1 Setup

We introduce a model for studying the adiabatic piston problem. A schematic illustration is shown in Fig. 3.1. First, we provide a mechanical description of the wall of mass M. We take the x-axis along the axial direction of an infinitely long tube of cross-sectional area S, and assume that the wall moves without friction along x-axis. We denote by V the velocity of the wall, which is the only degree of freedom of the wall. When discussing time evolution of V, we denote by $V(t)$ its value at time t, and by $\hat{V} = (V(t))_{t\in[0,\tau]}$ its path during the time interval $[0, \tau]$.

Next, we provide an effective description of rarefied gas particles of mass m. The gases in the left and right regions separated by the wall are initially prepared at equal pressure p but different temperatures T_{L} and T_{R}, respectively. In the following, we focus on the gas on the left side; the gas on the right side can be described similarly. We study a rarefied gas such that the characteristic time of the dissipation process inside each gas is much longer than the time during which we observe the steady state motion of the wall. Therefore, gas particles that have yet to collide with the wall are in equilibrium at the temperature T_{L}, the pressure p, and the number density $n_{\mathrm{L}} = p\beta_{\mathrm{L}}$. We also assume that the gas particles elastically and instantaneously collide with the wall only once. Furthermore, for simplicity, we assume that the surface of the wall is perpendicular to the x-axis, so that we consider only the x-component of the velocity of each gas particle.

For this setup, the interaction between the wall and the gas on the left side can

be described by random collisions with the collision rate $\lambda_{\rm L}(v,V)$ for the gas particle velocity v and the wall velocity V. The collision rate is explicitly written as

$$\lambda_{\rm L}(v,V) = n_{\rm L} S(v-V)\theta(v-V) f^{\rm L}_{\rm eq}(v), \tag{3.1}$$

where $f^{\rm L}_{\rm eq}(v) = \sqrt{\beta_{\rm L} m/2\pi}\exp(-\beta_{\rm L} m v^2/2)$ is the Maxwell–Boltzmann distribution and θ represents the Heaviside step function. Similarly, the collision rate of the gas on the right side is given by

$$\lambda_{\rm R}(v,V) = n_{\rm R} S(V-v)\theta(V-v) f^{\rm R}_{\rm eq}(v). \tag{3.2}$$

By these effective descriptions of the gases, our model becomes a continuous-time Markov jump process.

3.2.2 Time evolution equations

We explicitly write an equation of motion of the wall. When, due to collision, the velocities of a gas particle and the wall change from v to v' and from V to V', respectively, the laws of the conservation of energy and momentum are written as

$$v - V = -v' + V', \tag{3.3}$$

$$mv + MV = mv' + MV'. \tag{3.4}$$

Then, the impulse of the collision is given by

$$\begin{aligned} I(v,V) &= MV' - MV \\ &= \frac{2mM}{m+M}(v-V). \end{aligned} \tag{3.5}$$

The i-th collision time of a gas particle and the wall at the left side is determined according to the Poisson process with the rate function, $\int dv\, \lambda_{\rm L}(v,V)$. Suppose that a gas particle in the left side with a velocity $v_i^{\rm L}$ collides with the wall at $t = t_i^{\rm L}$. The equation of motion of the wall is

$$M\frac{{\rm d}V}{{\rm d}t} = F_{\rm L} + F_{\rm R}, \tag{3.6}$$

with

$$F_{\rm L} = \sum_i I\left(v_i^{\rm L}, \tilde{V}\right)\delta\left(t - t_i^{\rm L}\right), \tag{3.7}$$

where $F_{\rm L}$ is the force exerted by the elastic collisions of the gas particles on the left side and $\tilde{V}(t) \equiv \lim_{t' \nearrow t} V(t')$ the velocity just before the collision when $t = t_i^{\rm L}$. $F_{\rm R}$ is determined as well. (3.6) describes the time evolution of $V(t)$ (or the path of $V(t)$).

Then, we derive a time evolution equation of the velocity distribution function at time t, $P(V,t)$, based on the equation of motion (3.6). By using (3.1), (3.2), (3.3),

and (3.4), we obtain the following transition rate density from a state V to another state V':

$$\omega\left(V \to V'\right) = \lambda(v, V)\frac{\mathrm{d}v}{\mathrm{d}V'}, \tag{3.8}$$

where

$$\lambda(v, V) \equiv \lambda_{\mathrm{L}}(v, V) + \lambda_{\mathrm{R}}(v, V), \tag{3.9}$$

and

$$v = \frac{(M+m)V' - (M-m)V}{2m}. \tag{3.10}$$

Moreover, by using (3.8), the escape rate is given by

$$\begin{aligned}\kappa(V) &= \int \mathrm{d}V'\, \omega\left(V \to V'\right) \\ &= \int \mathrm{d}v\, \lambda(v, V).\end{aligned} \tag{3.11}$$

In terms of the transition rate density and the escape rate, we express the time evolution equation of $P(V,t)$ as

$$\frac{\partial P(V,t)}{\partial t} = \int \mathrm{d}V''\, \omega(V'' \to V)P(V'',t) - \kappa(V)P(V,t). \tag{3.12}$$

By using (3.8), we can rewrite (3.12) as

$$\frac{\partial P(V,t)}{\partial t} = \int \mathrm{d}v\, \lambda(v, V'')\frac{\mathrm{d}V''}{\mathrm{d}V}P(V'',t) - \kappa(V)P(V,t), \tag{3.13}$$

where

$$V'' = V - \frac{2m}{M-m}(v - V). \tag{3.14}$$

(3.13) is called the master-Boltzmann equation. It should be noted that, when $T_{\mathrm{L}} = T_{\mathrm{R}} = T$, (3.1), (3.2), (3.3), (3.4), and (3.8) lead to the detailed balance condition:

$$P_{\mathrm{eq}}(V)\omega(V \to V'') = P_{\mathrm{eq}}(-V'')\omega(-V'' \to -V), \tag{3.15}$$

where we denote the Maxwell–Boltzmann distribution by

$$P_{\mathrm{eq}}(V) = \sqrt{\frac{\beta M}{2\pi}}\mathrm{e}^{-\beta\frac{MV^2}{2}}. \tag{3.16}$$

This supports the validity of our model in equilibrium.

3.2.3 Notations

For later convenience, we define physical quantities. Given a path $\hat{V}$, we denote the total number of collisions as n, the time at the i-th collision as t_i, and the velocity after the i-th collision as V_i, where $t_0 \equiv 0$, $t_{n+1} \equiv \tau$, and $V(0) \equiv V_0$. We write the time reversal of V and $\hat{V}$ as $V^* = -V$ and $\hat{V}^\dagger = (V^*(\tau - t))_{t\in[0,\tau]}$, respectively. In the following, we denote the mean inverse temperature and the degree of non-equilibrium by $\beta \equiv (\beta_{\rm L} + \beta_{\rm R})/2$ and $\Delta \equiv (\beta_{\rm L} - \beta_{\rm R})/\beta$, respectively. Throughout this chapter, calligraphic fonts mean that its quantity depends on the path $\hat{V}$.

3.3 Local detailed balance condition

3.3.1 Naive consideration

In order to elucidate the energetics of this model, we first calculate $\omega(V \to V')/\omega(V'^* \to V^*)$ because it has been known that the ratio is related to the entropy production of the heat baths in many cases. We consider the case where, due to collision, the velocities of a gas particle and the wall change from v to v' and from V to V', respectively. Then, by using (3.3) and (3.4), we can show that the velocity of the wall changes from V'^* to V^* when that of the bath particle changes from v'^* to v^*. Furthermore, we obtain

$$V - v = \frac{m+M}{2m}(V - V') = V'^* - v'^*, \tag{3.17}$$

which means that $V < v \Leftrightarrow V < V' \Leftrightarrow V'^* < v'^*$. Thus, (3.8) leads to

$$\begin{aligned}\frac{\omega(V \to V')}{\omega(V'^* \to V^*)} &= \frac{\lambda_{\rm L}(v,V)}{\lambda_{\rm L}(v'^*,V'^*)}\theta(v-V) + \frac{\lambda_{\rm R}(v,V)}{\lambda_{\rm R}(v'^*,V'^*)}\theta(V-v) \\ &= \mathrm{e}^{-\beta_{\rm L}\left[\frac{mv^2}{2} - \frac{mv'^2}{2}\right]\theta(v-V) - \beta_{\rm R}\left[\frac{mv^2}{2} - \frac{mv'^2}{2}\right]\theta(V-v)} \\ &= \mathrm{e}^{-\beta_{\rm L}\left[\frac{MV'^2}{2} - \frac{MV^2}{2}\right]\theta(V'-V) - \beta_{\rm R}\left[\frac{MV'^2}{2} - \frac{MV^2}{2}\right]\theta(V-V')},\end{aligned} \tag{3.18}$$

where we have used the conservation of kinetic energy in elastic collisions. Therefore, given a path $\hat{V}$, we obtain

$$\prod_{i=1}^{n} \frac{\omega(V_{i-1} \to V_i)}{\omega(V_i^* \to V_{i-1}^*)} = \mathrm{e}^{-\beta_{\rm L}\mathcal{K}_{\rm L}(\hat{V}) - \beta_{\rm R}\mathcal{K}_{\rm R}(\hat{V})}, \tag{3.19}$$

with

$$\begin{aligned}\mathcal{K}_{\rm L}(\hat{V}) &\equiv \sum_{i=1}^{n}\left(\frac{MV_i^2}{2}-\frac{MV_{i-1}^2}{2}\right)\theta(V_i-V_{i-1}),\\ \mathcal{K}_{\rm R}(\hat{V}) &\equiv \sum_{i=1}^{n}\left(\frac{MV_i^2}{2}-\frac{MV_{i-1}^2}{2}\right)\theta(V_{i-1}-V_i),\end{aligned} \tag{3.20}$$

where we denote the total increment of the kinetic energy of the wall by the collisions of the gas particles on the left and right side during the time interval $[0,\tau]$ by $\mathcal{K}_{\rm L}(\hat{V})$ and $\mathcal{K}_{\rm R}(\hat{V})$, respectively. They satisfy

$$\mathcal{K}_{\rm L}(\hat{V})+\mathcal{K}_{\rm R}(\hat{V})=\frac{MV_n^2}{2}-\frac{MV_0^2}{2}. \tag{3.21}$$

Since collisions between the wall and each gas particle are elastic, $\mathcal{K}_{\rm L}(\hat{V})$ is equal to the decrease in the total kinetic energy of the gas particles on the left side. Thus, in this model, $\mathcal{K}_{\rm L}(\hat{V})$ and $\mathcal{K}_{\rm R}(\hat{V})$ are the energy transferred from the left and right side to the wall during the time interval $[0,\tau]$, respectively.

If the wall is fixed, which is a case considered in many examples, the energy transferred $\mathcal{K}_{\rm L}(\hat{V})$ may be interpreted as the heat transferred from the left side to the wall. Indeed, it was assumed that the ratio of the transition rates $\omega(V\to V')$ and $\omega(V'^*\to V^*)$ is equal to the exponential of the entropy production in the formal arguments [96]. However, since the wall can move in the model under consideration, work is done by the gas particles on each side. In order to obtain the proper entropy production, instead of the transition rate $\omega(V\to V')$, we have to precisely consider the probability density of the path $\hat{V}$ under the condition that V_0 is given.

3.3.2 True expression

The probability density of the path $\hat{V}$ for a given V_0 is expressed as

$$\mathcal{P}_\Delta(\hat{V}|V_0)=\mathrm{e}^{-\kappa(V_0)\times(t_1-t_0)}\prod_{i=1}^{n}\omega(V_{i-1}\to V_i)\,\mathrm{e}^{-\kappa(V_i)\times(t_{i+1}-t_i)}. \tag{3.22}$$

By using a certain initial distribution, $P_{\rm ini}(V_0)$, the expectation of any path-dependent quantity $\mathcal{A}(\hat{V})$ over all paths is given by

$$\langle\mathcal{A}\rangle_\Delta\equiv\int\mathcal{D}\hat{V}\;P_{\rm ini}(V_0)\mathcal{P}_\Delta(\hat{V}|V_0)\mathcal{A}(\hat{V}), \tag{3.23}$$

where we denote the integral over all paths by

$$\int\mathcal{D}\hat{V}\;\equiv\sum_{n=0}^{\infty}\int_{-\infty}^{\infty}dV_n\cdots\int_{-\infty}^{\infty}dV_0\int_0^{\tau}dt_n\int_0^{t_n}dt_{n-1}\cdots\int_0^{t_2}dt_1, \tag{3.24}$$

which satisfies $\mathcal{D}\hat{V} = \mathcal{D}\hat{V}^\dagger$. We also denote the probability density in equilibrium ($T_{\rm L} = T_{\rm R}$) by $\mathcal{P}_0(\hat{V}|V_0)$ and the expectation of $\mathcal{A}(\hat{V})$ in equilibrium by

$$\langle \mathcal{A} \rangle_0 \equiv \int \mathcal{D}\hat{V}\ P_{\rm ini}(V_0)\mathcal{P}_0(\hat{V}|V_0)\mathcal{A}(\hat{V}). \tag{3.25}$$

Here, the escape rate $\kappa(V)$ is calculated as

$$\begin{aligned}\kappa(V) &= \int {\rm d}v\ \lambda(v,V) \\ &= pS\beta_{\rm L}\int_V^\infty {\rm d}v\ (v-V)f_{\rm eq}^{\rm L}(v) + pS\beta_{\rm R}\int_{-\infty}^V {\rm d}v\ (V-v)f_{\rm eq}^{\rm R}(v).\end{aligned} \tag{3.26}$$

This leads to

$$\begin{aligned}\kappa(V) - \kappa(V^*) &= pS\beta_{\rm L}\int_{-\infty}^\infty {\rm d}v\ (v-V)f_{\rm eq}^{\rm L}(v) + pS\beta_{\rm R}\int_{-\infty}^\infty {\rm d}v\ (V-v)f_{\rm eq}^{\rm R}(v) \\ &= -(\beta_{\rm L}-\beta_{\rm R})pSV.\end{aligned} \tag{3.27}$$

It should be noted that $\kappa(V) \neq \kappa(V^*)$ when $\beta_{\rm L} \neq \beta_{\rm R}$.

Thus, by using (3.19), (3.22), and (3.27), we obtain

$$\begin{aligned}\frac{\mathcal{P}_\Delta(\hat{V}|V_0)}{\mathcal{P}_\Delta(\hat{V}^\dagger|V_n^*)} &= \prod_{i=1}^n \frac{\omega(V_{i-1}\to V_i)}{\omega(V_i^*\to V_{i-1}^*)}\prod_{i=0}^n {\rm e}^{-[\kappa(V_i)-\kappa(V_i^*)]\times(t_{i+1}-t_i)} \\ &= {\rm e}^{-\beta_{\rm L}\left[\mathcal{K}_{\rm L}(\hat{V})-pS\mathcal{X}(\hat{V})\right]-\beta_{\rm R}\left[\mathcal{K}_{\rm R}(\hat{V})+pS\mathcal{X}(\hat{V})\right]},\end{aligned} \tag{3.28}$$

where we have defined

$$\mathcal{X}(\hat{V}) \equiv \sum_{i=0}^n V_i\ (t_{i+1}-t_i), \tag{3.29}$$

which represents the displacement of the wall during the time interval $[0,\tau]$. Here, we define

$$\begin{aligned}\mathcal{Q}_{\rm L}(\hat{V}) &\equiv \mathcal{K}_{\rm L}(\hat{V}) - pS\mathcal{X}(\hat{V}), \\ \mathcal{Q}_{\rm R}(\hat{V}) &\equiv \mathcal{K}_{\rm R}(\hat{V}) + pS\mathcal{X}(\hat{V}).\end{aligned} \tag{3.30}$$

If $\mathcal{Q}_{\rm L}$ and $\mathcal{Q}_{\rm R}$ are the heat transferred from the left and right side to the wall during the time interval $[0,\tau]$, the equality (3.28) is called the local detailed balance condition, the microscopically reversible condition [25], or the detailed fluctuation theorem [27]. When the system in contact with a single heat bath obeys the canonical distribution at the temperature of the heat bath, we can expect that the local detailed balance condition is valid. Indeed, these definitions of the heat transferred are reasonable, because the work done by the gas particles in the left side is equal to

$pS\mathcal{X}(\hat{V})$ and (3.30) corresponds to the first law of thermodynamics. Once we derive the true expression of the local detailed balance condition, there is no difficulty of the understanding. Nevertheless, we wish to emphasize that it is not easy to conjecture that the difference of the escape rates, $\kappa(V_i) - \kappa(V_i^*)$, contributes to the entropy production in a concrete physical model although it is known in general cases [97]. By studying a concrete example on the basis of the local detailed balance condition, we have reached the consistent decomposition of the energy transferred into the heat transferred and the work.

Furthermore, we define the heat transferred from right to left by

$$\mathcal{Q}(\hat{V}) \equiv \frac{\mathcal{Q}_{\mathrm{R}}(\hat{V}) - \mathcal{Q}_{\mathrm{L}}(\hat{V})}{2}. \tag{3.31}$$

Then, by using

$$\begin{aligned} \mathcal{Q}_{\mathrm{L}}(\hat{V}) + \mathcal{Q}_{\mathrm{R}}(\hat{V}) &= \mathcal{K}_{\mathrm{L}}(\hat{V}) + \mathcal{K}_{\mathrm{R}}(\hat{V}) \\ &= \frac{MV_n^2}{2} - \frac{MV_0^2}{2}, \end{aligned} \tag{3.32}$$

we can rewrite the local detailed balance condition (3.28) as

$$\frac{P_{\mathrm{eq}}(V_0)\mathcal{P}_\Delta(\hat{V}|V_0)}{P_{\mathrm{eq}}(V_n^*)\mathcal{P}_\Delta(\hat{V}^\dagger|V_n^*)} = \mathrm{e}^{\Delta\beta\mathcal{Q}(\hat{V})}. \tag{3.33}$$

This expression of the local detailed balance condition leads to several types of fluctuation theorems and the formal expression of the steady-state distribution, which are useful for easily deriving the well-known relations [25]. It should be noted that the local detailed balance condition can also be derived from Hamiltonian systems, where the degrees of freedom of the gas particles are explicitly considered. See Appendix 3.A for a detailed explanation.

3.4 Fluctuation theorem

In order to obtain concise expressions, we assume that the initial distribution of the velocity of the wall, $P_{\mathrm{ini}}(V_0)$, is given by the Maxwell–Boltzmann distribution, $P_{\mathrm{eq}}(V_0)$. For any path-dependent quantity $\mathcal{A}(\hat{V})$, we define its time reversal by $\mathcal{A}^\dagger(\hat{V}) \equiv \mathcal{A}(\hat{V}^\dagger)$.

First, by using (3.33), we obtain

$$\begin{aligned} \langle\mathcal{A}\rangle_\Delta &= \int \mathcal{D}\hat{V}\ P_{\mathrm{eq}}(V_0)\mathcal{P}_\Delta(\hat{V}|V_0)\mathcal{A}(\hat{V}) \\ &= \int \mathcal{D}\hat{V}^\dagger\ P_{\mathrm{eq}}(V_n^*)\mathcal{P}_\Delta(\hat{V}^\dagger|V_n^*)\mathcal{A}^\dagger(\hat{V}^\dagger)\mathrm{e}^{\Delta\beta\mathcal{Q}^\dagger(\hat{V}^\dagger)} \\ &= \left\langle \mathcal{A}^\dagger \mathrm{e}^{\Delta\beta\mathcal{Q}^\dagger} \right\rangle_\Delta. \end{aligned} \tag{3.34}$$

By setting $\mathcal{A}(\hat{V}) \equiv 1$ and using $\mathcal{Q}^\dagger(\hat{V}) = -\mathcal{Q}(\hat{V})$, we obtain the integral fluctuation theorem:

$$\left\langle \mathrm{e}^{-\Delta\beta\mathcal{Q}} \right\rangle_\Delta = 1. \tag{3.35}$$

Jensen's inequality leads to

$$\Delta\beta\langle\mathcal{Q}\rangle_\Delta \geq 0. \tag{3.36}$$

Next, we derive the symmetry of the generating function [22, 23]. We define the energy transferred from right to left by

$$\mathcal{K}(\hat{V}) \equiv \frac{\mathcal{K}_\mathrm{R}(\hat{V}) - \mathcal{K}_\mathrm{L}(\hat{V})}{2}, \tag{3.37}$$

and the scaled cumulant generating function by

$$G(h_1, h_2) \equiv \lim_{\tau\to\infty} -\frac{1}{\tau} \log \left\langle \mathrm{e}^{-h_1\mathcal{K}-h_2\mathcal{X}} \right\rangle_\Delta . \tag{3.38}$$

By using (3.34) with $\mathcal{A}(\hat{V}) = \mathrm{e}^{-h_1\mathcal{K}(\hat{V})-h_2\mathcal{X}(\hat{V})}$, $\mathcal{K}^\dagger(\hat{V}) = -\mathcal{K}(\hat{V})$, and $\mathcal{X}^\dagger(\hat{V}) = -\mathcal{X}(\hat{V})$, we obtain

$$G(h_1, h_2) = G(\Delta\beta - h_1, \Delta\beta pS - h_2). \tag{3.39}$$

Finally, we derive the steady-state distribution of the velocity of the wall. We denote the path ensemble average of $\mathcal{A}(\hat{V})$ in equilibrium with the initial condition $V_0 = V$ as

$$\overline{\mathcal{A}}(V) \equiv \lim_{\tau\to\infty} \int \mathcal{D}\hat{V}\ \delta(V_0 - V)\mathcal{P}_0(\hat{V}|V_0)\mathcal{A}(\hat{V}). \tag{3.40}$$

The steady state distribution function $P_\mathrm{st}(V)$ is formally obtained as

$$P_\mathrm{st}(V) = \lim_{\tau\to\infty} \langle\delta(V(\tau) - V)\rangle_\Delta . \tag{3.41}$$

Thus, by using (3.34) with $\mathcal{A}(\hat{V}) = \delta(V(\tau) - V)$, $\delta(V_0^* - V) = \delta(V_0 - V^*)$, and space-reflection symmetry in equilibrium that leads to $\overline{\mathcal{Q}}(V^*) = -\overline{\mathcal{Q}}(V)$, we obtain

$$\begin{aligned} P_\mathrm{st}(V) &= \lim_{\tau\to\infty} \left\langle \delta(V_0 - V^*)\mathrm{e}^{-\Delta\beta\mathcal{Q}} \right\rangle_\Delta \\ &= P_\mathrm{eq}(V^*)\ \mathrm{e}^{-\Delta\beta\overline{\mathcal{Q}}(V^*)+O(\Delta^2)} \\ &= P_\mathrm{eq}(V)\ \mathrm{e}^{\Delta\beta\overline{\mathcal{Q}}(V)+O(\Delta^2)}, \end{aligned} \tag{3.42}$$

which is called the McLennan ensemble [4, 30, 98, 99].

3.5 Linear response theory

3.5.1 Onsager theory for adiabatic piston problem

In this subsection, we denote the pressures of the gases on the left and right sides by p_{L} and p_{R}, respectively. In the following, we assume that the system settles to a unique non-equilibrium steady state when it evolves for a sufficiently long time. Furthermore, we assume that thermodynamic forces, $\beta_{\mathrm{L}} - \beta_{\mathrm{R}}$ and $\beta_{\mathrm{L}} p_{\mathrm{L}} - \beta_{\mathrm{R}} p_{\mathrm{R}}$, are small compared to respective reference values. We define by J_K and J_V the steady energy flux from right to left and the steady velocity of the wall in the linear response regime, respectively. Within the linear response regime, Onsager's phenomenological equations relate the thermodynamic forces and fluxes as

$$\begin{cases} J_K = \mathrm{L}_{11}(\beta_{\mathrm{L}} - \beta_{\mathrm{R}}) + \mathrm{L}_{12}(\beta_{\mathrm{L}} p_{\mathrm{L}} - \beta_{\mathrm{R}} p_{\mathrm{R}}), \\ J_V = \mathrm{L}_{21}(\beta_{\mathrm{L}} - \beta_{\mathrm{R}}) + \mathrm{L}_{22}(\beta_{\mathrm{L}} p_{\mathrm{L}} - \beta_{\mathrm{R}} p_{\mathrm{R}}), \end{cases} \tag{3.43}$$

where L_{ij} are Onsager coefficients. Onsager's reciprocity relation states that $\mathrm{L}_{12} = \mathrm{L}_{21}$. Considering $\mathcal{Q} = \mathcal{K} + pS\mathcal{X}$, we define the steady heat flux from right to left in the linear response regime by

$$J_Q \equiv J_K + \overline{p} J_V, \tag{3.44}$$

with

$$\overline{p} \equiv \frac{p_{\mathrm{L}} + p_{\mathrm{R}}}{2}. \tag{3.45}$$

Then, we obtain

$$\begin{cases} J_Q = \widetilde{\mathrm{L}}_{11}(\beta_{\mathrm{L}} - \beta_{\mathrm{R}}) + \widetilde{\mathrm{L}}_{12}\beta(p_{\mathrm{L}} - p_{\mathrm{R}}), \\ J_V = \widetilde{\mathrm{L}}_{21}(\beta_{\mathrm{L}} - \beta_{\mathrm{R}}) + \widetilde{\mathrm{L}}_{22}\beta(p_{\mathrm{L}} - p_{\mathrm{R}}), \end{cases} \tag{3.46}$$

with

$$\begin{pmatrix} \widetilde{\mathrm{L}}_{11} & \widetilde{\mathrm{L}}_{12} \\ \widetilde{\mathrm{L}}_{21} & \widetilde{\mathrm{L}}_{22} \end{pmatrix} = \begin{pmatrix} \mathrm{L}_{11} + \mathrm{L}_{12}\overline{p} + \mathrm{L}_{21}\overline{p} + \mathrm{L}_{22}\overline{p}^2 & \mathrm{L}_{12} + \mathrm{L}_{22}\overline{p} \\ \mathrm{L}_{21} + \mathrm{L}_{22}\overline{p} & \mathrm{L}_{22} \end{pmatrix}, \tag{3.47}$$

where we have used

$$\beta_{\mathrm{L}} p_{\mathrm{L}} - \beta_{\mathrm{R}} p_{\mathrm{R}} = \overline{p}(\beta_{\mathrm{L}} - \beta_{\mathrm{R}}) + \beta(p_{\mathrm{L}} - p_{\mathrm{R}}). \tag{3.48}$$

In this form, the reciprocity relation, $\widetilde{\mathrm{L}}_{12} = \widetilde{\mathrm{L}}_{21}$, is also satisfied. In order to calculate J_Q and J_V, we express the Onsager coefficients in terms of the time correlation functions. It should be noted that $p_{\mathrm{L}} = p_{\mathrm{R}} = p$ in our model.

3.5.2 Linear response formula

By using (3.34) with $\mathcal{A}(\hat{V}) = \mathcal{K}(\hat{V})/(\tau S)$, we obtain

$$\lim_{\tau\to\infty}\left\langle\frac{\mathcal{K}}{\tau S}\right\rangle_{\Delta} = \lim_{\tau\to\infty}\left\langle-\frac{\mathcal{K}}{\tau S}\,\mathrm{e}^{-\Delta\beta\mathcal{Q}}\right\rangle_{\Delta} = \lim_{\tau\to\infty}\left[-\left\langle\frac{\mathcal{K}}{\tau S}\right\rangle_{\Delta} + \frac{\Delta\beta}{\tau S}\left\langle\mathcal{K}\mathcal{Q}\right\rangle_0 + O(\Delta^2)\right]. \tag{3.49}$$

This leads to

$$\lim_{\tau\to\infty}\left\langle\frac{\mathcal{K}}{\tau S}\right\rangle_{\Delta} = \Delta\beta\lim_{\tau\to\infty}\frac{1}{2\tau S}\left\langle\mathcal{K}\mathcal{Q}\right\rangle_0 + O(\Delta^2) = \Delta\beta\lim_{\tau\to\infty}\frac{1}{2\tau S}\left\langle\mathcal{K}\left[\mathcal{K}+pS\mathcal{X}\right]\right\rangle_0 + O(\Delta^2). \tag{3.50}$$

Similarly, by using (3.34) with $\mathcal{A}(\hat{V}) = \mathcal{X}(\hat{V})/\tau$, we obtain

$$\lim_{\tau\to\infty}\left\langle\frac{\mathcal{X}}{\tau}\right\rangle_{\Delta} = \Delta\beta\lim_{\tau\to\infty}\frac{1}{2\tau}\left\langle\mathcal{X}\mathcal{Q}\right\rangle_0 + O(\Delta^2) = \Delta\beta\lim_{\tau\to\infty}\frac{1}{2\tau}\left\langle\mathcal{X}\left[\mathcal{K}+pS\mathcal{X}\right]\right\rangle_0 + O(\Delta^2). \tag{3.51}$$

It should be noted that these universal relations, (3.50) and (3.51), hold for any $\epsilon = \sqrt{m/M}$. Considering (3.43), (3.50), and (3.51), we obtain

$$\begin{pmatrix}\mathrm{L}_{11} & \mathrm{L}_{12}\\ \mathrm{L}_{21} & \mathrm{L}_{22}\end{pmatrix} = \begin{pmatrix}\lim_{\tau\to\infty}\frac{1}{2\tau S}\left\langle\mathcal{K}\mathcal{K}\right\rangle_0 & \lim_{\tau\to\infty}\frac{1}{2\tau}\left\langle\mathcal{K}\mathcal{X}\right\rangle_0\\ \lim_{\tau\to\infty}\frac{1}{2\tau}\left\langle\mathcal{X}\mathcal{K}\right\rangle_0 & \lim_{\tau\to\infty}\frac{S}{2\tau}\left\langle\mathcal{X}\mathcal{X}\right\rangle_0\end{pmatrix}. \tag{3.52}$$

Furthermore, (3.47) and (3.52) lead to

$$\begin{pmatrix}\widetilde{\mathrm{L}}_{11} & \widetilde{\mathrm{L}}_{12}\\ \widetilde{\mathrm{L}}_{21} & \widetilde{\mathrm{L}}_{22}\end{pmatrix} = \begin{pmatrix}\lim_{\tau\to\infty}\frac{1}{2\tau S}\left\langle\mathcal{Q}\mathcal{Q}\right\rangle_0 & \lim_{\tau\to\infty}\frac{1}{2\tau}\left\langle\mathcal{Q}\mathcal{X}\right\rangle_0\\ \lim_{\tau\to\infty}\frac{1}{2\tau}\left\langle\mathcal{X}\mathcal{Q}\right\rangle_0 & \lim_{\tau\to\infty}\frac{S}{2\tau}\left\langle\mathcal{X}\mathcal{X}\right\rangle_0\end{pmatrix}. \tag{3.53}$$

We note that (3.50) and (3.51) can be derived by the symmetry of the generating function (3.39). By considering

$$\left.\frac{\partial G(h_1,h_2)}{\partial h_1}\right|_{h_1=h_2=0} = \left.\frac{\partial G(\Delta\beta-h_1,\Delta\beta pS-h_2)}{\partial h_1}\right|_{h_1=h_2=0}, \tag{3.54}$$

we obtain

$$\lim_{\tau\to\infty}\left\langle\frac{\mathcal{K}}{\tau S}\right\rangle_{\Delta}=\lim_{\tau\to\infty}-\frac{1}{\tau S}\frac{\left\langle\mathcal{K}\mathrm{e}^{-\Delta\beta\mathcal{Q}}\right\rangle_{\Delta}}{\left\langle\mathrm{e}^{-\Delta\beta\mathcal{Q}}\right\rangle_{\Delta}}. \tag{3.55}$$

By using (3.35), this equation is the same as (3.49). Similarly, by considering

$$\left.\frac{\partial G(h_1,h_2)}{\partial h_2}\right|_{h_1=h_2=0}=\left.\frac{\partial G(\Delta\beta-h_1,\Delta\beta pS-h_2)}{\partial h_2}\right|_{h_1=h_2=0}, \tag{3.56}$$

we obtain the same equation as (3.51).

Moreover, the McLennan ensemble (3.42) provides another expression of (3.51). We denote by $\langle\ \rangle_{\mathrm{st}}$ and $\langle\ \rangle_{\mathrm{eq}}$ the ensemble averages defined by P_{st} and P_{eq}, respectively. Then, by using (3.42) and $\langle V\rangle_{\mathrm{eq}}=0$, we obtain

$$\begin{aligned}\langle V\rangle_{\mathrm{st}}&=\Delta\beta\left\langle V\overline{\mathcal{Q}}\right\rangle_{\mathrm{eq}}+O(\Delta^2)\\&=\Delta\beta\left\langle V\left[\overline{\mathcal{K}}+pS\overline{\mathcal{X}}\right]\right\rangle_{\mathrm{eq}}+O(\Delta^2),\end{aligned} \tag{3.57}$$

which is equivalent to (3.51). Thus, $\widetilde{\mathrm{L}}_{21}$ is also expressed as

$$\widetilde{\mathrm{L}}_{21}=\left\langle V\overline{\mathcal{Q}}\right\rangle_{\mathrm{eq}}. \tag{3.58}$$

By evaluating the dynamics of $V(t)$ and $\mathcal{K}(\hat{V})$ in equilibrium, one can calculate the Onsager coefficients.

3.5.3 Calculation of Onsager coefficients

First, by using perturbation expansion in the small parameter $\epsilon=\sqrt{m/M}$, we can derive the Fokker–Planck equation from (3.13), and we obtain the time evolution equation of $V(t)$. In this subsection, we consider the case where $\beta_{\mathrm{L}}=\beta_{\mathrm{R}}$. By using

a test function, $\Phi(V)$, and the fact that $2\epsilon^2/(1+\epsilon^2) \ll 1$, (3.13) leads to

$$\begin{aligned}\int \mathrm{d}V\ \Phi(V)\frac{\partial P(V,t)}{\partial t} &= \int \mathrm{d}v \int \mathrm{d}V''\ \Phi(V)\lambda(v,V'')P(V'',t) \\ &\quad - \int \mathrm{d}V\ \Phi(V)\kappa(V)P(V,t) \\ &= \int \mathrm{d}v \int \mathrm{d}V''\ \sum_{i=1}^{\infty}\frac{1}{i!}\left(\frac{I(v,V'')}{M}\right)^i \frac{\partial^i \Phi(V'')}{\partial V''^i} \\ &\quad \times \lambda(v,V'')P(V'',t) \\ &= \int \mathrm{d}V''\ \Phi(V'')\sum_{i=1}^{\infty}\frac{(-1)^i}{i!}\times \\ &\quad \frac{\partial^i}{\partial V''^i}\left[\int \mathrm{d}v \left(\frac{I(v,V'')}{M}\right)^i \lambda(v,V'')P(V'',t)\right], \end{aligned} \tag{3.59}$$

where we have used

$$V = V'' + \frac{I(v,V'')}{M}. \tag{3.60}$$

Thus, we can rewrite (3.13) as the following formal series in powers of $2\epsilon^2/(1+\epsilon^2)$ [42]:

$$\begin{aligned}\frac{\partial P(V,t)}{\partial t} &= \sum_{i=1}^{\infty}\frac{(-1)^i}{i!}\frac{\partial^i}{\partial V^i}\left[\int \mathrm{d}v\ \left(\frac{I(v,V)}{M}\right)^i \lambda(v,V)P(V,t)\right] \\ &= \sum_{i=1}^{\infty}\frac{(-1)^i}{i!}\left(\frac{2\epsilon^2}{1+\epsilon^2}\right)^i \frac{\partial^i}{\partial V^i}\left[\int \mathrm{d}v\ (v-V)^i\lambda(v,V)P(V,t)\right]. \end{aligned} \tag{3.61}$$

By considering $f_{\mathrm{eq}}^{\mathrm{L}}(v) = f_{\mathrm{eq}}^{\mathrm{R}}(v) = \epsilon\sqrt{\beta M/(2\pi)}\mathrm{e}^{-\epsilon^2\beta M v^2/2}$, we obtain the following formula:

$$\begin{aligned}\int_V^{\infty} dv\ v^l f_{\mathrm{eq}}^{\mathrm{L}}(v) &= \int_0^{\infty} dv\ v^l f_{\mathrm{eq}}^{\mathrm{L}}(v) + O(\epsilon) \\ &= \epsilon^{-l}\frac{1}{2\sqrt{\pi}}\left(\frac{2}{\beta M}\right)^{l/2}\Gamma\left(\frac{l+1}{2}\right) + O(\epsilon), \end{aligned} \tag{3.62}$$

$$\begin{aligned}\int_{-\infty}^{V} dv\ v^l f_{\mathrm{eq}}^{\mathrm{R}}(v) &= \int_{-\infty}^{0} dv\ v^l f_{\mathrm{eq}}^{\mathrm{R}}(v) + O(\epsilon) \\ &= \epsilon^{-l}\frac{(-1)^l}{2\sqrt{\pi}}\left(\frac{2}{\beta M}\right)^{l/2}\Gamma\left(\frac{l+1}{2}\right) + O(\epsilon), \end{aligned} \tag{3.63}$$

where l is a non-negative integer. Then, using (3.1), (3.2), (3.61), (3.62), and (3.63), we obtain the Fokker–Planck equation up to order ϵ^2 as

$$\frac{\partial P(V,t)}{\partial t} = -\frac{\partial}{\partial V}\left[\left(-\frac{\gamma V}{M}\right)P(V,t)\right] + \frac{\gamma}{\beta M^2}\frac{\partial^2 P(V,t)}{\partial V^2}, \tag{3.64}$$

with

$$\begin{aligned}\gamma &\equiv \epsilon(n_{\mathrm{L}} + n_{\mathrm{R}})S\sqrt{\frac{8M}{\pi\beta}} \\ &= 4\epsilon p S\sqrt{\frac{2\beta M}{\pi}},\end{aligned} \tag{3.65}$$

where γ is interpreted as a friction constant. It should be noted that the friction effect originates from the change in the collision rate due to the motion of the wall. (3.64) leads to the following time evolution equation of $V(t)$ [102]:

$$M\frac{dV(t)}{dt} = -\gamma V(t) + \sqrt{\frac{2\gamma}{\beta}}\xi(t), \tag{3.66}$$

where ξ is Gaussian white noise with $\langle \xi(t)\xi(t')\rangle_0 = \delta(t-t')$. By solving (3.66), we obtain

$$V(t) = V(0)e^{-\frac{\gamma}{M}t} + \sqrt{\frac{2\gamma}{\beta M^2}}\int_0^t ds\; e^{-(t-s)\frac{\gamma}{M}}\xi(s). \tag{3.67}$$

Next, we derive the time evolution equation of $\mathcal{K}(\hat{V})$. We define the energy and heat flux from the gas particles on the left side to the wall by

$$k_{\mathrm{L}}(\tau;\hat{V}) \equiv \frac{1}{S}\frac{\mathrm{d}\mathcal{K}_{\mathrm{L}}(\hat{V})}{\mathrm{d}\tau}, \tag{3.68}$$

and

$$\begin{aligned}q_{\mathrm{L}}(\tau;\hat{V}) &\equiv \frac{1}{S}\frac{\mathrm{d}\mathcal{Q}_{\mathrm{L}}(\hat{V})}{\mathrm{d}\tau} \\ &= k_{\mathrm{L}}(\tau;\hat{V}) - pV(\tau),\end{aligned} \tag{3.69}$$

respectively. $k_{\mathrm{R}}(\tau;\hat{V})$ and $q_{\mathrm{R}}(\tau;\hat{V})$ are defined as well. We denote the energy and heat flux from right to left by

$$k(\tau;\hat{V}) \equiv \frac{k_{\mathrm{R}}(\tau;\hat{V}) - k_{\mathrm{L}}(\tau;\hat{V})}{2}, \tag{3.70}$$

and

$$q(\tau;\hat{V}) \equiv \frac{q_{\mathrm{R}}(\tau;\hat{V}) - q_{\mathrm{L}}(\tau;\hat{V})}{2}, \tag{3.71}$$

respectively. We also denote by $K(v,V)$ the change in the kinetic energy of the wall for the elastic collision of the wall of velocity V with a gas particle of velocity v, which is given by

$$K(v,V) = -\frac{2\epsilon^2}{(1+\epsilon^2)^2} M(V-v)(V+\epsilon^2 v). \tag{3.72}$$

By considering the time evolution equation of the joint distribution function for V and $\mathcal{K}_{\rm L}$, we obtain in the same way as in deriving (3.66)

$$k_{\rm L}(t) \simeq \int dv\ \lambda_{\rm L}(v, V(t)) K(v, V(t))/S, \tag{3.73}$$

where $\simeq$ means that we ignore the fluctuation terms, which vanish when we take the average value of them. It should be noted that when we ignore the fluctuation terms, $k_{\rm L}(t)$ is determined uniquely by $V(t)$. By using (3.62), we can rewrite (3.73) up to order ϵ^2 as

$$k_{\rm L}(t) \simeq \left(1 - 4\epsilon^2 + \epsilon^2 \beta M V(t)^2\right) pV(t) - \frac{\gamma}{MS}\left(\frac{1}{2} MV(t)^2 - \frac{1}{2\beta}\right). \tag{3.74}$$

Similarly, we obtain up to order ϵ^2

$$k_{\rm R}(t) \simeq -\left(1 - 4\epsilon^2 + \epsilon^2 \beta M V(t)^2\right) pV(t) - \frac{\gamma}{MS}\left(\frac{1}{2} MV(t)^2 - \frac{1}{2\beta}\right). \tag{3.75}$$

Thus, (3.74) and (3.75) lead to

$$\begin{aligned} k(t) &= \frac{k_{\rm R}(t) - k_{\rm L}(t)}{2} \\ &\simeq -\left(1 - 4\epsilon^2 + \epsilon^2 \beta M V(t)^2\right) pV(t) + O(\epsilon^3), \end{aligned} \tag{3.76}$$

and

$$\begin{aligned} q(t) &= k(t) + pV(t) \\ &\simeq \epsilon^2 \left(4 - \beta M V(t)^2\right) pV(t) + O(\epsilon^3). \end{aligned} \tag{3.77}$$

Finally, we calculate $\widetilde{\rm L}_{21}$ explicitly. To lowest order in ϵ, (3.67) and (3.77) lead to

$$\begin{aligned} \overline{\mathcal{X}}(V) &= \lim_{\tau\to\infty} \left\langle \int_0^\tau dt\ V(t)|_{V(0)=V} \right\rangle_0 \\ &= \frac{MV}{\gamma}, \end{aligned} \tag{3.78}$$

and

$$\begin{aligned} \overline{\mathcal{Q}}(V) &= \lim_{\tau\to\infty} \left\langle \int_0^\tau dt\ Sq(t)|_{V(0)=V} \right\rangle_0 \\ &= 2\epsilon^2 \frac{pSMV}{\gamma} - \epsilon^2 \frac{pS\beta M^2 V^3}{3\gamma}. \end{aligned} \tag{3.79}$$

Using (3.79), $\langle V^2 \rangle_{\rm eq} = 1/(\beta M)$, and $\langle V^4 \rangle_{\rm eq} = 3/(\beta^2 M^2)$, we obtain to lowest order in ϵ

$$\begin{aligned} \widetilde{\mathrm{L}}_{21} &= \langle V \overline{\mathcal{Q}} \rangle_{\rm eq} \\ &= \frac{\epsilon^2 pS}{\beta\gamma}. \end{aligned} \tag{3.80}$$

Using (3.46), (3.65), and (3.80), we obtain up to order ϵ

$$\begin{aligned} J_V &= \widetilde{\mathrm{L}}_{21} \Delta\beta \\ &= \Delta\epsilon^2 \frac{pS}{\gamma} \\ &= \frac{\Delta\epsilon}{4} \sqrt{\frac{\pi}{2\beta M}}. \end{aligned} \tag{3.81}$$

Within the linear response regime, this result is consistent with the previous study [92].

3.6 Concluding remarks

In this chapter, we elucidate the energetics of the adiabatic piston problem on the basis of the local detailed balance condition. Owing to the condition, we can decompose the energy transferred from each gas to the wall into the work and the heat transferred. In the course of the calculation of the condition, we find that the difference of the escape rates, $\kappa(V_i) - \kappa(V_i^*)$, contributes to the entropy production. In addition, by using the condition, we obtain the linear response formula for the steady velocity of the wall and steady energy flux through the wall. By using perturbation expansion in the small parameter $\epsilon \equiv \sqrt{m/M}$, we derive the steady velocity up to order ϵ. It should be noted that we can derive the local detailed balance condition for the more general case where the wall consists of many atoms.

The adiabatic piston problem will be important in future studies. First, since the wall moves despite the same pressure on both sides, this phenomenon cannot be described by the standard hydrodynamic equations, and thus this problem will provide a good example for studying the hydrodynamic equations more deeply. In particular, the determination of the boundary condition of the fluctuating hydrodynamic equations may be directly related to the description of the observed phenomenon. Second, since this problem is the simplest example of two interacting systems, one may obtain a mechanical representation of the information exchange process in two interacting stochastic systems [100, 101]. As seen in these two examples, one can deepen the understanding of non-equilibrium statistical mechanics by developing the analysis of the adiabatic piston problem.

Before ending this chapter, we discuss the force from the bath $\widetilde{F}_{\rm L}$, which plays an essential role on the phenomenon. The simplest model of $\widetilde{F}_{\rm L}$ that yields the T-p

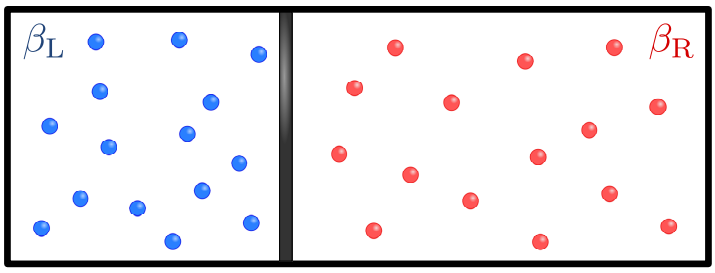

Fig. 3.2 (color online) Schematic illustration of our total system, which consists of a wall and two heat baths. The wall consists of only one degree of freedom and separates the left heat bath from the right heat bath. The left and right heat bath consist of N_{L} and N_{R} particles, and are initially prepared at different inverse temperatures, β_{L} and β_{R}, respectively.

ensemble of the system in equilibrium is give by a Langevin force [87, 88]

$$\widetilde{F}_{\mathrm{L}} = pS - \gamma_{\mathrm{L}} V + \sqrt{2T_{\mathrm{L}}\gamma_{\mathrm{L}}}\xi_{\mathrm{L}}, \tag{3.82}$$

where ξ_{L} is Gaussian white noise with unit variance [102] and γ_{L} a friction constant. $\widetilde{F}_{\mathrm{R}}$ is similarly defined. In this case, we can write the equation of motion of the wall as

$$\begin{aligned} M\frac{\mathrm{d}V}{\mathrm{d}t} &= \widetilde{F}_{\mathrm{L}} + \widetilde{F}_{\mathrm{R}} \\ &= -(\gamma_{\mathrm{L}} + \gamma_{\mathrm{R}})V + \sqrt{2T_{\mathrm{L}}\gamma_{\mathrm{L}}}\xi_{\mathrm{L}} + \sqrt{2T_{\mathrm{R}}\gamma_{\mathrm{R}}}\xi_{\mathrm{R}}. \end{aligned} \tag{3.83}$$

Then, by considering $\langle \mathrm{d}V/\mathrm{d}t\rangle_{\mathrm{st}} = \langle \xi_{\mathrm{L}}\rangle_{\mathrm{st}} = \langle \xi_{\mathrm{R}}\rangle_{\mathrm{st}} = 0$, it is easily confirmed that

$$\langle V\rangle_{\mathrm{st}} = 0. \tag{3.84}$$

That is, the steady state velocity depends on the type of stochastic force. This result raises the question what is the condition of proper description of the baths. To understand the proper bath model in non-equilibrium is of great importance.

3.A Local detailed balance condition for Hamiltonian systems

We provide the microscopic description of our model. The model is illustrated in Fig. 3.2. The system consists of a wall and two heat baths. We assume that the wall of area S consists of only one degree of freedom and separates the left heat bath from the right heat bath. The wall moves freely along a long tube and we take x-axis as the direction of movement of the wall. The position and momentum of the wall are denoted as $\gamma = (X, P)$. We also assume that the left and right heat bath consist of N_{L} and N_{R} particles, respectively. A collection of the positions and momenta

of $N_{\rm L}$ particles in the left heat bath is denoted as $\Gamma^{\rm L} = (\boldsymbol{r}_1^{\rm L}, \dots, \boldsymbol{r}_{N_{\rm L}}^{\rm L}, \boldsymbol{p}_1^{\rm L}, \dots, \boldsymbol{p}_{N_{\rm L}}^{\rm L})$, and that of $N_{\rm R}$ particles in the right heat bath is similarly denoted as $\Gamma^{\rm R}$. Then, the microscopic state of the total system is expressed as a point of the phase space $\Gamma \equiv (\gamma, \Gamma^{\rm L}, \Gamma^{\rm R})$. For any state Γ, we denote by Γ^* its time reversal, namely, the state obtained by reversing all the momenta, and denote the time reversal of $\boldsymbol{p}_i$ as $\boldsymbol{p}_i^* = -\boldsymbol{p}_i$. We assume that all interactions are short-range, and ignore the interaction between the left and right heat bath particles for simplicity. We denote by $\mathcal{H}(\gamma)$, $H_{\rm L}(\Gamma^{\rm L};\gamma)$, and $H_{\rm R}(\Gamma^{\rm R};\gamma)$ the Hamiltonian of the wall, the left heat bath, and the right heat bath, respectively, where $H_{\rm L}(\Gamma^{\rm L};\gamma)$ and $H_{\rm R}(\Gamma^{\rm R};\gamma)$ include the interaction potential between the particles in each heat bath and the wall. Then, the time evolution of Γ is determined by the following total Hamiltonian:

$$H(\Gamma) \equiv \mathcal{H}(\gamma) + H_{\rm L}(\Gamma^{\rm L};\gamma) + H_{\rm R}(\Gamma^{\rm R};\gamma). \tag{3.85}$$

We denote by Γ_t the solution of the Hamiltonian equations at time t for any initial state Γ. We assume that the total Hamiltonian satisfies the time-reversal symmetry:

$$H(\Gamma) = H(\Gamma^*). \tag{3.86}$$

In this setup, we obtain Liouville's theorem:

$$\left| \frac{\partial \Gamma_t}{\partial \Gamma} \right| = 1, \tag{3.87}$$

and the law of conservation of energy:

$$H(\Gamma_t) = H(\Gamma). \tag{3.88}$$

In the following, we consider the time evolution in the time interval $[0, \tau]$.

Next, we determine initial conditions. We fix the initial state of the wall as $\gamma = \gamma_{\rm i}$ and the final state of the wall as $\gamma_\tau = \gamma_{\rm f}$. We initially prepare the left and right heat baths at different inverse temperatures, $\beta_{\rm L}$ and $\beta_{\rm R}$, respectively. Thus, the initial states of the heat baths are sampled according to the probability density

$$P_{\rm B}(\Gamma^{\rm L}, \Gamma^{\rm R};\gamma) = {\rm e}^{\beta_{\rm L}[F_{\rm L}(\gamma) - H_{\rm L}(\Gamma^{\rm L};\gamma)] + \beta_{\rm R}[F_{\rm R}(\gamma) - H_{\rm R}(\Gamma^{\rm R};\gamma)]}, \tag{3.89}$$

with

$$F_{\rm L}(\gamma) = -\frac{1}{\beta_{\rm L}} \log \left[\int {\rm d}\Gamma^{\rm L} \ {\rm e}^{-\beta_{\rm L} H_{\rm L}(\Gamma^{\rm L};\gamma)} \right], \tag{3.90}$$

$$F_{\rm R}(\gamma) = -\frac{1}{\beta_{\rm R}} \log \left[\int {\rm d}\Gamma^{\rm R} \ {\rm e}^{-\beta_{\rm R} H_{\rm R}(\Gamma^{\rm R};\gamma)} \right], \tag{3.91}$$

where $F_{\rm L}(\gamma)$ and $F_{\rm R}(\gamma)$ represent the Helmholtz free energies of the left and right heat baths, respectively. By using the Helmholtz free energy, we can define the pressure of

the left heat bath to the wall by

$$\begin{aligned} p_{\mathrm{L}}(\gamma) &\equiv -\frac{\partial F_{\mathrm{L}}(\gamma)}{\partial(SX)} \\ &= \int \mathrm{d}\Gamma^{\mathrm{L}}\ \mathrm{e}^{\beta_{\mathrm{L}}[F_{\mathrm{L}}(\gamma)-H_{\mathrm{L}}(\Gamma^{\mathrm{L}};\gamma)]}\left[-\frac{\partial H_{\mathrm{L}}(\Gamma^{\mathrm{L}};\gamma)}{\partial(SX)}\right]. \end{aligned} \tag{3.92}$$

The pressure of the right heat bath to the wall is similarly defined by

$$p_{\mathrm{R}}(\gamma) \equiv \frac{\partial F_{\mathrm{R}}(\gamma)}{\partial(SX)}. \tag{3.93}$$

It should be noted that the direction of the pressure force to the wall on the left side is opposite to that on the right side. In this setup, we can write the probability density for paths of the wall starting at γ_{i} and ending at γ_{f} as

$$\mathcal{W}(\gamma_{\mathrm{i}} \to \gamma_{\mathrm{f}}) = \int \mathrm{d}\Gamma\ P_{\mathrm{B}}(\Gamma^{\mathrm{L}}, \Gamma^{\mathrm{R}}; \gamma)\delta(\gamma - \gamma_{\mathrm{i}})\delta(\gamma_\tau - \gamma_{\mathrm{f}}), \tag{3.94}$$

which satisfies

$$\int \mathrm{d}\gamma_{\mathrm{f}}\ \mathcal{W}(\gamma_{\mathrm{i}} \to \gamma_{\mathrm{f}}) = 1. \tag{3.95}$$

For any physical quantity $A(\Gamma)$, we define its time reversal by

$$A^\dagger(\Gamma) \equiv A(\Gamma^*_\tau), \tag{3.96}$$

and the ensemble average of $A(\Gamma)$ with the initial and final conditions of the wall γ_{i} and γ_{f}, respectively, by

$$\langle A \rangle_{\gamma_{\mathrm{i}} \to \gamma_{\mathrm{f}}} \equiv \frac{\int \mathrm{d}\Gamma\ P_{\mathrm{B}}(\Gamma^{\mathrm{L}}, \Gamma^{\mathrm{R}}; \gamma)\delta(\gamma - \gamma_{\mathrm{i}})\delta(\gamma_\tau - \gamma_{\mathrm{f}})A(\Gamma)}{\mathcal{W}(\gamma_{\mathrm{i}} \to \gamma_{\mathrm{f}})}. \tag{3.97}$$

Finally, we derive the local detailed balance condition. We define the decrease in the internal energy of the left and right heat bath by

$$\begin{cases} U_{\mathrm{L}}(\Gamma) \equiv H_{\mathrm{L}}(\Gamma^{\mathrm{L}}; \gamma) - H_{\mathrm{L}}(\Gamma^{\mathrm{L}}_\tau; \gamma_\tau), \\ U_{\mathrm{R}}(\Gamma) \equiv H_{\mathrm{R}}(\Gamma^{\mathrm{R}}; \gamma) - H_{\mathrm{R}}(\Gamma^{\mathrm{R}}_\tau; \gamma_\tau). \end{cases} \tag{3.98}$$

By using (3.86) and (3.89), we obtain

$$\frac{P_{\mathrm{B}}(\Gamma^{\mathrm{L}}, \Gamma^{\mathrm{R}}; \gamma)}{P_{\mathrm{B}}(\Gamma^{\mathrm{L}*}_\tau, \Gamma^{\mathrm{R}*}_\tau; \gamma^*_\tau)} = \mathrm{e}^{\beta_{\mathrm{L}}[F_{\mathrm{L}}(\gamma^*) - F_{\mathrm{L}}(\gamma^*_\tau) - U_{\mathrm{L}}(\Gamma)] + \beta_{\mathrm{R}}[F_{\mathrm{R}}(\gamma^*) - F_{\mathrm{R}}(\gamma^*_\tau) - U_{\mathrm{R}}(\Gamma)]}. \tag{3.99}$$

Thus, according to Liouville's theorem (3.87), we obtain

$$\begin{aligned}\mathcal{W}(\gamma_{\rm i}\to\gamma_{\rm f})\left\langle A\right\rangle_{\gamma_{\rm i}\to\gamma_{\rm f}} &= \int {\rm d}\Gamma\ P_{\rm B}(\Gamma^{\rm L},\Gamma^{\rm R};\gamma)\delta(\gamma-\gamma_{\rm i})\delta(\gamma_\tau-\gamma_{\rm f})A(\Gamma)\\ &= \int {\rm d}\Gamma^*_\tau\ P_{\rm B}(\Gamma^{{\rm L}*}_\tau,\Gamma^{{\rm R}*}_\tau;\gamma^*_\tau)\delta(\gamma^*_\tau-\gamma^*_{\rm f})\delta(\gamma^*-\gamma^*_{\rm i})A^\dagger(\Gamma^*_\tau)\\ &\quad\times {\rm e}^{\beta_{\rm L}[F_{\rm L}(\gamma^*)-F_{\rm L}(\gamma^*_\tau)-U^\dagger_{\rm L}(\Gamma^*_\tau)]+\beta_{\rm R}[F_{\rm R}(\gamma^*)-F_{\rm R}(\gamma^*_\tau)-U^\dagger_{\rm R}(\Gamma^*_\tau)]}.\end{aligned} \tag{3.100}$$

Here we assume that the displacement of the wall is much shorter than the length of the long tube in the x-direction, and therefore that the pressures of the left and right heat bath are kept constant over time. Furthermore, $F_{\rm L}$ depends only on X. Then, by using (3.92), we obtain

$$F_{\rm L}(\gamma_\tau)=F_{\rm L}(\gamma)-p_{\rm L}(\gamma)S(X_\tau-X). \tag{3.101}$$

$p_{\rm L}(\gamma)S(X_\tau-X)$ is the work done by the particles in the left heat bath. Here, with the following definitions

$$\begin{cases}Q_{\rm L}(\Gamma)\equiv U_{\rm L}(\Gamma)-p_{\rm L}(\gamma)S(X_\tau-X),\\ Q_{\rm R}(\Gamma)\equiv U_{\rm R}(\Gamma)+p_{\rm R}(\gamma)S(X_\tau-X),\end{cases} \tag{3.102}$$

(3.100) leads to

$$\mathcal{W}(\gamma_{\rm i}\to\gamma_{\rm f})\left\langle A\right\rangle_{\gamma_{\rm i}\to\gamma_{\rm f}}=\mathcal{W}(\gamma^*_{\rm f}\to\gamma^*_{\rm i})\left\langle A^\dagger {\rm e}^{-\beta_{\rm L}Q^\dagger_{\rm L}-\beta_{\rm R}Q^\dagger_{\rm R}}\right\rangle_{\gamma^*_{\rm f}\to\gamma^*_{\rm i}}. \tag{3.103}$$

From the first law of thermodynamics, $Q_{\rm L}(\Gamma)$ and $Q_{\rm R}(\Gamma)$ are interpreted as the heat transferred from the left and right heat bath to the wall, respectively. Now, we define the mean inverse temperature by $\beta=(\beta_{\rm L}+\beta_{\rm R})/2$, the degree of non-equilibrium by $\Delta=(\beta_{\rm L}-\beta_{\rm R})/\beta$, and the Helmholtz free energy for the wall by

$$F\equiv-\frac{1}{\beta}\log\left[\int {\rm d}\gamma\ {\rm e}^{-\beta\mathcal{H}(\gamma)}\right]. \tag{3.104}$$

By using (3.88), we obtain

$$U_{\rm L}(\Gamma)+U_{\rm R}(\Gamma)=\mathcal{H}(\gamma_\tau)-\mathcal{H}(\gamma). \tag{3.105}$$

Thus, by setting $p_{\rm L}(\gamma_{\rm i})=p_{\rm R}(\gamma_{\rm i})=p$, we can rewrite (3.103) as

$$\widetilde{P}_{\rm eq}(\gamma_{\rm i})\mathcal{W}(\gamma_{\rm i}\to\gamma_{\rm f})\left\langle A\right\rangle_{\gamma_{\rm i}\to\gamma_{\rm f}}=\widetilde{P}_{\rm eq}(\gamma^*_{\rm f})\mathcal{W}(\gamma^*_{\rm f}\to\gamma^*_{\rm i})\left\langle A^\dagger {\rm e}^{\Delta\beta\frac{Q^\dagger_{\rm R}-Q^\dagger_{\rm L}}{2}}\right\rangle_{\gamma^*_{\rm f}\to\gamma^*_{\rm i}}, \tag{3.106}$$

with

$$\widetilde{P}_{\rm eq}(\gamma) \equiv {\rm e}^{\beta[F-\mathcal{H}(\gamma)]}. \tag{3.107}$$

By setting $A = 1$, (3.103) and (3.106) are consistent with the local detailed balance conditions in the main text (3.28) and (3.33), respectively. The form of the heat transferred and the work from each gas to the wall in our stochastic model is also consistent with that in the description of Hamiltonian systems under the assumption that gas regions are so large that thermodynamic quantities of the heat baths are kept constant over observation time.

Chapter 4

Macroscopically measurable force induced by temperature discontinuities at solid-gas interfaces

4.1 Introduction

Nontrivial phenomena occur at the interface between a solid and a fluid. Indeed, the description of behavior near the interface has not been established, because its characteristic length scale is too small for macroscopic phenomenological descriptions. Although imposing appropriate boundary conditions at the interface for macroscopic equations often gives a good description, there are cases where the assumptions of the boundary conditions should be seriously considered. In this chapter, we study a phenomenon associated with temperature gaps at the interfaces between a solid and gases.

In order to demonstrate our findings clearly, we employ the special-purpose systems shown in Fig. 4.1. A solid (say, silicon), which consists of many atoms, is placed in a long tube of cross-sectional area S. Dilute gases (say, helium) at the same pressure p but different temperatures T_{L} and T_{R} are contained in the left and right regions, respectively, at an initial time. The gases are well approximated by ideal gases and cannot mix with each other because the solid acts as a separating wall. It is assumed that the pressure and temperatures of gas particles before colliding with the solid are kept constant over time. In this setup, despite the equal pressure, momentum flows from one gas to the other owing to the energy transfer from the hot side to the cold side. Recently, a phenomenological mechanism for the emergence of a force from such cross-coupling has been proposed in Refs. [43, 44]. In this chapter, we provide a quantitative estimation of the force acting on the solid on the basis of a microscopic description of the system under some assumptions. An important finding is that the

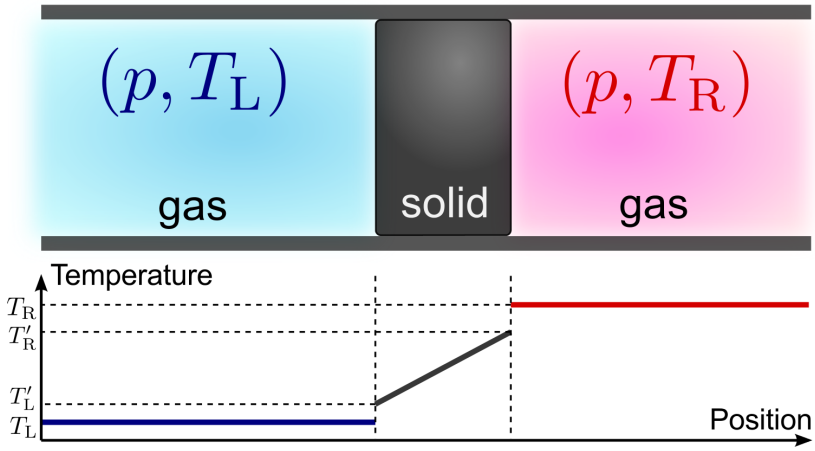

Fig. 4.1 Schematic illustration of the experimental systems. The solid separates two gases at the same pressure but different temperatures. The pressures and temperatures are kept constant over time. Temperature gaps appear on the solid surface.

force is determined by the temperature gaps at the interface of the solid and gases.

More precisely, we denote by T'_{L} and T'_{R} the kinetic temperatures of the solid particles at the left and right ends, respectively, which are different from T_{L} and T_{R} in general. Such a temperature discontinuity at an interface has been measured in experiments [103–105]. For the mass of gas particles m_{G} and the mass of solid particles m, we define $\epsilon \equiv \sqrt{m_{\mathrm{G}}/m}$, which is assumed to be small. We then show that the temperature gaps $T'_{\mathrm{L}} - T_{\mathrm{L}}$ and $T'_{\mathrm{R}} - T_{\mathrm{R}}$ generate the force F_{gap} given by

$$F_{\mathrm{gap}} = \epsilon^2 pS \left(\frac{T'_{\mathrm{L}} - T_{\mathrm{L}}}{T_{\mathrm{L}}} + \frac{T_{\mathrm{R}} - T'_{\mathrm{R}}}{T_{\mathrm{R}}} \right). \tag{4.1}$$

By assuming Fourier's law in the solid, we can estimate the temperature gaps in terms of the thermal conductivity of the solid. Surprisingly, the result shows that F_{gap} takes a macroscopically measurable value. It should be noted that steady-state motion of the solid is observed because the force F_{gap} may be balanced with a friction force induced by collision with gas particles.

In the argument below, we describe the microscopic model that we employ. We then derive the aforementioned result. Finally, we discuss the possibility of experimental realization of the phenomenon in laboratories. Throughout this chapter, β represents the inverse temperature and k_{B} the Boltzmann constant. The subscripts or superscripts L and R represent quantities on the left and right sides, respectively.

4.2 Model

We provide a three-dimensional mechanical description of the solid in Fig. 4.2. We take the x axis along the axial direction of the tube. We assume that the solid consists

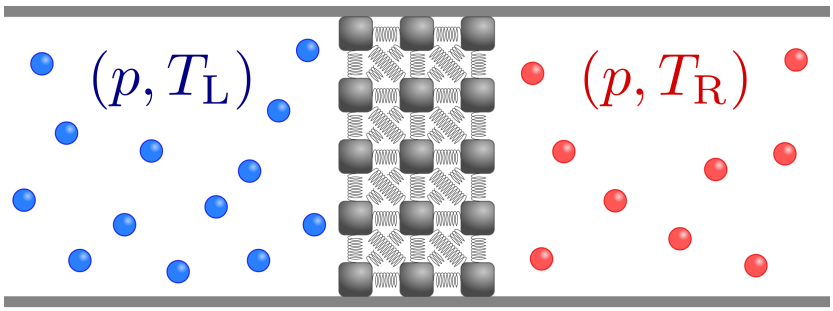

Fig. 4.2 Schematic illustration of a cross section of our model in three dimensions. The solid particles are connected by a spring. Gas particles collide with the solid particles according to a Poisson process.

of $N \times M$ particles of mass m, where N and M are the number of particles along the x direction and in a plane perpendicular to the x axis, respectively. A collection of the positions and momenta of $N \times M$ solid particles, which we distinguish by subscripts i and j ($1 \le i \le N$, $1 \le j \le M$), are denoted by $\Gamma = (\boldsymbol{r}_{1,1}, \dots, \boldsymbol{r}_{N,M}; \boldsymbol{p}_{1,1}, \dots, \boldsymbol{p}_{N,M})$, which gives the microscopic state of the solid. The x components of $\boldsymbol{r}_{i,j}$ and $\boldsymbol{p}_{i,j}$ are denoted by $x_{i,j}$ and $p_{i,j}$, respectively, and the corresponding velocity is given by $v_{i,j} \equiv p_{i,j}/m$. The position and velocity of the center of mass of the solid in the x direction are denoted by X and V, respectively.

The Hamiltonian of the solid, $H(\Gamma)$, is given by

$$H(\Gamma) = \sum_{i,j} \left[\frac{|\boldsymbol{p}_{i,j}|^2}{2m} + U_{\mathrm{w}}(\boldsymbol{r}_{i,j}) \right] + \sum_{\langle i,j;i',j' \rangle} U_{\mathrm{int}}(\boldsymbol{r}_{i,j}, \boldsymbol{r}_{i',j'}), \tag{4.2}$$

where $\langle i,j;i',j' \rangle$ represents the nearest- and second-nearest-neighbor pair of solid particles. U_{int} is the interaction potential between two solid particles, and U_{w} is the potential between a solid particle and the tube wall. The tube wall is assumed to be frictionless, and $U_{\mathrm{w}}(\boldsymbol{r}_{i,j})$ does not depend on $x_{i,j}$. The motion of solid particles except for left and right ends is described by the Hamiltonian equations.

Next, we provide an effective description of the gases. We focus on the gas on the left side; the gas on the right side can be described similarly. Employing a dilute gas that consists of particles of mass m_{G}, we may assume that the characteristic time of the dissipation process inside each gas is much longer than the time during which we observe the steady-state motion of the solid. Therefore, gas particles that have yet to collide with the solid are in equilibrium at the temperature T_{L}, the pressure p, and the number density $n_{\mathrm{L}} = p\beta_{\mathrm{L}}$. We also assume that gas particles elastically and instantaneously collide with the solid only once. More precisely, the instantaneous collision means that the characteristic time of the solid-gas interaction is much shorter than the relaxation time of all solid particles. It should be noted that this situation is completely different from a case where the solid is effectively described as a wall with one degree of freedom. For convenience, we make a list of characteristic time

Table 4.1 Characteristic time scales.

symbol	definition
τ_1	relaxation time of the dissipation process inside gas
τ_2	relaxation time of V
τ_3	relaxation time of all solid particles
τ_4	solid-gas interaction time

scales in Table 4.1. Our assumption means that $\tau_1 \gg \tau_2 > \tau_3 \gg \tau_4$. Furthermore, for simplicity, we assume that the tangent plane at the collision point is perpendicular to the x axis, so that the x component of the velocity of each solid particle at both ends is independent of the other components at the collisions.

For this setup, the interaction between the solid and the gas on the left side can be described by random collisions with the collision rate $\lambda_{\mathrm{L}}(v_{\mathrm{G}}, v_{1,j})$ per unit area for the gas particle velocity v_{G} and the solid particle velocity $v_{1,j}$. The collision rate is explicitly written as

$$\lambda_{\mathrm{L}}(v_{\mathrm{G}}, v_{1,j}) = n_{\mathrm{L}}(v_{\mathrm{G}} - v_{1,j})\theta(v_{\mathrm{G}} - v_{1,j})f_{\mathrm{eq}}^{\mathrm{L}}(v_{\mathrm{G}}) \tag{4.3}$$

with

$$f_{\mathrm{eq}}^{\mathrm{L}}(v_{\mathrm{G}}) = \sqrt{\frac{\beta_{\mathrm{L}} m_{\mathrm{G}}}{2\pi}} \exp\left(-\beta_{\mathrm{L}} \frac{m_{\mathrm{G}} v_{\mathrm{G}}^2}{2}\right), \tag{4.4}$$

where θ represents the Heaviside step function and $f_{\mathrm{eq}}^{\mathrm{L}}(v_{\mathrm{G}})$ is the Maxwell–Boltzmann distribution.

The l-th collision time of a gas particle and the j-th solid particle at the left end is determined according to the Poisson process. Suppose that a gas particle with a velocity in the x direction $v_{\mathrm{G},j}^{\mathrm{L},l}$ collides with the j-th solid particle at $t = t_j^{\mathrm{L},l}$. The equation of motion for the j-th solid particle in the x direction is written as

$$\frac{dp_{1,j}}{dt} = -\frac{\partial H(\Gamma)}{\partial x_{1,j}} + F_{\mathrm{L},j}, \tag{4.5}$$

with

$$F_{\mathrm{L},j} = \sum_l I\left(v_{\mathrm{G},j}^{\mathrm{L},l}, \tilde{v}_{1,j}\right) \delta\left(t - t_j^{\mathrm{L},l}\right), \tag{4.6}$$

and

$$I(v_{\mathrm{G}}, v) = \frac{2m_{\mathrm{G}} m}{m_{\mathrm{G}} + m}(v_{\mathrm{G}} - v), \tag{4.7}$$

where $F_{\mathrm{L},j}$ is the force exerted by the elastic collisions of the gas particles, $I(v_{\mathrm{G}}, v)$ the impulse of the collision, and $\tilde{v}_{1,j}(t) \equiv \lim_{t' \nearrow t} v_{1,j}(t')$ the velocity just before the collision when $t = t_j^{\mathrm{L},l}$. Similarly, the collision rate of the gas on the right side is given by

$$\lambda_{\mathrm{R}}(v_{\mathrm{G}}, v_{N,j}) = n_{\mathrm{R}}(v_{N,j} - v_{\mathrm{G}})\theta(v_{N,j} - v_{\mathrm{G}})f_{\mathrm{eq}}^{\mathrm{R}}(v_{\mathrm{G}}), \tag{4.8}$$

and the equation of motion for the solid particles at the right end is determined as well.

The Hamiltonian equations in combination with the Poisson processes yield a unique steady state. The expectation value in the steady state is denoted by $\langle \cdot \rangle$. We then have $\langle v_{i,j} \rangle = \langle V \rangle$ for any i and j, and we assume that the statistical properties in the steady state are homogeneous in the vertical direction.

4.3 Analysis

We consider the equation of motion for the center of mass. From the law of action and reaction, the equation in the x direction is written as

$$mNM\frac{dV}{dt} = \sum_{j=1}^{M} \left[F_{\mathrm{L},j} + F_{\mathrm{R},j} \right]. \tag{4.9}$$

Thus, the total force acting on the solid in the x direction is generated by the elastic collisions of the gas particles, where the collision rate depends on the velocity of the solid particles. Because $d\langle V \rangle / dt = 0$, we have the force balance equation in the steady state as

$$\sum_{j=1}^{M} \left[\langle F_{\mathrm{L},j} \rangle + \langle F_{\mathrm{R},j} \rangle \right] = 0. \tag{4.10}$$

Here, we note that

$$\langle F_{\mathrm{L},j} \rangle = \left\langle \int dv_{\mathrm{G}} \lambda_{\mathrm{L}}(v_{\mathrm{G}}, v_{1,j}) I(v_{\mathrm{G}}, v_{1,j}) \right\rangle \frac{S}{M}. \tag{4.11}$$

We then expand the total force $\sum_{j=1}^{M} \left[\langle F_{\mathrm{L},j} \rangle + \langle F_{\mathrm{R},j} \rangle \right]$ in $\epsilon \equiv \sqrt{m_{\mathrm{G}}/m}$. Defining $\gamma_{\mathrm{L}} \equiv \epsilon n_{\mathrm{L}} \sqrt{8mk_{\mathrm{B}}T_{\mathrm{L}}/\pi}$ and $\gamma_{\mathrm{R}} \equiv \epsilon n_{\mathrm{R}} \sqrt{8mk_{\mathrm{B}}T_{\mathrm{L}}/\pi}$, we obtain

$$\sum_{j=1}^{M} \left[-\gamma_{\mathrm{L}} \langle v_{1,j} \rangle - \gamma_{\mathrm{R}} \langle v_{N,j} \rangle + \epsilon^2 p \beta_{\mathrm{L}} m \left\langle v_{1,j}^2 \right\rangle - \epsilon^2 p \beta_{\mathrm{R}} m \left\langle v_{N,j}^2 \right\rangle \right] \frac{S}{M} + O(\epsilon^3) = 0. \tag{4.12}$$

See Appendix 4.A for the derivation. The first and second terms in (4.12) are interpreted as the friction force that originates from the change in the collision rate due to the motion of the solid particles. The terms proportional to ϵ^2 in (4.12) are expressed in the form (4.1), where $T'_{\mathrm{L}} \equiv m(\langle v_{1,j}^2 \rangle - \langle v_{1,j} \rangle^2)/k_{\mathrm{B}}$ and $T'_{\mathrm{R}} \equiv m(\langle v_{N,j}^2 \rangle - \langle v_{N,j} \rangle^2)/k_{\mathrm{B}}$ are different from T_{L} and T_{R}, respectively. By using F_{gap} given in (4.1), we rewrite (4.12) as

$$-(\gamma_{\mathrm{L}} + \gamma_{\mathrm{R}}) S \langle V \rangle + F_{\mathrm{gap}} + O(\epsilon^3) = 0. \tag{4.13}$$

It should be noted that $\langle v_{i,j} \rangle = \langle V \rangle = O(\epsilon)$.

We now derive the temperature gaps for the model we consider. First, we shall find a relation connecting the temperature gap with the heat flux. Let $J_{\mathrm{L},j}$ be the heat flux transferred from the gas to the j-th solid particle at the left end, and $\dot{K}_{\mathrm{L},j}$ be the increasing rate of the kinetic energy per unit area of the j-th solid particle at the left end. The energy conservation law leads to

$$J_{\mathrm{L},j} = \dot{K}_{\mathrm{L},j} - pv_{1,j}. \tag{4.14}$$

Similarly, $J_{\mathrm{R},j} = \dot{K}_{\mathrm{R},j} + pv_{N,j}$. We denote by $\Delta K(v_{\mathrm{G}}, v)$ the change in the kinetic energy of a solid particle for the collision of a solid particle of velocity v with a gas particle of velocity v_{G}, which is given by

$$\Delta K(v_{\mathrm{G}}, v) = \frac{2m_{\mathrm{G}}m}{m_{\mathrm{G}}+m}\frac{m_{\mathrm{G}}v_{\mathrm{G}}+mv}{m_{\mathrm{G}}+m}(v_{\mathrm{G}}-v). \tag{4.15}$$

We then calculate $\langle J_{\mathrm{L},j}\rangle$ as

$$\langle J_{\mathrm{L},j}\rangle = \left\langle \int dv_{\mathrm{G}}\lambda_{\mathrm{L}}(v_{\mathrm{G}}, v_{1,j})\Delta K(v_{\mathrm{G}}, v_{1,j}) \right\rangle - p\langle v_{1,j}\rangle . \tag{4.16}$$

Expanding this expression in ϵ, we obtain

$$\langle J_{\mathrm{L},j}\rangle = \frac{\gamma_{\mathrm{L}}}{m}k_{\mathrm{B}}\left(T_{\mathrm{L}} - T'_{\mathrm{L}}\right) + O(\epsilon^2), \tag{4.17}$$

$$\langle J_{\mathrm{R},j}\rangle = \frac{\gamma_{\mathrm{R}}}{m}k_{\mathrm{B}}\left(T_{\mathrm{R}} - T'_{\mathrm{R}}\right) + O(\epsilon^2). \tag{4.18}$$

See Appendix 4.A for the derivation. These equations mean that the heat flux is related to the temperature gap [106, 107]. The average heat flux through the solid from the left to the right is written as $\langle J\rangle \equiv \langle J_{\mathrm{L},j}\rangle = -\langle J_{\mathrm{R},j}\rangle$ for any j.

Second, we consider the heat flux. In general, the heat flux depends on the interaction potential between solid particles, and it is difficult to calculate it from a microscopic description. Nevertheless, by selecting a proper short-range interaction between solid particles in our model, we may phenomenologically assume Fourier's law in the form

$$\langle J\rangle = \kappa(T'_{\mathrm{L}} - T'_{\mathrm{R}})/L, \tag{4.19}$$

where κ and L represent the thermal conductivity and the axial length of the solid, respectively, and the temperature dependence of κ is ignored. From (4.17), (4.18), and (4.19), we obtain

$$\langle J\rangle = \frac{\kappa(T_{\mathrm{L}} - T_{\mathrm{R}})/L}{1 + \kappa m(1/\gamma_{\mathrm{L}} + 1/\gamma_{\mathrm{R}})/(k_{\mathrm{B}}L)} + O(\epsilon^2), \tag{4.20}$$

and

$$T'_{\mathrm{L}} - T_{\mathrm{L}} = \frac{\gamma_{\mathrm{R}}/(\gamma_{\mathrm{L}}+\gamma_{\mathrm{R}})}{1 + k_{\mathrm{B}}L\gamma_{\mathrm{L}}\gamma_{\mathrm{R}}/[\kappa m(\gamma_{\mathrm{L}}+\gamma_{\mathrm{R}})]}(T_{\mathrm{R}} - T_{\mathrm{L}}) + O(\epsilon). \tag{4.21}$$

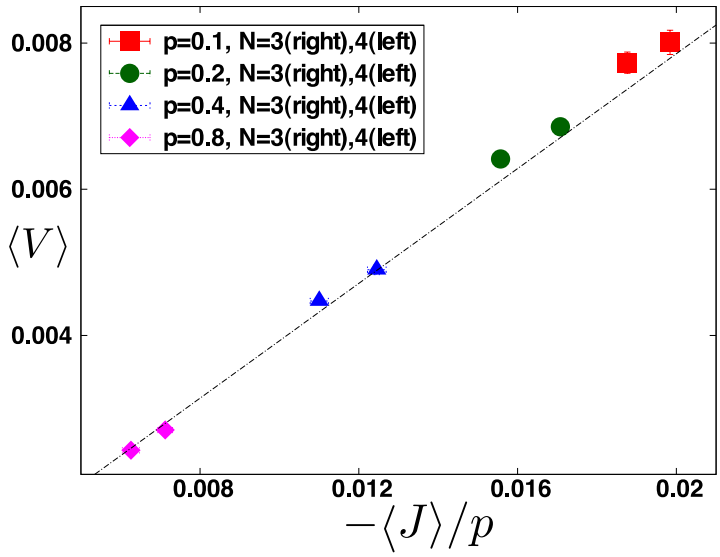

Fig. 4.3 Steady-state velocity $\langle V \rangle$ versus the heat flux over the pressure $-\langle J \rangle / p$ for $p = 0.1, N = 3, 4$ (square, red), $p = 0.2, N = 3, 4$ (circle, green), $p = 0.4, N = 3, 4$ (triangle, blue), and $p = 0.8, N = 3, 4$ (diamond, pink). The dotted line represents $\langle V \rangle = -\pi \langle J \rangle / (8p)$.

By substituting this result into (4.1), we obtain an expression for F_{gap} in terms of the experimental parameters. Furthermore, (4.1), (4.13), (4.17), and (4.18) lead to the simple relation

$$\langle V \rangle = -\frac{\pi \langle J \rangle}{8p} + O(\epsilon^2), \tag{4.22}$$

which connects the moving velocity with the heat flux passing inside the solid. See Refs. [43, 44] for an intuitive explanation of the result.

In order to directly demonstrate the validity of our theory, we performed numerical experiments by solving the Hamiltonian equations in combination with the Poisson process. Here, for simplicity, we consider the case that the system is defined in two dimensions. Concretely, we use the potentials $U_{\mathrm{int}}(\boldsymbol{r}, \boldsymbol{r}') = k(|\boldsymbol{r} - \boldsymbol{r}'| - \sqrt{d}a)^2/2$ for the d-th nearest neighbor pair of solid particles ($d = 1, 2$) and $U_{\mathrm{w}}(\boldsymbol{r}) = 1/|\boldsymbol{r} - \boldsymbol{r}_{\mathrm{w}}(\boldsymbol{r})|^6$, where k is the spring constant, $\sqrt{d}a$ the natural length, and $\boldsymbol{r}_{\mathrm{w}}(\boldsymbol{r})$ the nearest position of the tube wall from $\boldsymbol{r}$. All the quantities are converted into dimensionless forms by setting $k = a = m = 1$. We then set the parameter values as $k_{\mathrm{B}}T_{\mathrm{L}} = 0.07$, $k_{\mathrm{B}}T_{\mathrm{R}} = 0.1$, and $\epsilon = \sqrt{1/10}$. Because the equations are nonlinear, we observed the temperature gradient inside the solid and the temperature gaps at the surface of the solid. We then measured $\langle V \rangle$ and $\langle J \rangle$ for several values of p and $N = M$, and plotted $(-\langle J \rangle / p, \langle V \rangle)$ in Fig. 4.3. We find that the obtained data is consistent with the nontrivial relation (4.22).

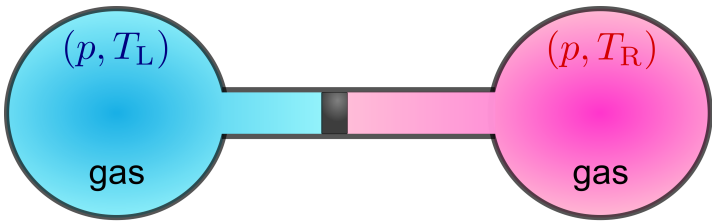

Fig. 4.4 Simple realization of the phenomenon under consideration in an experiment. Large reservoirs of equilibrium gas are connected to the tube, and the length of the tube is assumed to be shorter than the mean free path of the gas particles.

4.4 Experiments

Let us discuss the experimental feasibility of the phenomenon under consideration. As one example of laboratory experiments, we consider silicon and helium of atomic weight 28 and 4, respectively, where $\epsilon = \sqrt{1/7}$. The thermal conductivity of silicon at room temperature is $\kappa \simeq 149\,\mathrm{J/(m \cdot s \cdot K)}$, and the density of silicon is $\rho \simeq 2.33\,\mathrm{g/cm^3}$. We set $T_{\mathrm{L}} = 293\,\mathrm{K}$, $T_{\mathrm{R}} = 303\,\mathrm{K}$, $p = 1\,\mathrm{atm}$, $S = 7\,\mathrm{cm^2}$, and $L = 1\,\mathrm{cm}$. By using (4.1), (4.20), (4.21), and (4.22), we obtain the velocity of the solid $\langle V \rangle \simeq 3.9 \times 10\,\mathrm{cm/s}$, the temperature gap $T'_{\mathrm{L}} - T_{\mathrm{L}} \simeq 1.6\,\mathrm{K}$, and the temperature-gap-induced force $F_{\mathrm{gap}} \simeq 1.1 \times 10^{-1}\,\mathrm{N}$. These estimated values are large enough to be measured in careful experiments. We next consider several possible difficulties that may arise in experiments.

First, there is the friction between the solid and the tube. Because the coefficient of static friction of a lubricant is at most 0.5 [108], the static friction force is about $0.5 \times 9.8\,\mathrm{m/s^2} \times \rho \mathrm{SL} \simeq 8.0 \times 10^{-2}\,\mathrm{N}$, which is less than $F_{\mathrm{gap}} \simeq 1.1 \times 10^{-1}\,\mathrm{N}$. Thus, the effect of the friction can be mitigated by the use of a lubricant.

Second, one may worry that the relaxation time of the motion of the solid is longer than the observation time. However, since the relaxation time is estimated as $mNM/(\gamma_{\mathrm{L}} + \gamma_{\mathrm{R}})S = \rho L/(\gamma_{\mathrm{L}} + \gamma_{\mathrm{R}}) \simeq 5.7 \times 10^{-2}\,\mathrm{s}$, the velocity of the solid is rapidly relaxed to the steady-state value.

Lastly, the most difficult experimental setup may be the control of the temperatures of the gases. One method is to connect the tube with baths of dilute gas, where the length of the tube is chosen to be shorter than the mean-free path of the dilute gas as shown in Fig. 4.4. The mean-free path of the helium atoms at 1 atm and 300 K is about 200 nm and is inversely proportional to the pressure. Therefore, when the length of the tube is 20 cm, we have to set the pressure at $1 \times 10^{-6}\,\mathrm{atm}$, and F_{gap} becomes very small. On the contrary, when the mean-free path is much shorter than the length of the tube, a temperature gradient appears in the gases. This makes $T_{\mathrm{R}} - T_{\mathrm{L}}$ small, and as a result F_{gap} becomes small. The simplest realization is to control the temperatures from the side wall of the tube. In this case, we immobilize

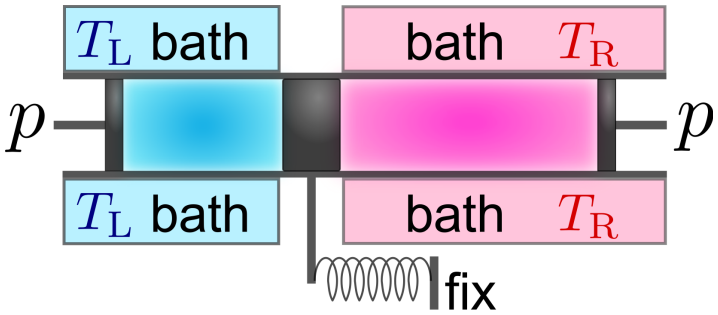

Fig. 4.5 Two heat baths are in thermal contact with two dilute-gas regions, respectively. The solid material is immobilized by a spring. $F_{\rm gap}$ can be measured in the experiment, while the steady-state motion is not observed.

the solid by linking a spring to it (see Fig. 4.5). Because the value of the stall force is equal to $F_{\rm gap}$, we can measure its value, whereas we cannot observe the steady-state motion.

Setting aside the quantitative aspects, we may observe phenomena to which $F_{\rm gap}$ makes a dominant contribution. One example is a Brownian particle under a temperature gradient [65–68]. If the thermal conductivity of the particle is much larger than that of a solution, heat flux passes inside the particle. Then, because the temperature gap appears on the solid surface, the force $F_{\rm gap}$ is generated. It should be noted, however, that other types of forces appear on the particle under a temperature gradient [68]. It is a stimulating challenge to separate $F_{\rm gap}$ from the total force.

4.5 Concluding remarks

In this chapter, we have predicted that the temperature gap at the interface between a solid and a gas yields the force $F_{\rm gap}$. Because this force is not described by standard continuum theory such as hydrodynamics and elastic theory, further experimental and theoretical studies are necessary so as to obtain a systematic understanding of the nature of the force. Before ending this chapter, we provide a few remarks.

With regard to our setup, similar models were studied in the context of the so-called adiabatic piston problem [1,39,42,89]. Indeed, for the case $\kappa \gg Lk_{\rm B}\gamma_{\rm L}\gamma_{\rm R}/[m(\gamma_{\rm L}+\gamma_{\rm R})]$ or $N = 1$, we obtain

$$\langle J\rangle = \frac{k_{\rm B}(T_{\rm L} - T_{\rm R})}{m(\gamma_{\rm L}^{-1} + \gamma_{\rm R}^{-1})} + O(\epsilon^2), \tag{4.23}$$

and

$$\langle V\rangle = \epsilon\sqrt{\frac{\pi}{8}}\left(\sqrt{\frac{k_{\rm B}T_{\rm R}}{m}} - \sqrt{\frac{k_{\rm B}T_{\rm L}}{m}}\right) + O(\epsilon^2), \tag{4.24}$$

where $T'_{\rm L} = T'_{\rm R}$. These expressions for $\langle J\rangle$ and $\langle V\rangle$ are identical to those derived in Refs. [92, 93]. Here, it should be noted that m in the preceding studies was assumed

to be the total mass of the solid, which gives much smaller values of $\langle J \rangle$ and $\langle V \rangle$ than ours.

In contrast to the interface case, there exists no force due to temperature differences at the atomic scale in the bulk. In order to clearly understand the difference between the two cases, we should derive $F_{\rm gap}$ on the basis of a mechanical description of solids and gases. This fundamental question might be solved by considering hydrodynamics of a binary mixture fluid in the phase separation state. Because hydrodynamics may involve the discontinuity of the temperature profile at the interface between the two materials, the standard assumption of slowly varying thermodynamic quantities may not be valid. The derivation may be obtained as an extension of a recent work [36] in which the hydrodynamic equations for a simple fluid are derived from a Hamiltonian description of identical particles. Obviously, the experimental measurement of $F_{\rm gap}$ is of great importance even for the theory. By clarifying the mechanism of nonstandard forces, we hope to develop the understanding of nonequilibrium systems.

4.A Derivation of (4.12), (4.17), and (4.18)

By considering $f_{\rm eq}^{\rm L(R)}(v) = \epsilon\sqrt{\beta_{\rm L(R)}m/2\pi}\exp(-\epsilon^2\beta_{\rm L(R)}mv^2/2)$, we obtain

$$\begin{aligned}\int_V^\infty v^k f_{\rm eq}^{\rm L}(v)dv &= \int_0^\infty v^k f_{\rm eq}^{\rm L}(v)dv + O(\epsilon)\\ &= \frac{\epsilon^{-k}}{2\sqrt{\pi}}\left(\frac{2}{\beta_{\rm L}m}\right)^{\frac{k}{2}}\Gamma\left(\frac{k+1}{2}\right) + O(\epsilon), \qquad (4.25)\\ \int_{-\infty}^V v^k f_{\rm eq}^{\rm R}(v)dv &= \int_{-\infty}^0 v^k f_{\rm eq}^{\rm R}(v)dv + O(\epsilon)\\ &= \frac{(-\epsilon)^{-k}}{2\sqrt{\pi}}\left(\frac{2}{\beta_{\rm R}m}\right)^{\frac{k}{2}}\Gamma\left(\frac{k+1}{2}\right) + O(\epsilon), \qquad (4.26)\end{aligned}$$

where k is a non-negative integer. By using (4.25) and (4.26), we obtain

$$\begin{aligned}\int \lambda_{\rm L}(v,V)I(v,V)dv &= \frac{2\epsilon^2 m n_{\rm L}}{1+\epsilon^2}\int_V^\infty (v-V)^2 f_{\rm eq}^{\rm L}(v)dv \\ &= (1-\epsilon^2)p - \gamma_{\rm L}V + \epsilon^2 p\beta_{\rm L} m V^2 + O(\epsilon^3), \qquad (4.27)\\ \int dv\ \lambda_{\rm R}(v,V)I(v,V) &= -\frac{2\epsilon^2 m n_{\rm R}}{1+\epsilon^2}\int_{-\infty}^V dv(V-v)^2 f_{\rm eq}^{\rm R}(v) \\ &= -(1-\epsilon^2)p - \gamma_{\rm R}V - \epsilon^2 p\beta_{\rm R} m V^2 + O(\epsilon^3), \qquad (4.28)\\ \int \lambda_{\rm L}(v,V)\Delta K(v,V)dv &= \frac{2\epsilon^2 m n_{\rm L}}{(1+\epsilon^2)^2}\int_V^\infty (v-V)^2(\epsilon^2 v+V) f_{\rm eq}^{\rm L}(v)dv \\ &= pV - \gamma_{\rm L}V^2 + \frac{\gamma_{\rm L}k_{\rm B}T_{\rm L}}{m} + O(\epsilon^2), \qquad (4.29)\\ \int \lambda_{\rm R}(v,V)\Delta K(v,V)dv &= -\frac{2\epsilon^2 m n_{\rm R}}{(1+\epsilon^2)^2}\int_{-\infty}^V (V-v)^2(\epsilon^2 v+V) f_{\rm eq}^{\rm R}(v)dv \\ &= -pV - \gamma_{\rm R}V^2 + \frac{\gamma_{\rm R}k_{\rm B}T_{\rm R}}{m} + O(\epsilon^2), \qquad (4.30)\end{aligned}$$

where we have used $p = n_{\rm L}/\beta_{\rm L} = n_{\rm R}/\beta_{\rm R}$, $\gamma_{\rm L} = \epsilon n_{\rm L}\sqrt{8mk_{\rm B}T_{\rm L}/\pi}$, and $\gamma_{\rm R} = \epsilon n_{\rm R}\sqrt{8mk_{\rm B}T_{\rm R}/\pi}$. Here, we assume that $\langle O(\epsilon^k)\rangle = O(\epsilon^k)$. Then, (4.27) and (4.28) lead to

$$\begin{aligned}\sum_{j=1}^M \Big[\langle F_{{\rm L},j}\rangle + \langle F_{{\rm R},j}\rangle\Big] &= \sum_{j=1}^M \left[\left\langle \int dv_{\rm G}\lambda_{\rm L}(v_{\rm G},v_{1,j})I(v_{\rm G},v_{1,j})\right\rangle \right. \\ &\qquad \left. + \left\langle \int dv_{\rm G}\lambda_{\rm R}(v_{\rm G},v_{N,j})I(v_{\rm G},v_{N,j})\right\rangle\right]\frac{S}{M} \\ &= \sum_{j=1}^M \left[-\gamma_{\rm L}\langle v_{1,j}\rangle - \gamma_{\rm R}\langle v_{N,j}\rangle + \epsilon^2 p\beta_{\rm L} m\langle v_{1,j}^2\rangle \right. \\ &\qquad \left. -\epsilon^2 p\beta_{\rm R} m\langle v_{N,j}^2\rangle\right]\frac{S}{M} + O(\epsilon^3). \qquad (4.31)\end{aligned}$$

By using $\langle v_{i,j} \rangle = \langle V \rangle = O(\epsilon)$, (4.29), and (4.30), we obtain

$$\begin{aligned}
\langle J_{\mathrm{L},j} \rangle &= \left\langle \int dv_{\mathrm{G}} \lambda_{\mathrm{L}}(v_{\mathrm{G}}, v_{1,j}) \Delta K(v_{\mathrm{G}}, v_{1,j}) \right\rangle - p \langle v_{1,j} \rangle \\
&= \frac{\gamma_{\mathrm{L}}}{m} k_{\mathrm{B}} \left(T_{\mathrm{L}} - m \left\langle v_{1,j}^2 \right\rangle / k_{\mathrm{B}} \right) + O(\epsilon^2) \\
&= \frac{\gamma_{\mathrm{L}}}{m} k_{\mathrm{B}} \left(T_{\mathrm{L}} - T'_{\mathrm{L}} \right) + O(\epsilon^2), \qquad (4.32) \\
\langle J_{\mathrm{R},j} \rangle &= \left\langle \int dv_{\mathrm{G}} \lambda_{\mathrm{R}}(v_{\mathrm{G}}, v_{N,j}) \Delta K(v_{\mathrm{G}}, v_{N,j}) \right\rangle + p \langle v_{N,j} \rangle \\
&= \frac{\gamma_{\mathrm{R}}}{m} k_{\mathrm{B}} \left(T_{\mathrm{R}} - m \left\langle v_{N,j}^2 \right\rangle / k_{\mathrm{B}} \right) + O(\epsilon^2) \\
&= \frac{\gamma_{\mathrm{R}}}{m} k_{\mathrm{B}} \left(T_{\mathrm{R}} - T'_{\mathrm{R}} \right) + O(\epsilon^2). \qquad (4.33)
\end{aligned}$$

Chapter 5

Conclusions

In this thesis, aiming at the construction of non-equilibrium statistical mechanics for fluid dynamics, we have studied fluid stresses on the basis of a microscopic mechanical description. In Chapter 2, we have related the surface stress correlation to the bulk stress correlation in a viscous fluid at low Reynolds number with the aid of large deviation theory, and have derived Stokes' law from Kirkwood's formula and the Green–Kubo formula without explicitly employing the hydrodynamic equations. In Chapter 3, by considering the local detailed balance condition, we have elucidated the energetics of the adiabatic piston problem that cannot be described by the hydrodynamic equations. We also have shown that the adiabatic piston problem is understood based on the linear response theory. In Chapter 4, we have shown that the force induced by the temperature discontinuities at solid-gas interfaces is large enough to be observed by a macroscopic measurement. The temperature discontinuities break the standard assumption of slowly varying thermodynamic quantities in fluid mechanics, which is the reason why the adiabatic piston problem cannot be described by the hydrodynamic equations. Before ending this thesis, we make some remarks.

As shown in previous studies and this thesis, non-equilibrium identities and large deviation theory are useful for understanding the relation between microscopic mechanics and macroscopic hydrodynamics. However, many problems of statistical mechanics for fluid phenomena still remain unsolved. For example, as we pointed out in Chapter 1, it is difficult to determine the microscopic conditions for realizing macroscopic non-slip boundary conditions. Macroscopic boundary conditions may be related to the roughness of boundaries. In future, we want to elucidate these relations. Furthermore, by understanding the fluid behavior near boundaries, we wish to investigate the validity of hydrodynamic description in the small-scale system given in Ref. [37] and the adiabatic piston problem.

As another example more related to our study, the fluctuation properties of fluid stresses are still poorly understood. In Chapter 2, we have derived

$$\left\langle (\bar{\sigma}_*)^2 \right\rangle_{\rm eq} \propto \frac{1}{\tau \mathcal{R}^3}. \tag{5.1}$$

However, because $\bar{\sigma}_*$ is the time-averaged force per unit area on the surface of the

sphere, the central limit theorem would naively indicate that

$$\left\langle (\bar{\sigma}_*)^2 \right\rangle_{\rm eq} \propto \frac{1}{\tau \mathcal{R}^2}. \tag{5.2}$$

which is realized in a dilute gas. This implies that collisions between a bath particle and the sphere are independent of each other in the dilute gas whereas the collisions are correlated in a viscous fluid. In addition, since $\mathcal{R}$ is the macroscopic quantity, (5.1) and (5.2) mean that the surface stress fluctuations are suppressed in the viscous fluid, which is called hyperuniformity [109]. We do not know other examples of phenomena showing hyperuniformity in viscous fluids, and then hope to develop the understanding of them.

In general, it is difficult to understand macroscopic non-equilibrium phenomena based on a microscopic mechanical description because available methods for connecting different hierarchies are limited. By extending the methods developed in this thesis, we hope to construct statistical mechanics for non-equilibrium phenomena.

Acknowledgments

First of all, I would like to express the deepest appreciation to my supervisor, Shinichi Sasa, for his thoughtful guidance and encouragement during my doctoral studies. He always give me insightful comments on my studies. Without his persistent help, I would not have been able to do research.

I would like to thank Ken Sekimoto, Shinji Takesue, Masaki Sano, Hal Tasaki, Sadayoshi Toh, Hisao Hayakawa, Akira Yoshimori, Naoko Nakagawa, Keiji Saito, Takeaki Araki, Takeshi Matsumoto, Hirofumi Wada, Kazumasa Takeuchi, Takahiro Sagawa, Yohei Nakayama, Kyogo Kawaguchi, Kiyoshi Kanazawa, Sosuke Ito, Tomohiko G. Sano, Satoshi Takada, and Yuki Uematsu for useful discussions.

I also thank (former) members of the Sasa group, Michikazu Kobayashi, Andreas Dechant, Yuki Minami, Masahiko Ueda, Taiki Haga, Hiroyoshi Takagi, Akito Inoue, Hayato Miyake, Takahiro Hatano, Michio Otsuki, Takenobu Nakamura, Masamichi Miyama, Hiroki Ohta, Taiki Kanda, Michihiro Nakamura, Takahiro Nemoto, Makoto Wakasugi, Junya Iwai, Hisato Komatsu, Naoto Shiraishi, and Daisuke Sato. They helped me many times on my research, and also on my daily life problems.

References

[1] Callen, H.B.: Thermodynamics and an Introduction to Thermostatistics, 2nd edn. Wiley, New York (1985)

[2] Lieb, E.H., Yngvason, J.: The physics and mathematics of the second law of thermodynamics. Phys. Rep. **310**, 1–96 (1999)

[3] Landau, L.D., Lifshitz, E.M.: Statistical Physics, Vol. 5, 3rd ed. Pergamon Press, Oxford (1980)

[4] Zubarev, D.N.: Nonequilibrium Statistical Thermodynamics. Consultants Bureau, New York (1974)

[5] Kubo, R., Toda, M., Hashitsume, N.: Statistical Physics II: Nonequilibrium Statistical Mechanics. Springer-Verlag, Berlin (1985)

[6] Sasa, S., Tasaki, H.: Steady state thermodynamics. J. Stat. Phys. **125**, 125–224 (2006)

[7] Landau, L.D., Lifshitz, E.M.: Fluid Mechanics, Vol. 6, 1st ed. Pergamon Press, Oxford (1959)

[8] Chapman, S., Cowling, T.G.: The Mathematical Theory Of Non-Uniform Gases, 3rd ed. Cambridge University Press, Cambridge (1970)

[9] Chaikin, P.M., Lubensky, T.C.: Principles of Condensed Matter Physics. Cambridge University Press, Cambridge (1995)

[10] Sasa, S.: Continuum Mechanics. Class lecture, The University of Tokyo, Tokyo (2012)

[11] Onsager, L.: Reciprocal Relations in Irreversible Processes. I. Phys. Rev. **37**, 405–426 (1931)

[12] Onsager, L.: Reciprocal Relations in Irreversible Processes. II. Phys. Rev. **38**, 2265–2279 (1931)

[13] Hashitsume, N.: A statistical theory of linear dissipative systems. Prog. Theor. Phys. **8**, 461–478 (1952).

[14] Onsager, L., Machlup, S.: Fluctuations and Irreversible Processes. Phys. Rev. **91**, 1505–1512 (1953)

[15] Machlup, S., Onsager, L.: Fluctuations and Irreversible Process. II. Systems with Kinetic Energy. Phys. Rev. **991**, 1512–1515 (1953)

[16] De Groot, S.R., Mazur, P.: Non-Equilibrium Thermodynamics. Dover, New York, (1984)

[17] Green, M.S.: Markoff Random Processes and the Statistical Mechanics of Time-Dependent Phenomena. J. Chem. Phys. **20**, 1281–1295 (1952)

[18] Green, M.S.: Markoff Random Processes and the Statistical Mechanics of Time-

Dependent Phenomena. II. Irreversible Processes in Fluids. J. Chem. Phys. **22**, 398–413 (1954)
[19] Irving, J.H., Kirkwood, J.G.: The statistical mechanical theory of transport processes. IV. The equations of hydrodynamics. J. Chem. Phys. **18**, 817–829 (1950)
[20] Evans, D.J., Cohen, E.G.D., Morriss, G.P.: Probability of second law violations in shearing steady states. Phys. Rev. Lett. **71**, 2401–2404 (1993)
[21] Gallavotti, G., Cohen, E.G.D.: Dynamical ensembles in nonequilibrium statistical mechanics. Phys. Rev. Lett. **74**, 2694–2697 (1995)
[22] Kurchan, J.: Fluctuation theorem for stochastic dynamics. J. Phys. A **31**, 3719–3729 (1998)
[23] Lebowitz, J.L., Spohn, H.: A Gallavotti–Cohen-type symmetry in the large deviation functional for stochastic dynamics. J. Stat. Phys. **95**, 333–365 (1999)
[24] Maes, C.: The fluctuation theorem as a Gibbs property. J. Stat. Phys. **95**, 367–392 (1999)
[25] Crooks, G.E.: Entropy production fluctuation theorem and the nonequilibrium work relation for free energy differences. Phys. Rev. E **60**, 2721–2726 (1999)
[26] Crooks, G.E.: Path-ensemble averages in systems driven far from equilibrium. Phys. Rev. E **61**, 2361–2366 (2000)
[27] Jarzynski, C.: Hamiltonian derivation of a detailed fluctuation theorem. J. Stat. Phys. **98**, 77–102 (2000)
[28] Seifert, U.: Entropy production along a stochastic trajectory and an integral fluctuation theorem. Phys. Rev. Lett. **95**, 040602 (2005)
[29] Jarzynski, C,: Nonequilibrium equality for free energy differences. Phys. Rev. Lett. **78**, 2690–2693 (1997)
[30] Hayashi, K., Sasa, S.: Linear response theory in stochastic many-body systems revisited. Physica A **370**, 407–429 (2006)
[31] Seifert, U.: Stochastic thermodynamics, fluctuation theorems and molecular machines. Rep. Prog. Phys. **75**, 126001 (2012)
[32] Liphardt, J., Dumont, S., Smith, S.B., Tinoco, I. Jr., Bustamante, C.: Equilibrium information from nonequilibrium measurements in an experimental test of Jarzynski's equality. Science **296**, 1832–1835 (2002)
[33] Wang, G.M., Sevick, E.M., Mittag, E., Searles, D.J., Evans, D.J.: Experimental demonstration of violations of the second law of thermodynamics for small systems and short time scales. Phys. Rev. Lett. **89**, 050601 (2002)
[34] Collin, D.F., Ritort F., Jarzynski C., Smith S.B., Tinoco I. Jr., Bustamante C.: Verification of the Crooks fluctuation theorem and recovery of RNA folding free energies. Nature **437** 231–234 (2005)
[35] Hayashi, K., Ueno, H., Iino, R., Noji, H.: Fluctuation theorem applied to F_1-ATPase. Phys. Rev. Lett. **104**, 218103 (2010)
[36] Sasa, S.: Derivation of Hydrodynamics from the Hamiltonian description of particle systems. Phys. Rev. Lett. **112**, 100602 (2014)
[37] Zhu, Y., Granick, S.: Rate-Dependent Slip of Newtonian Liquid at Smooth Surfaces. Phys. Rev. Lett. **87**, 096105 (2001)

[38] Sausset, F., Biroli, G., Kurchan, J.: Do solids flow? J. Stat. Phys. **140**, 718–727 (2010)
[39] Feynman, R.P., Leighton, R.B., Sands, M.: The Feynman Lectures on Physics, Vol. 1, Chap. 39.4. Addison Wesley, Boston, (1963)
[40] Lieb, E.H.: Some problems in statistical mechanics that I would like to see solved. Physica A **263**, 491–499 (1999)
[41] Chernov, N.I., Lebowitz, J.L., Sinai, Ya.G.: Dynamics of a massive piston in an ideal gas. Russ. Math. Surv. **57**, 1045–1125 (2002)
[42] Gruber Ch., Lesne, A.: Adiabatic Piston. In: Françoise, J.P., Naber, G., Tsun, T.S. (eds.) Encyclopedia of Mathematical Physics, pp. 160–174. Elsevier, Amsterdam (2006)
[43] Fruleux, A., Kawai, R., Sekimoto, K.: Momentum Transfer in Nonequilibrium Steady States. Phys. Rev. Lett. **108**, 160601 (2012)
[44] Kawai, R., Fruleux, A., Sekimoto, K.: A hard disc analysis of momentum deficit due to dissipation. Phys. Scr. **86**, 058508 (2012)
[45] Kawaguchi, K., Nakayama, Y.: Fluctuation theorem for hidden entropy production. Phys. Rev. E **88**, 022147 (2013)
[46] Kirkwood, J.: The statistical mechanical theory of transport processes I. General theory. J. Chem. Phys. **14**, 180–201 (1946)
[47] Lebowitz, J.L., Rubin, E.: Dynamical Study of Brownian Motion. Phys. Rev. **131**, 2381–2396 (1963)
[48] Zwanzig, R.: Elementary Derivation of Time-Correlation Formulas for Transport Coefficients. J. Chem. Phys. **40**, 2527–2533 (1964)
[49] Mazur, P., Oppenheim, I.: Molecular theory of Brownian motion. Physica **50**, 241–258 (1970)
[50] Lagar'kov, A.N., Sergeev, V.H.: Molecular dynamics method in statistical physics. Sov. Phys. Usp. **27**, 566–588 (1978)
[51] Brey, J.J., Ordóñez, J.G.: Computer studies of Brownian motion in a Lennard–Jones fluid: The Stokes law. J. Chem. Phys. **76**, 3260–3263 (1982)
[52] Español, P., Zúñiga, I.: Force autocorrelation function in Brownian motion theory. J. Chem. Phys. **98**, 574–580 (1993)
[53] Ould-Kaddour, F., Levesque, D.: Determination of the friction coefficient of a Brownian particle by molecular-dynamics simulation. J. Chem. Phys. **118**, 7888–7891 (2003)
[54] Lee, S.H., Kapral, R.: Friction and diffusion of a Brownian particle in a mesoscopic solvent. J. Chem. Phys. **121**, 11163–11169 (2004)
[55] Lorentz, H.A.: Les Theories Statistiques en Thermodynamique. B.G. Teubner, Leipzig (1912)
[56] Green, M.S.: Brownian motion in a gas of noninteracting molecules. J. Chem. Phys. **19**, 1036–1046 (1951)
[57] Zwanzig, R.: Hydrodynamic fluctuations and Stokes' law friction. J. Res. Natl. Bur. Std.(US) B **68**, 143–145 (1964)
[58] Schmitz, R.: Fluctuations in nonequilibrium fluids. Phys. Rep. **171**, 1–58 (1988)
[59] Kim S., Karrila, S.J.: Microhydrodynamics: Principles and Selected Applica-

tions. Butterworth-Heinemann, Newton, MA (1991)
[60] Dembo, A., Zeitouni, O.: Large Deviations Techniques and Applications, 2nd edn. Springer, New York (1998)
[61] Touchette, H.: The large deviation approach to statistical mechanics. Phys. Rep. **478**, 1–69 (2009)
[62] Shiraishi, N.: Anomalous System Size Dependence of Large Deviation Functions for Local Empirical Measure. J. Stat. Phys. **152**, 336–352 (2013)
[63] Bodineau, T., Derrida, B.: Current fluctuations in nonequilibrium diffusive systems: an additivity principle. Phys. Rev. Lett. **92**, 180601 (2004)
[64] Bertini, L., De Sole, A., Gabrielli, D., Jona-Lasinio, G., Landim, C.: Current fluctuations in stochastic lattice gases. Phys. Rev. Lett. **94**, 030601 (2005)
[65] Duhr, S., Braun, D.: Why molecules move along a temperature gradient. Proc. Natl. Acad. Sci. U.S.A. **103**, 19678–19682 (2006)
[66] Piazza R., Parola, A.: Thermophoresis in colloidal suspensions. J. Phys. Condens. Matter **20**, 153102 (2008)
[67] Jiang, H.R., Wada, H., Yoshinaga, N., Sano, M.: Manipulation of Colloids by a Nonequilibrium Depletion Force in a Temperature Gradient. Phys. Rev. Lett. **102**, 208301 (2009)
[68] Würger, A.: Thermal non-equilibrium transport in colloids. Rep. Prog. Phys. **73**, 126601 (2010)
[69] Marchetti, M.C., Joanny, J.F., Ramaswamy, S., Liverpool, T.B., Prost, J., Rao, M., Simha, R.A.: Hydrodynamics of soft active matter. Rev. Mod. Phys. **85**, 1143–1189 (2013)
[70] Bursac, P., Lenormand, G., Fabry, B., Oliver, M., Weitz, D.A., Viasnoff, V., Butlerm J.P., Fredberg, J.J.: Cytoskeletal remodelling and slow dynamics in the living cell. Nat. Mater. **4**, 557–561 (2005)
[71] Mizuno, D., Tardin, C., Schmidt, C.F., MacKintosh, F.C.: Nonequilibrium Mechanics of Active Cytoskeletal Networks. Science **315**, 370–373 (2007)
[72] Trepat, X., Deng, L., An, S.S., Navajas, D., Tschumperlin, D.J., Gerthoffer, W.T., Butler, J.P., Fredberg, J.J.: Universal physical responses to stretch in the living cell. Nature **447**, 592–595 (2007)
[73] Fletcher, D.A., Mullins, R.D.: Cell mechanics and the cytoskeleton. Nature **463**, 485–492 (2010)
[74] Albert, R., Pfeifer, M.A., Barabási, A.-L., Schiffer, P.: Slow drag in a granular medium. Phys. Rev. Lett. **82**, 205–208 (1999)
[75] Katsuragi, H., Durian, D.J.: Unified force law for granular impact cratering. Nat. Phys. **3**, 420–423 (2007)
[76] Goldman, D.I., Umbanhowar, P.: Scaling and dynamics of sphere and disk impact into granular media. Phys. Rev. E **77**, 021308 (2008)
[77] Takehara, Y., Okumura, K.: High-Velocity Drag Friction in Granular Media near the Jamming Point. Phys. Rev. Lett. **112**, 148001 (2014)
[78] Yang, X., Manning, M.L., Marchetti, M.C.: Aggregation and segregation of confined active particles. Soft matter **10**, 6477–6484 (2014)
[79] Takatori, S.C., Yan, W., Brady, J.F.: Swim Pressure: Stress Generation in

Active Matter. Phys. Rev. Lett. **113**, 028103 (2014)
[80] Ginot, F., Theurkauff, I., Levis, D., Ybert, C., Bocquet, L., Berthier, L., Cottin-Bizonne, C.: Nonequilibrium Equation of State in Suspensions of Active Colloids. Phys. Rev. X **5**, 011004 (2015)
[81] Solon, A.P., Fily, Y., Baskaran, A., Cates, M.E., Kafri, Y., Kardar, M., Tailleur J.: Pressure is not a state function for generic active fluids. Nature Phys. **11**, 673–678 (2015)
[82] Maldacena, J.M.: The large N limit of superconformal field theories and supergravity. Adv. Theor. Math. Phys. **2**, 231–252 (1998)
[83] Gubser, S.S., Klebanov, I.R., Polyakov, A.M.: Gauge theory correlators from non-critical string theory. Phys. Lett. B. **428**, 105–114 (1998)
[84] Witten, E.: Anti-de Sitter space and holography. Adv. Theor. Math. Phys. **2**, 253–291 (1998)
[85] Aharony, O., Gubser, S.S., Maldacena, J.M., Ooguri, H., Oz, Y.: Large N field theories, string theory and gravity. Phys. Rep. **323**, 183–386 (2000)
[86] Ryu, S., Takayanagi, T.: Holographic Derivation of Entanglement Entropy from the anti-de Sitter Space/Conformal Field Theory Correspondence. Phys. Rev. Lett. **96**, 181602 (2006)
[87] Sekimoto, K.: Kinetic characterization of heat bath and the energetics of thermal ratchet models. J. Phys. Soc. Jpn **66**, 1234–1237 (1997)
[88] Sekimoto, K.: Stochastic Energetics. Springer, Berlin (2010)
[89] Kestemont, E., Van den Broeck, C., Mansour, M.M.: The "adiabatic" piston: And yet it moves. Europhys. Lett. **49**, 143–149 (2000)
[90] Munakata T., Ogawa, H.: Dynamical aspects of an adiabatic piston. Phys. Rev. E **64**, 036119 (2001)
[91] Van den Broeck, C., Kawai, R., Meurs, P.: Microscopic Analysis of a Thermal Brownian Motor. Phys. Rev. Lett. **93**, 090601 (2004)
[92] Gruber Ch., Piasecki, J.: Stationary motion of the adiabatic piston. Physica A **268**, 412–423 (1999)
[93] Gruber, Ch., Frachebourg, L.: On the adiabatic properties of a stochastic adiabatic wall: Evolution, stationary non-equilibrium, and equilibrium states. Physica A **272**, 392–428 (1999)
[94] Gruber, Ch., Pache, Séverine., Lesne, Annick.: Two-time-scale relaxation towards thermal equilibrium of the enigmatic piston. J. Stat. Phys. **112**, 1177–1206 (2003)
[95] Plyukhin A.V., Schofield, J.: Langevin equation for the extended Rayleigh model with an asymmetric bath. Phys. Rev. E **69**, 021112 (2004)
[96] Sagawa, T., Hayakawa, H.: Geometrical expression of excess entropy production. Phys. Rev. E **84**, 051110 (2011)
[97] Maes, C., Netočnỳ, K., Wynants, B.: On and beyond entropy production: the case of Markov jump processes. Markov Proc. Rel. Fields **14**, 445-464 (2008)
[98] McLennan, J.A.: Introduction to Nonequilibrium Statistical Mechanics. Prentice-Hall, Englewood Cliffs, NJ (1989)
[99] Maes, C., Netočnỳ, K.: Rigorous meaning of McLennan ensembles. J. Math.

Phys. **51**, 015219 (2010)
[100] Sagawa, T., Ueda, M.: Fluctuation theorem with information exchange: Role of correlations in stochastic thermodynamics. Phys. Rev. Lett. **109**, 180602 (2012)
[101] Ito, S., Sagawa, T.: Information thermodynamics on causal networks. Phys. Rev. Lett. **111**, 180603 (2013)
[102] Gardiner, C.W.: Handbook of Stochastic Methods. Springer, Heidelberg (1983)
[103] Swartz, E.T., Pohl, R.O.: Thermal boundary resistance. Rev. Mod. Phys. **61**, 605–668 (1989)
[104] Fang, G., Ward, C.A.: Temperature measured close to the interface of an evaporating liquid. Phys. Rev. E **59**, 417–428 (1999)
[105] Cahill, D.G., Ford, W.K., Goodson, K.E., Mahan, G.D., Majumdar, A., Maris, H.J., Merlin, R., Phillpot, S.R.: Nanoscale thermal transport. J. Appl. Phys. **93**, 793–818 (2003)
[106] Parrondo, J.M.R., Español, P.: Criticism of Feynman's analysis of the ratchet as an engine. Am. J. Phys. **64**, 1125–1129 (1996)
[107] Lepri, S., Livi, R., Politi, A.: Thermal conduction in classical low-dimensional lattices. Phys. Rep. **377**, 1–80 (2003)
[108] Anderson, A.E. *et al.*: ASM Handbook: Friction, Lubrication, and Wear Technology, Vol. 18. ASM International, Materials Park (1992)
[109] Torquato, S., Stillinger, F.H.: Local density fluctuations, hyperuniformity, and order metrics. Phys. Rev. E **68**, 041113 (2003)